Exploiting the adenoassociated virus Rep protein to mediate site-specific integration into the human genome and optimisation of Ad/AAV vector design

Thesis

FABIO AVOLIO

Exploiting the Adenoassociated virus Rep protein to mediate site-specific integration into the human genome and optimisation of Ad/AAV vector design

Degree of Doctor of Philosophy (PhD)
in Molecular and Cellular Biology

October 2007

Sponsoring establishment:
San Raffaele Dibit (HSR-Dibit)
Milan, ITALY

Director of studies:
Professor Fulvio Mavilio

External supervisor:
Professor Michael Antoniou

DATE OF SUBMISSION 15 MAY 2007
DATE OF AWARD 08 FEBRUARY 2008

ProQuest LLC.
789 East Eisenhower Parkway
P.O. Box 1346
Ann Arbor, MI 48106 – 1346

Declaration

This thesis has been composed by myself and has not been used in any previous application for a degree. The results presented here were obtained by myself.

All sources and information are acknowledged by means of references.

Some of the results presented and discussed here are contained in the following articles:

Mickaël Guilbaud, Gilliane Chadeuf, **Fabio Avolio**, Achille François, Philippe Moullier, Alessandra Recchia and Anna Salvetti. **Relative influence of the AAV-2 minimal p5 element for rAAV plasmid and vector site-specific integration.** Submitted

To my family…

Ringrazio

I miei genitori... per tutto e perché è anche grazie a loro che sono arrivato fin qui e che non ho mai ringraziato... Grazie...

Erika... Che mi è sempre stata vicina anche quando era meglio starmi lontano... per i consigli... per le critiche mai risparmiate (e serve coraggio...). Per essere un buon navigatore nella vita ed in macchina... Grazie... Senza di te non sarebbe stato possibile...

Me... Perché... Perché... Perché alcune cose si devono mandare giù con l'aiuto delle persone care...

Quelli che mi hanno dato forza, sostegno ed entusiasmo... Non servirebbe menzionarli... Comunque grazie a Claudio per i consigli e per essere stato il mio mentore...

Sara per i consigli, le pause caffè e le e-mails di svago...

Ile per la compagnia in ufficio durante le correzioni...

Guby perché è stato una piacevole sorpresa e per avermi allietato alcuni momenti bui...

Clè perché mi ha aiutato nel lavoro e mi ha tenuto compagnia stando ai miei stupidi scherzi e battute...

ClaCla per la compagnia in aeroporto...

La AS906YZ... Grazie dei 145000 Km e della protezione... E scusa per l'ingloriosa fine il 17/08/2007...

Emily... E alcune persone care che no ci sono più...

Abstract

Gene therapy is an approach to treating diseases in which an exogenous gene is introduced to correct for a defective or missing protein or to affect a biochemical pathway. Few successes have been reported in humans (0), as several technical issues limit its broader application.

One question is how to deliver DNA to the appropriate cells. Nature provides one solution in the form of viruses, which are in essence protected gene delivery packages with native ability to introduce their genomes into cells.

Once the desired gene is delivered to target cells, another issue that arises is the fate of the DNA.

Some strategies rely on long-term expression from extra-chromosomal DNA, but there are cases, such as dividing cells, where it would be highly beneficial to permanently insert the gene into chromosomes.

Certain viral genomes can be integrated into host DNA by non-homologous recombination or, in the case of retroviruses, by virally encoded integrases. While integration seems to be not dependent on target sequence, *in vivo*, retroviruses, such as HIV and murine leukemia virus, integrate preferentially into active genes (1, 2), introducing the possibility of insertional mutagenesis.

The theoretical danger inherent in retrovirus-based gene therapy has been concretely demonstrated in a recent clinical trial in which the modified retrovirus integrated into the *LMO2* locus, causing leukemia in three of the patients (4).

A powerful system to circumvent this critical issue could be to develop a system to site-specific integrate the exogenous gene into a safety zone into the genome.

To date, only one animal virus, the adenoassociated virus (AAV), has been identified that integrates its genome into a particular location into human chromosomal DNA. When cells are infected in the absence of helper virus, AAV establishes a latent infection in which the

AAV genome integrates into a locus known as AAVS1 on the q arm of chromosome 19 (4). Recombinant AAV (rAAV) vectors too have a series of limitations as gene therapy vectors: they can accommodate only small genes and moreover eliminating most of wild-type AAV (wt AAV) sequences they have lost almost all the site-specific integration capability.

On the basis of AAV site-specific integration machinery a series of effort to re-introduce wt AAV's integration efficiency have been done. Different viruses have been engineered using the AAV's integration machinery to transform them to target and integrate site-specifically large genes into the chr 19.

Development of a maximized integrating, large capacity DNA viral vector is still an unmet goal of gene transfer technology.

The initial aim of this project was to characterize the combination of the attributes of both the AAV and adenovirus (Ad) gene therapy vectors to develop an Ad/AAV hybrid virus system able to target site-specifically a large fragment of DNA into the host cell genome.

In executing our experimental strategy, we found that, in addition to the known incompatibility of Rep expression and Ad growth, an equally large obstacle was presented by the inefficiency of the integration event when using traditional rAAV integrating elements. The finding that traditional rAAV plasmid vectors lack integration potency compared to wt AAV plasmid constructs led recently to the discovery of an AAV integration enhancer sequence element which functions in *cis* to an AAV inverted terminal repeat-flanked target gene. This study has addressed both of these problems.

Moreover the project aimed also the capability of such vectors to target a large integrating cassette and the differences in the system integration efficiency compairing the dimension of the integrating cassettes.

We demonstrated that an Ad can be generated that expresses Rep proteins and that Rep-mediated AAV persistence can occur in the presence of Ad vectors.

We exploited the size limit capability introducing a large integrating cassette (12 kb) into the Ad/AAV vector and we obtained a good level of integration into the human genome. Specifically we succeeded in integrating it without any recombination event and in a site-specific fashion at good level.

The model we extensively tested in human cell lines was also used successfully into human primary cells where we obtained site-specific integration into human chromosome 19 as expected.

Another problem analysed was the flexibility of Ad vector system.

Adenoviral vectors maintain the cellular specificity of adenoviruses from which they derive. A good gene therapy vector should have a broad tropism to ensure a good transduction efficiency, and moreover should be able to transduce cells of interest, such as $CD34^+$ cells and other primary cells.

We tried to expand Ad tropism engineering the commonly used Ad 5 vector (not able to transduce very well $CD34^+$ and hematopoietic cells), transforming it to an Ad 5/35 modified vector. This approach permitted us to have better $CD34^+$ cell transduction and a very good efficiency with hematopoietic cell lines.

List of contents

Abbreviations used in this thesis (unless otherwise stated in the text).

kb	kilobases
bp	base pairs
RNA	Ribonucleic Acid
DNA	Deoxyribonucleic acid
IL-#	Interleukin- # = number
ITR	Inverted Terminal Repeat
SCF	Stem Cell Factor
TPO	Trombopoietin
PCR	Polimerase Chain Reaction
kDa	KiloDalton
HD	Helper Dependent
AAV	Adenoassociated Virus
Ad	Adenovirus
Dox	Doxicyclin
O.D.	Optical Density
L.B	Luria Bertani
T.B	Terrific Broth
S.O.C	Super Optimal Catabolite repression
TU	Transducing Unit
MOI	Multiplicity Of Infection

rAAV	recombinant Adeno Associated Virus
wt	wild type

Chapter 1

Introduction

1.1 Gene therapy: an overview.

Gene transfer in somatic cells has without any doubt a big potential to treat a number of genetic and acquired diseases. Among the several delivery systems developed for gene therapy purposes, viral vectors derived from retroviruses, moreover murine retroviruses, are the most widely used.

Retroviruses are distinguished from other viruses by two characteristic steps in their life cycle: reverse transcription, resulting in a double strand DNA copy of the viral RNA genome, and integration, leading to the covalent attachment of the viral DNA to host cell DNA.

Integration process is an unequalled, and often indispensable tool to obtain high efficiency and stable gene transfer.

Up to now retroviral and lentiviral vectors are the only available tools to integrate foreign genes into human cells at reasonable efficiency. However their use involves some important problems and limitations:

1. Retroviral vectors (both gammaretroviral and lentiviral) can generally integrate only transgenes with a size limit of 5-7 kb.
2. Independent regulation of multiple transcription units is difficult in a retroviral vector context.
3. Integration of retroviral vectors into the target cell genome occurs randomly, preferentially into active genes. In the last years to this phenomenon has been associated an important risk of insertional mutagenesis and oncogenesis due to the deregulation of gene/s near the genomic region in which the provirus integrates (0, 1 , 2, 3).

Alternative to retroviruses are present but at the moment not well studied and developed.

1.2 Adeno-Associated Viruses.

Adeno-Associated viruses (AAV), a single-stranded DNA virus of the family *Parvoviridae*, genus *Dependovirus*, is among the smallest known viruses. The serotype 2 virus (AAV-2) has a genome of 4,680 bases contained in an icosahedral capsid of ≈24 nm (20) (Fig. 1.1).

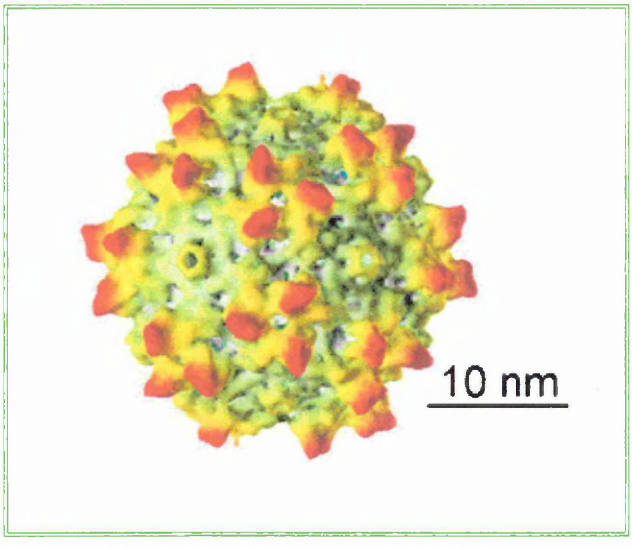

Fig. 1.1 Schematic representation of an AAV particle.

The defining characteristic of this class of viruses is their dependence on co-infection with a helper virus (or certain perturbed cellular states) to provide the functions necessary for productive infection (21).

Although virus infection appears to be widespread, with over 80% of humans testing seropositive, AAV causes no known pathology (21). The infectivity, moderate immunogenicity, and apparent lack of pathogenicity have made AAV a promising candidate as a vector for human gene therapy (22).

Recently, random integration and subsequent activation of cellular genes have created safety concerns about retrovirus vectors (23), and recombinant AAV vectors have also been shown to disrupt cellular genes (24, 25). Randomly integrating recombinant AAV vectors are severely compromised in integration efficiency (26) and site-specific

integration, as mediated by wt AAV, may have both safety and efficiency advantages in certain gene therapy applications.

AAV is unique among animal viruses in that its latent state involves insertion into the host genome at a preferred site (4, 5). This site, referred to as AAVS1, is found at chromosome 19q13.4qter and has been mapped to the first exon of myosin binding subunit 85 of protein phosphatase 1 (28) (Fig. 1.2).

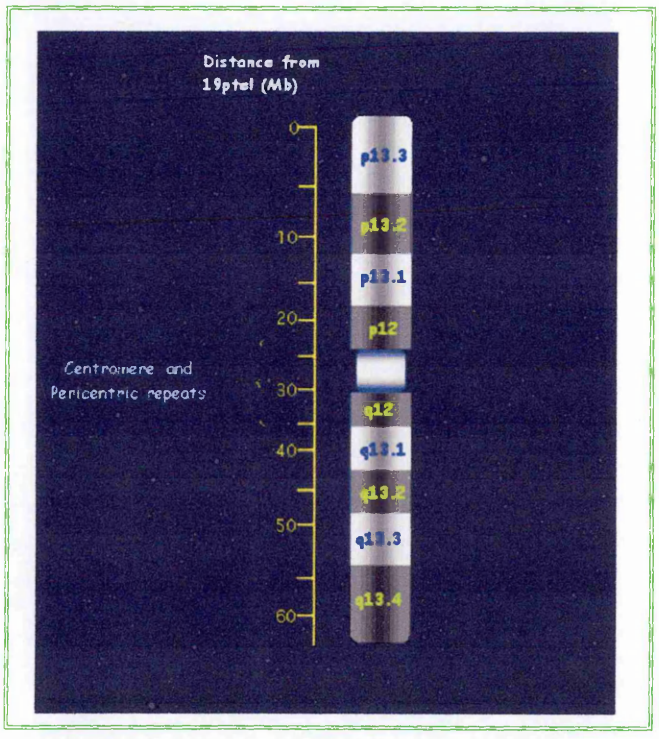

Fig. 1.2 Schematic representation of human chromosome 19. AAVS1 locus is located in chromosome 19q13.4qter.

Integration has been associated with gross disruptions in the AAVS1 locus, including both duplications and deletions (29). Disruption of a nearby gene has also been reported in only one case (30).

1.2.1 Viral DNA.

The viral DNA contains two open reading frames (ORFs), *rep* and *cap*, encoding the regulatory (Rep78, Rep68, Rep52, and Rep40) and structural (VP1, VP2, and VP3) proteins, respectively (Fig. 1.3).

The genome is flanked by two inverted terminal repeats (ITRs) (31). The ITRs are 145 nucleotides including the D element and are considered to be the only *cis* elements required for replication and site-specific integration of the AAV genome.

In addition to the ITR elements, the *rep* gene is necessary in *trans* to target the integration event to the AAVS1 site (19, 16, 14). The *rep* ORF encodes four non-structural proteins: Rep40, Rep52, Rep68, and Rep78, which are involved in the replication of the AAV genome (20). Rep68 and Rep78 are gene products of alternatively spliced mRNA transcribed from the AAV p5 promoter. A structural difference between Rep78 and Rep68 is that Rep78 possesses a zinc finger-like motif at its carboxyl terminus.

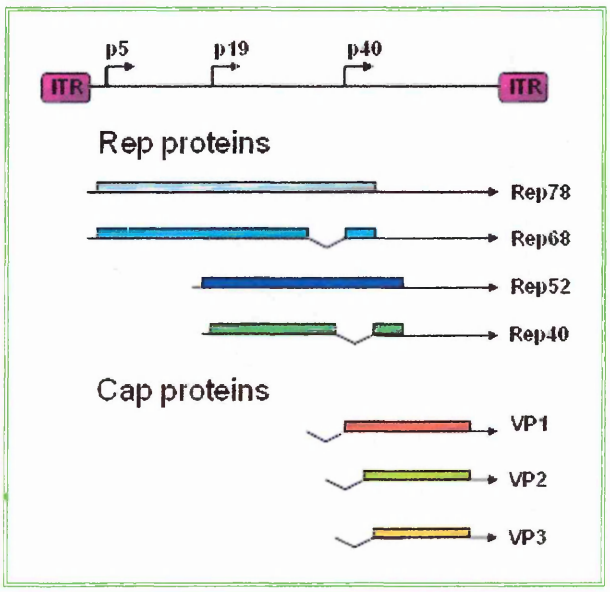

Fig. 1.3 Schematic representation of AAV genome structure and transcripts. Rep68 is the spliced form of Rep78 generated from the p5 promoter. Rep40 is the spliced form of Rep52 generated from the p19 promoter. The structural proteins (VP1, 2 and 3) are under the control of p40 promoter.

Both Rep proteins share essentially the same functions: strand-specific DNA binding (6), site-specific nicking and ATP-dependent helicase activity (7). Either Rep protein alone is sufficient for replication of the AAV genome (32) and for AAVS1-specific integration (14). The multifunctional Rep proteins inhibit cellular transformation by heterologous genes (33) and suppress heterologous promoters, including the c-*fos*, c-*myc*, H-*ras* and LTR of human immunodeficiency virus type 1 (HIV-1) (34, 35, 36). The Rep proteins also

modulate cell cycle-regulating proteins (37). These results indicate that over-expression of Rep proteins has negative effects on cells and is, on occasion, lethal to cells.

1.2.2 AAV-2 DNA replication.

The current model for AAV-2 DNA replication predicts that viral DNA replicates by a self-priming displacement mechanism that is initiated from the ITR and requires cellular polymerases, helper virus-derived factors and AAV-2 Rep proteins (38, 39). In particular, two AAV-2 regulatory proteins, Rep78 and Rep68, are essential for the replication process. Transcription from the p19 promoter generates Rep52 and Rep40 (Fig. 1.3); Rep52 is known to have helicase and ATPase activities but not DNA binding or endonuclease activity (16). Rep68 and Rep78 down-regulate the p5 and p19 promoters (40), and this stringent control of Rep expression helps to minimize cell death caused by the cytotoxicity of the Rep proteins (41).

Although the precise molecular mechanisms of AAV site-specific integration are not well understood, it appears that Rep68 or Rep78 are critical. They were shown to bind the ITRs at a specific site, called the Rep binding site (RBS), and to cleave it at the terminal resolution site (*trs*) between two thymidine residues (34, 42, 43). This process is essential for the completion of the synthesis of a double-stranded monomer form, which is then used as the template for the reinitiation of DNA synthesis (38). Through poorly understood interactions, the Rep protein/AAV-DNA complex localizes to AAVS1 site, and a non-homologous deletion-insertion recombination event occurs, resulting in integration of the AAV genome (44, 45). The endonuclease activity of the two larger Rep proteins allows them to nick at the *trs*, which is positioned 8 or 11 bp away from the Rep Binding Elements (RBEs) in AAV and AAVS1 respectively. There then follows an interaction between Rep molecules that are bound to the AAV genome and those that are bound to the AAVS1 site, a non homologous recombination event occurs, resulting in integration of the AAV genome (45). It has been shown previously that head-to-tail concatamers of the wt

AAV genome are able to site-specifically integrate in this manner (29). Preferred AAV recombination junction sites have been localized to both left and right AAV ITR elements as well as the p5-*rep* promoter region of the AAV genome (26, 47). Different studies have demonstrated that efficient nicking at the *trs* required, besides the Rep-binding site, the contact of Rep with a five-base sequence called RBE', present at the tip of one of the ITR arms (48, 49, 50). In addition, the sequence surrounding the *trs* was shown to be important for the formation of a stem-loop structure that exposed the *trs* on the single-stranded loop (51). Recent crystallographic data have confirmed that the N-terminal domain of Rep interacted with RBE' and suggested that this interaction was implicated in the orientation of the Rep molecules bound at the ITR as well as in the stimulation of the extrusion of the *trs* by the Rep helicase activity. Two of these elements, the RBS and the *trs*, are also present within the chromosome 19 AAVS1 locus, where wild-type AAV-2 was shown to site-specifically integrate (45, 5).

1.2.3 The role of Rep.

AAV vectors lacking the *rep* gene fail to integrate into AAVS1, showing an apparent random integration into the host chromosomal DNA (51). A non-viral plasmid-based system capable of integrating a transgene specifically into AAVS1 has been described; this was achieved by transferring the transgene flanked by the ITRs with transient expression of Rep78 or Rep68 (19, 16, 14). Thus, this system is potentially safer than integrating retrovirus and AAV vectors. A strategy utilizing two plasmids, one harbouring the transgene cassette between the ITR sequences and the other for Rep expression, allows only the transgene plasmid to integrate into the AAVS1 locus (14). This method successfully introduced the transgene into AAVS1 in haematopoietic K562 cells (53).

The frequency of AAVS1-specific integration by the plasmid-based methods has differed among studies.

Shelling & Smith (18) reported that 9 of 12 cell clones (75%) obtained by transfecting HeLa or 293 cells with an AAV vector plasmid on which the Neo gene was placed under the control of the p40 promoter, the original promoter for Cap proteins, had rearranged AAVS1 and mentioned that approximately 50% of the rearranged bands also hybridized to an AAV probe.

Another strategy using one plasmid on which both a Rep cassette and an ITR-flanked transgene cassette were placed has targeted the transgene to AAVS1 in 6 of 21 (29%) 293 cell clones (19). Similar methods applied to other cell lines, HeLa and Huh-7 cells, have been able to insert the transgene to AAVS1 in up to 20% of clones (16).

All the studies mentioned used a one plasmid system and the p5 promoter for Rep expression.

These results indicated that a high-level expression of the Rep proteins increased the frequency of AAVS1 rearrangement and rather decreased the frequency of AAVS1-specific integration of the transgene.

1.2.4 AAV nuclear transport.

Helper virus has been shown to potentially influence the biology of AAV by facilitating virus transport to the nucleus (54) and by enhancing conversion of the single-stranded AAV genome into a transcriptionally active duplex DNA substrate.

In the absence of helper virus, AAV is dependent on interaction with the cell for internalization and genome transport to the nucleus.

What are the steps that lead to AAV integration into AAVS1?

Studies in dividing cells demonstrate that AAV uptake is efficient, and virions localize to the perinuclear region within two hours post-internalization (54).

The efficiency of capsid uncoating and transport of viral DNA to the nucleus is a potential rate-limiting step that may be influenced by viral MOI. The model presented in Fig. 1.4 indicates a proposed sequence of events that occur during the process of AAV integration.

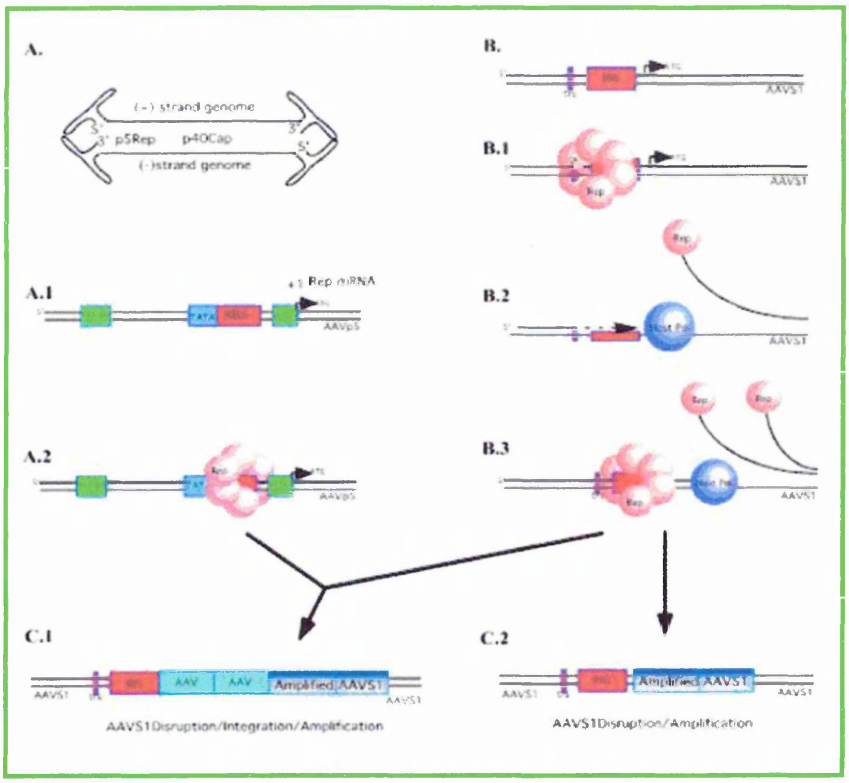

Fig. 1.4 Proposed model for Rep-mediated AAVS1 disruption and AAV site-specific integration. (A) Representation of the AAV genome with the inverted terminal repeats hairpinned. (A.1), minimum p5 integration element including Rep binding sites (RBS), the transcription factor YY1, and the TATA box. (B) Representation of AAVS1, including the RBS and the nicking site for Rep endonuclease activity (*trs*). Panels (B.1) to (B.3) diagram Rep binding and replication initiated with host polymerase. Note that Rep is covalently attached to the 5′ end of the nick site. Rep may reinitiate this process several times, perhaps accounting for amplification of AAVS1 (C.2). For integration to occur, a Rep-mediated recombination event between AAVS1 (B.3) and p5 (A.2) results in AAV sequence in the disrupted chromosome 19 locus (C.1). J Virol. 2004 August; 78(15): 7874–7882.

Following localization to the nucleus, cellular replication and/or DNA repair mechanisms are essential for second-strand synthesis of the AAV genome. Alternatively, in the absence of efficient second-strand synthesis, a second pathway for production of transcriptionally active duplex AAV genome would be through plus- and minus-strand hybridization.

Subsequent to the formation of duplex genome production, the p5 promoter is activated to transcribe Rep (Fig. 1.4). Transcription from the p5 promoter and translation of Rep mRNA yield the multifunctional Rep proteins (the focus will be on Rep68 and 78 because they are able to mediate integration in the absence of the smaller Rep proteins) (20).

Production of the duplex genome is a necessary prerequisite for p5 transcription of the *rep* gene and is a likely substrate target DNA for integration, as duplex plasmid DNA integrates with high efficiency. It is not possible to distinguish between duplex formation or Rep expression levels as a specific rate-limiting entity.

A limitation may simply be template copy number at low MOI. In a latent infection, Rep expression levels are presumably very low. Following Rep protein expression, there are three biologically active target DNAs that Rep can bind relevant to integration:

- Rep binds to the AAVS1 site on chromosome 19;
- Rep binds to the p5 Rep binding site of AAV;
- Rep binds to the inverted terminal repeat Rep binding site.

Data obtained through transfection of plasmid DNA corroborate previous studies which show that the inverted terminal repeat elements are not required for efficient integration; therefore, the role of the inverted terminal repeats is essential for maintaining the fidelity of the integrating genome and for rescue from latency but not as playing a role in mediating a Rep-dependent integration event.

Integration efficiency is defined by Rep interaction with the AAVS1 site (Fig. 1.4) and by Rep interaction with the p5 promoter (Fig. 1.4). Rep functions as a hexameric complex, but this has not been confirmed to be the complex that is acting on the AAVS1 site or on p5. Rep expression in the absence of helper virus or in the absence of integration substrate mediates a rearrangement of the AAVS1 site. The AAVS1 site rearrangements are consistent with a local amplification event (Fig. 1.4). When an integration substrate (Fig. 1.4) is present in sufficient quantities, localization of the p5 promoter (p5IEE) integration substrate to the AAVS1 integration site takes place, and integration occurs through what is predicted to be a strand switch mechanism or perhaps ligation between cellular and viral DNA mediated by Rep (55).

One important level of autonomous regulation of AAV integration is through regulation of Rep expression. Rep binding to the p5IEE has been shown to bring about a stringent block

to Rep transcription (40). The repression of *rep* transcription therefore implies that there is a narrow window of opportunity for Rep-mediated site-specific integration to occur. Consistent with this hypothesis, Huser et al. demonstrated that maximal integration of AAV into chromosome 19 occurs within the first 4 days post-infection. Studies by Giraud et al. demonstrated that targeting to plasmid-based AAVS1 targets occurred by 24 hours post-infection (56).

Because increasing the dose of virus does not yield an increase in the occurrence of integrants, it is possible to argue that there is an inherent limit to the number of discernible recombination events that can occur when a cell is infected, regardless of the number of available integration substrate targets. In this model, activation of AAVS1 establishes the kinetics of integration. Presentation of an integration substrate during the time of AAVS1 rearrangement creates the opportunity for a copy choice mechanism to integrate the AAV substrate DNA.

1.3 ITR-Rep mediated integration.

In current AAV-based transgene systems, *rep* is deleted since the small viral capsid does not have space for an exogenous gene; retaining *rep* would result in a genome too large to be packaged (17). Thus, *rep*$^{-}$ AAV-based vectors, which retain other inherent advantages of AAV, either do not integrate or integrate inefficiently in a nontargeted manner, a process that has been reported to occur preferentially into active genes (25). Promising alternatives are hybrid vectors that combine AAV ITRs and *rep* with a second virus with larger transgene capacity, such as adenovirus (57), herpes simplex virus (58), or baculovirus (59).

1.3.1 Rep acts on AAV ITRs.

The varied activities of Rep are needed for reactions on unique DNA structures known as inverted terminal repeats (ITRs) found at the ends of the single-stranded viral genome that serve as the viral origins of replication (Fig.1.5).

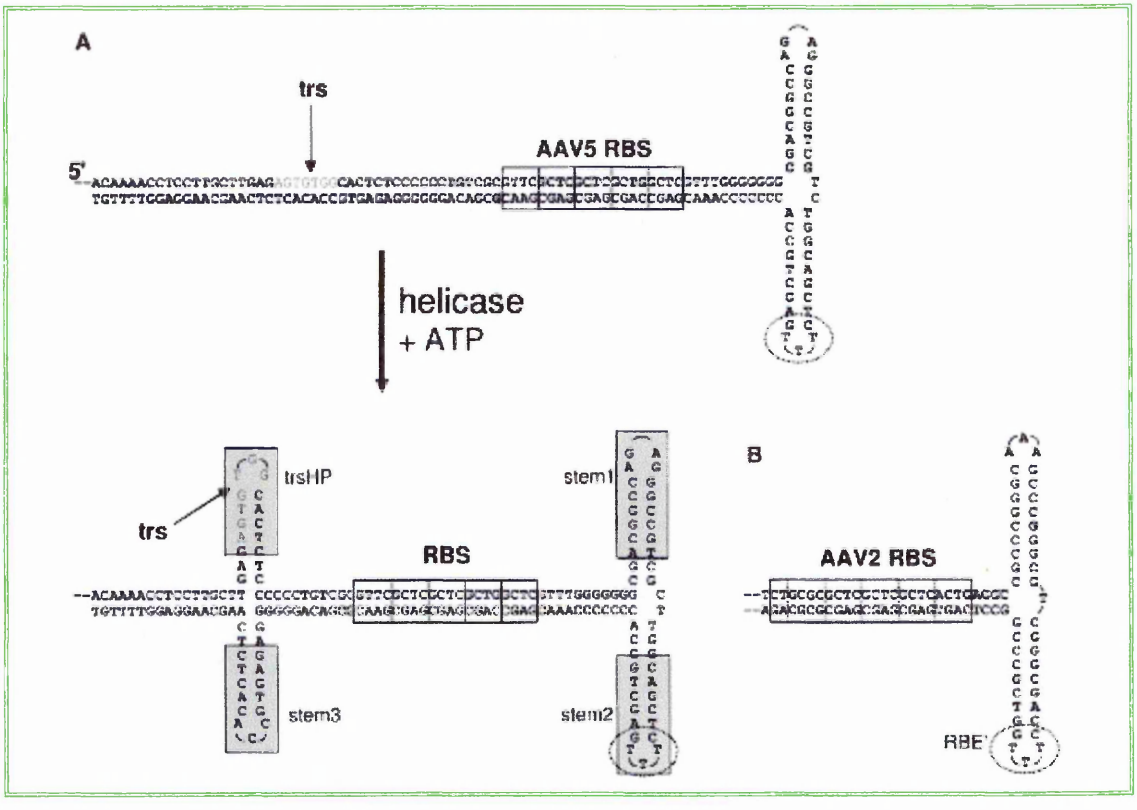

Fig. 1.5 Sequence and Folded Structure of the AAV Inverted Terminal Repeat. (A) One arm of the AAV-5 ITR contains the terminal resolution site (*trs*), at which Rep introduces a strand- and sequence-specific nick, and the Rep binding site (RBS), which contains a series of tetranucleotide repeats (shown in boxes; Chiorini et al., 1999). The other two arms of the three-way DNA junction consist of short hairpins. The helicase activity of Rep generates an alternate structure around the *trs* in which the cleavage site is single stranded. The four shaded boxes correspond to stem loops tested for Rep binding. (B) Sequence of the AAV-2 ITR. The box indicates the 22 bp binding element identified by Ryan et al. (1996); dotted lines demark tetranucleotide repeats. The circled tip of one of the hairpin arms is designated RBE′ (Brister and Muzyczka, 2000). Molecular Cell Volume 13, Issue 3 , 13 February 2004, Pages 403-414

Each ITR contains interrupted palindromic sequences that allow the formation of a three-way DNA junction with two short (~9 bp) hairpin arms. Within the ITRs are two sequences required for replication: a *Rep binding site* (RBS) consisting of several direct repeats of a 5′-GCTC-3′ motif and a *terminal resolution site*, *trs*. Viral replication requires Rep binding at the RBS and subsequent cleavage of the top strand at the *trs* to generate the

3′-OH group so that the viral ends can be converted into linear duplex DNA. Cleavage at the *trs* is strongly stimulated by the presence in *cis* of one of the ITR hairpin arms (49, 50, 51), an effect attributed to a five base sequence known as the RBE′, a *R*ep *b*inding *e*lement, at the tip of the hairpin. The endonuclease domain recognizes its *trs* substrate in the context of ssDNA or a stem loop generated by the Rep helicase activity (7, 42). Two of the important DNA sequences within the ITR, the RBS and the *trs*, also occur at AAVS1, suggesting that the same Rep-mediated DNA recognition and cleavage occur during integration. The 33 bp region within AAVS1 that encompass these two sequences are necessary and sufficient for targeted integration.

Methylation interference experiments and DNaseI protection assays indicate that AAV-2 Rep preferentially contacts one of the two hairpin arms of the ITR and that this arm corresponds to the one furthest away from the *trs*, whether the ITR is in the flip or the flop orientation (6). Ryan et al. (49) showed that five bases, 5′-CTTTG-3′, at the tip of one of the hairpin arms particularly contribute to Rep binding. The low efficiency of *trs* cleavage on linear duplex substrates compared to that on substrates with intact ITRs is unaffected by the addition of the hairpin arms in *trans*, suggesting that the Rep/RBE′ interaction stimulates cleavage by imposing a geometric constraint on Rep assembled on the RBS. It is possible that this stimulation is indirect and that the Rep/RBE′ interaction is important primarily to generate a single-stranded substrate rather than to stimulate the chemical steps of DNA cleavage (51). This is consistent with the idea that this structure, which shows that stem-loop binding does not induce any conformational changes at the enzyme active site.

The fine tuning of the cleavage activity by the RBE′ plays an important role in Rep's ability to discriminate between fully replicated dsDNA viral genomes, which still possess RBS and *trs* sequences, and genomes whose terminal hairpin arms identify them as unreplicated. Nevertheless, the Rep/RBE′ interaction must be modulatory rather than essential; otherwise, Rep would not be able to cleave the *trs* sequence present at the chromosomal AAVS1 site and the virus would be unable to integrate.

1.4 Rearrangement of the AAVS1 site.

'Abortive' integration into AAVS1, i.e. rearrangement of AAVS1 without foreign gene insertion, has been described in 293 or HeLa cells (19 18, 14). A similar disruption of AAVS1 has been detected in cell lines latently infected with wild-type AAV (4). This phenomenon may be explained in three ways.

First, the integrated transgene or AAV genome is disrupted during or after an integration event such that Southern blot analysis cannot detect it.

Second, recombination between the AAVS1 region and other sites may cause rearrangement of AAVS1 without integration of the transgene at AAVS1.

Third, the Rep protein may excise the integrated plasmid DNA or AAV genome, resulting in the loss of the pre-integrated sequences.

Lamartina *et al.* (15) reported no apparent difference between Rep78 and Rep68 in the ability to deliver foreign DNA to AAVS1 in HeLa cells. Some other studies have reported the functional differences between Rep78 and Rep68. Rep68 seems to be efficient in processing dimers to monomer duplex DNA and possesses a stronger nicking activity (39), while the helicase activity of Rep78 is stronger.

The differential effects of Rep78 and Rep68 on the p5, p19 and p40 promoters were described (61). In addition, Rep78 inhibits CREB-dependent transcription by interacting with protein kinase (62, 63). None of these findings explains why Rep78 appears to cause more abortive integration. Rep68 may be more suitable for the AAVS1-targeted integration system. To confirm the usefulness of Rep68 in the AAVS1-targeted integration system, further analysis of a larger population of cell clones would be required. Also, the exact functions of the Rep protein in AAVS1-specific integration should be elucidated.

1.5 The role of Rep Binding Elements (RBE) in Rep mediated integration.

The number of RBE sequences in the human genome, how Rep discriminates between these and the ch-19 target locus RBE sequence, and how Rep interacts with all sites and still facilitates targeted integration within a fixed time frame become of significant importance. Using a filter-binding assay and a highly purified source of Rep68 protein, it was established that genomic DNA will compete efficiently against a ch-19 target sequence. In this assay, a minimum Rep binding site of 8-bp in the context of large DNA fragments demonstrated competition, suggesting that as many as 200,000 potential binding sites may exist in the human genome.

Filter-binding analysis of genomic DNA successfully retained ch-19 target sequences, as well as a cellular RBE identified by BLAST analysis (69), corroborating the competition results.

Electron microscopy (EM) analysis was utilized to distinguish possible differences between Rep protein DNA interaction with ch-19 RBE compared to a minimum 8-bp RBE sequence. Identical multimeric Rep protein DNA complexes, which spanned about 60 bp, assembled on ch-19 target DNA, as well as a minimum RBE site, were observed, but never on heterologous DNA lacking these sequences.

Analysis of Rep expression in non-virus-infected cells demonstrated DNA rearrangement of the ch-19 target sequence, suggesting that this locus is a hot spot for Rep-induced DNA amplification and rearrangement that most likely influences AAV targeted integration.

Although higher affinity for ch-19 RBE sequences (2.7-fold) than for heterologous DNA carrying identical elements using this assay, the difference appears to be insufficient to explain AAV targeting. In fact, these experimental conditions didn't identify any features that would make the ch-19 locus a preferred site for Rep binding.

For example, EM analysis of Rep-DNA complexes demonstrated highly uniform multimeric complexes on both ch-19 and non-ch-19 RBE sequences. These protein structures covered about 60 bp of DNA and appeared to be indistinguishable for ch-19, non-ch-19, and AAV ITR RBE sites. Rep binding to control DNA was never observed with substrates lacking the RBE site.

These results imply that Rep may interact with numerous RBE sites distributed across the human genome as part of the integration mechanism.

Rep levels in a latent infection. The amount of Rep in a latent infection could be considered as a rate-limiting step for AAV site-specific integration. For this reason, the amount of Rep expressed in the first 24 hours of a non-lytic infection was determined. Analysis suggested that 1 to 4,000 copies of Rep78 and Rep68 are available for facilitating targeted integration. At present, the rate association constant for Rep and cellular RBE sites have not been determined. Other DNA-binding proteins (e.g., *Drosophila* doublesex and Lambda Cro) typically have rate association constants on the order of 10^6 (71) and 10^8 (72), respectively. Extrapolating from other known DNA association constants and the time observed for AAV integration (24 hours) (73), this would suggest that the level of Rep78 and Rep68 present in a non-productive infection (1 to 4,000 molecules) should be sufficient to interact with all 200,000 potential RBE sites. Even if Rep is inefficient at binding, it is important to note that, *in vivo*, it is unlikely that all 200,000 sites are accessible to Rep binding due to their chromatin structure. In fact, a recent study has shown that the ch-19 site is DNase hypersensitive (74), implying a chromatin structure that is accessible for protein interactions. This observation implies that ch-19 is always available for Rep interaction, whereas other sites may be subject to local chromatin environment during the cell cycle. These factors strengthen the notion that 1,000 to 4,000 molecules of Rep could be sufficient for targeting the viral genome in the absence of any other features.

Rep protein complexes. Characterization of purified Rep-DNA complexes by EM analysis represented the first visual identification of a multimeric-protein complex interacting with the Rep binding site. The fact that Rep complexes were multimeric is not surprising since it has been reported that Rep forms multiple protein-DNA complexes and may potentially bind as a hexamer (60). The observation that Rep can span a region of DNA of about 60 bp, however, does provide an explanation as to why Rep does not bind efficiently to small oligonucleotides. It is possible that the RBE DNA induces multimerization of the Rep protein since the Rep protein concentration used in the EM experiments (16nM) was significantly lower than that for Rep when it exists as a monomer in solution (380nM or 25ng/μl). It is interesting to note that previous studies have suggested Rep-Rep interactions when there is binding to the DNA RBE motif. Observations clearly establish that Rep complexes interacting with either AAV ITR, ch-19 RBE, or minimum RBE element derived from plasmid DNA form identical protein structures (Fig. 1.6).

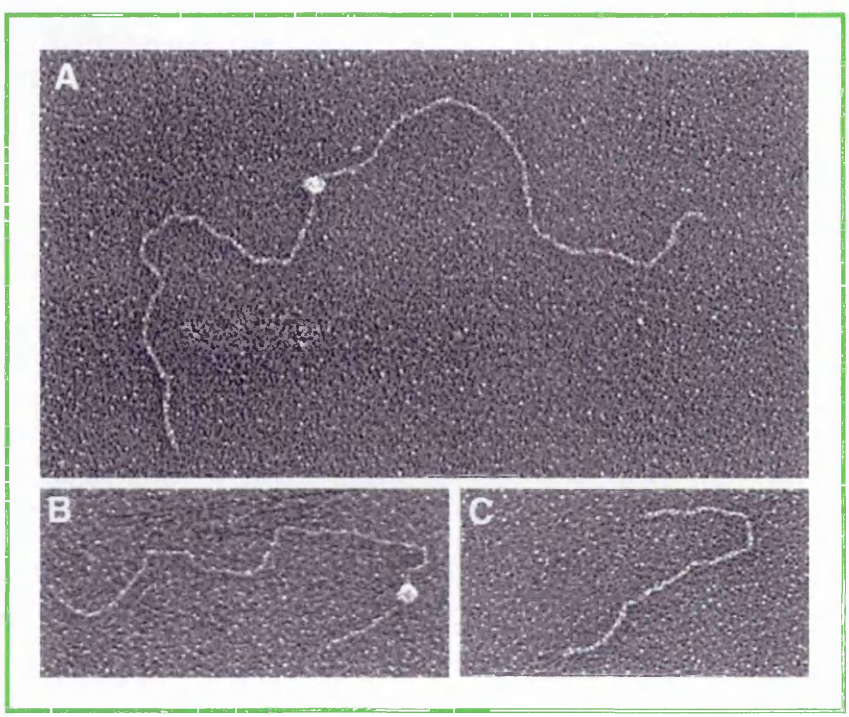

Fig. 1.6 EM analysis of Rep-DNA complexes at protein/DNA mass ratios of 1:1. (A) Rep68H6 protein bound to the center RBE of the 2.7 kb ch-19 integration fragment. (B) Rep68H6 protein bound to the asymmetric RBE of the 1.7 kb DNA fragment. (C) A 953-bp DNA fragment devoid of any RBE sequence and to which Rep68H6 did not bind. J Virol. 2000 May; 74(9): 3953–3966.

The presence of a strong RBE increases the local concentration of Rep enough to allow interaction with low-affinity sites on the same DNA strand. This may be a factor that is important in vivo, where competition for Rep (RBE sites) and the initiation for site-specific recombination may be influenced by the local concentration of Rep molecules (Rep-Rep interactions). Regardless, as previously indicated by gel shift assays, EM analysis also revealed a higher affinity of Rep for the ITR when it was compared to either ch-19 or analogous RBE sequences. Based on this observation it was hypothesized that Rep levels in a newly infected cell will allow constant occupation of the AAV ITR sequences compared to transient binding to cellular RBE elements other than ch-19. This would imply that a preformed AAV ITR-Rep complex is a separate substrate that may interact with chromosomal RBE sites or chromosomal Rep-RBE complexes. If the ITR-Rep complex interacts with a Rep-chromosome complex as a separate entity, then the formation of the appropriate Rep-chromosome RBE complex would become the rate-limiting determinant for targeted recombination.

Cellular factors. All of binding analyses were performed with purified Rep only. Recent evidence has demonstrated a role for high-mobility group (HMG) proteins in NS1 nicking of the MVM genome (75). This protein has also enhanced Rep binding and nicking activity on the AAV ITR and has enhanced in vitro targeting of AAV substrates (76). HMG proteins have been implicated in bending DNA and making it more flexible (79). Therefore, observations with purified Rep would likely be enhanced in the presence of HMG. Cellular proteins could clearly impact the efficiency of Rep-mediated integration.

Rep-dependent ch-19 replication. The ability to amplify ch-19 in the absence of viral integration substrates strongly suggest that Rep-mediated replication is a primary step for AAV targeting. These observations support studies by Urcelay et al. (46) that described an *in vitro* Rep-dependent replication of ch-19 DNA carrying the RBE-*trs* site. From these observations, it appears that a critical step in the AAV integration process involves Rep-dependent nicking of the ch-19 substrate. Cellular amplification in the absence of viral

targeting sequences, suggesting that Rep initiates a replication event on ch-19 that results in amplification and rearrangement. These observations also suggest the possibility that the head-to-tail configuration of viral integrants appears as a by-product of this replication event. Proviral structures for AAV vectors devoided of Rep result in identical head-to-tail concatemers, albeit at random sites in the genome (4, 73). In addition, recent analysis of simian virus 40 integration has documented identical head-to-tail proviral structures, implying that this may be an universal cellular mechanism for "amplified" integration (77). These data imply that host machinery is responsible for the head-to-tail amplification and that the role of Rep is to direct the recombination event through initiation of replication on a virus-like origin (RBE-*trs*) located on ch-19. These observations also provide an explanation as to why latent proviral structures (head to tail) generated by host enzymes do not resemble the Rep-dependent viral replication intermediates (head to head) seen in a lytic infection. EM data suggest that the Rep complex may be associated with the viral Terminal Repeats (TR) sequences prior to initiating replication on ch-19.

It is still undetermined whether the viral Rep-TR complex requires nicking in order to recombine with the ch-19 target sequence. While rescue of proviral AAV genomes requires functional terminal repeats for replication and packaging, the precise role in integration is still undefined. These data suggest that if Rep independently forms a complex on ch-19 and initiates replication, this may be a hot spot for Rep-Rep DNA complexes to assemble, in a manner similar to that of the punctate replication centers described by Hunter et al. (55), for wt AAV lytic infection.

At present, 1% of AAV infecting viral genomes integrate with approximately 70 to 90% of these proviruses targeted to ch-19 (78). Though this is an efficient reaction for targeting, the overall integration frequency is marginal at best. Five successive steps can be identified that would impact AAV targeted integration after infection:

- Conversion of single-stranded to double-stranded DNA, providing a template competent for mRNA expression;

- Expression of Rep proteins;
- Rep interaction and complex formation with viral ITR and/or chromosomal RBEs;
- Rep-dependent replication of the ch-19 locus;
- Rep-ITR complexes interacting with Rep–ch-19 replicated substrates, facilitating targeted recombination and resulting in head-to-tail proviral structures via host enzymes.

1.6 The role of the nicking sites (*trs*) recognition in Rep mediated integration.

Multiple evidence suggests that both binding and nicking of *AAVS1* by Rep68/78 are required for preferential integration (46, 69). This has led to the current hypothesis that *AAVS1* is the preferred integration locus for AAV-2 because it contains the best Rep68/78 nicking site within the human genome.

Analysis of the *trs* region has been problematic because nicking site recognition appears to require that the DNA strands be separated in the region of the *trs* (9, 55 42). Rep68/78 have two nucleoside triphosphate-dependent DNA helicase activities.

One helicase activity is non specific with regard to DNA sequence but requires a 3′ single-stranded tail (7, 50).

The second activity can unwind a blunt-ended fragment but requires an RBS.

The current model for nicking suggests that Rep68/78 first binds at the RBS and begins to separate bi-directionally the two strands (9, 42). Once the region of the *trs* is separated from its complementary strand, the *trs*-containing strand is hypothesized to fold into a stable secondary structure. Rep68 or Rep78 can then nick at a site that it recognizes by a combination of its base sequence and its secondary structural context (55). A putative

stem-loop structure has been identified in the region of the *trs* for AAV serotypes 1 through 6. Fig. 1.7 shows that a 5- to 7-bp stem could be formed by standard Watson-Crick base pairing (i.e. A-T and G-C) (69). Individual mutation of several of the bases within the putative stem of the AAV-2 *trs* region resulted in a reduction in the ability of the site to be nicked (69).

Comparison of the *AAVS1 trs* region with that of AAV-2 shows several regions of base identity (Fig. 1.7); the 5′-GT TGG-3′ core motif immediately flanking the *trs* (the gap represents the primary cut site), 2 of the 6 bases 5′ of the core motif, and 3 of the 11 bases 3′ of the core motif. Most of the bases believed to be involved in the AAV-2 *trs* stem structure are not conserved in *AAVS1* (46).

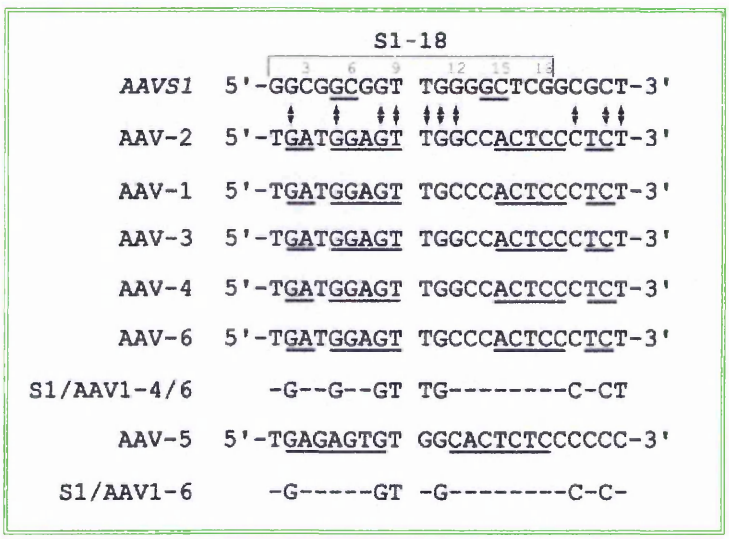

Fig. 1.7 Underlined bases have the potential to form a stem by Watson-Crick base pairing. Bases conserved between all sequences (S1/AAV1-6) and between all sequences except AAV-5 (S1/AAV1-4/6) are indicated. The double-pointed arrows indicate bases conserved between *AAVS1* and the AAV-2-ITR. The 18-base segment of *AAVS1* that is the focus of the present study (S1-18) is bracketed. Bases C3, C6, T9, G12, C15, and G18 of S1-18 are numbered. J Virol. 2005 March; 79(6): 3544–3556.

Furthermore, no stem-loop similar to those proposed for the AAV sequences could be formed in *AAVS1* by using Watson-Crick base pairing. In spite of this, previous works showed only about a twofold difference in the ability of Rep78 to nick the linear form of the AAV-2 ITR *trs*/RBS versus the *AAVS1 trs*/RBS. Maybe a stable secondary structure based, at least in part, on non-Watson-Crick base pairing, in the *AAVS1 trs* region is

present. Elements of this secondary structure may also contribute to the ability of *AAVS1* to be nicked by Rep68/78

1.7 p5 integration enhancer element.

Rep-mediated integration of recombinant AAV plasmids is extremely inefficient, with between 0,1 and 1% of transduced cells demonstrating rAAV genome persistence after 6 weeks (26). In contrast, plasmids that carry the entire AAV genome integrate at efficiencies of greater than 10%. This difference led several groups to postulate the presence within the AAV-2 genome of an additional *cis*-acting replication element, besides the ITRs, and to demonstrate its presence within the 5' portion of the *rep* gene (64).

A 350-bp sequence (previously named CARE) encompassing the p5 promoter and the 5' portion of the *rep* ORF (nucleotides 190 to 540 of wild-type AAV-2) was able to promote Rep-dependent replication of a plasmid containing the ITR-deleted *rep-cap* genome and the encapsidation of these sequences during recombinant AAV production (64). This element contained the binding sites for transcription factors such as YY1, and the major late transcription factor, a TATA box, a Rep-binding site, and a *trs*-like motif (66, 67). Binding of Rep78 and Rep68 to the p5 Rep-binding site was previously shown to mediate the transcriptional repression of the p5 promoter observed in both the absence and presence of adenovirus (68). The p5 *trs*-like motif was identified because it enabled Rep-dependent AAV-2 replication in the absence of the left ITR (67). In addition to its ability to behave as a *cis*-acting replication origin, the p5 region (nucleotides 151 to 289 of wild-type AAV-2) was recently shown to enhance Rep-mediated site-specific integration of plasmid DNA into the human chromosome 19 AAVS1 site (26, 27).

Replication assays performed in transfected cells (*in vivo*) indicated that a minimal functional p5 element was composed of a 55-bp region (nucleotides 250 to 304 of wild-

type AAV-2) containing the TATA box, the Rep-binding site, the *trs* present at the transcription initiation site (trs^{+1}), and a downstream 17-bp region that could potentially form a hairpin structure localizing the trs^{+1} at the top of the loop. Interestingly, the TATA box was seen to be absolutely required for *in vivo* but dispensable for *in vitro*, i.e. cell-free, replication. Finally, there was the demonstration that Rep binding and nicking at the trs^{+1} was enhanced in the presence of cellular TATA binding protein (TBP), and that the over-expression of this cellular factor increased the *in vivo* replication of the minimal p5 element. Together, these studies characterized the minimal AAV replication origin present within the p5 promoter region and demonstrated for the first time the involvement of the TATA box, in *cis*, and of the TBP, in *trans*, for the Rep-dependent replication of this element.

Philpot and co-workers (27) identified the p5 sequence investigating the hypothesis that an Ad vector could be adapted to utilize the integration mechanism of AAV and generate chimeric constructs that could bring closer to a system able to fulfil a long-term gene expression. An important finding emerged: traditional rAAV vectors are lacking an important integration efficiency element. In the presence of a p5-*rep* integration efficiency element, the vast majority of AAV integrants (over 90%) occurred in a site-specific manner.

Recchia and co-workers generated a helper-dependent Ad-Rep vector and tested its ability to mediate site-specific integration by co-infecting it with an Ad that contained ITR-flanked GFP and hygromycin resistance transgenes (57). In agreement with Philpott, Recchia et al. found a relatively low efficiency of persistently hygromycin-resistant cell lines (estimated at 0.3%). In their studies, a third of the selected cell lines contained GFP localized to chromosome 19, as indicated by fluorescent in situ hybridization analysis.

Using a vector containing p5-*rep* sequence (including the intact *rep* ORF) in *cis* but outside GFP-flanked ITRs, Balague and co-workers found that such a vector persisted in nine fold-more cell lines than did an equivalent plasmid without p5-*rep* sequence (19). In addition,

the p5-*rep* sequence mediated site-specific integration at a level comparable to the 12% targeted integration efficiency observed.

In another study, Pieroni et al. used similar plasmid vectors consisting of neomycin resistance and GFP transgenes between ITRs with and without p5-*rep* sequence (again expressing the full *rep* ORF) outside the ITR elements (16). Despite using antibiotic selection, they found that the p5-*rep* sequence was critical for site-specific integration of transgenes in HeLa cells. Both of these studies came to the conclusion that Rep is necessary in *trans* for targeted AAV integration. A new series of papers claim that Rep in *trans* is necessary but not sufficient for efficient site-specific integration to occur. These authors showed that co-transfection of Rep-expressing plasmids with an ITR-flanked transgene does not result in efficient integration. It seems that the Balague and Pieroni systems supplied two distinct elements, the Rep protein in *trans* and an AAV integration efficiency element in *cis*. Interestingly, based on the constructs used in their studies, the *cis* integration element can be located inside or outside the ITR-flanked transgene, indicating functional flexibility in position and orientation of the integration element.

Importantly, the results characterizing integration by the rAAV construct pGFPCap indicate that the entire *rep* ORF is not required in *cis* for efficient integration. This construct contains the dispensable *cap* sequence element but lacks the majority of the Rep coding region. The pGFPCap construct also includes 526 bp of DNA containing the entire p5 promoter, which flanks the left AAV ITR. Analysis of clonal cell lines isolated from transfections of pGFPCap with Rep supplied in *trans* pAAV/Ad showed that 5% were positive for GFP and AAVS1 disruptions. Although the level of integration was below that seen with wt AAV or pRepGFP, this is the first construct that separates the p5-*rep* promoter element from Rep expression and maintains a high level of site-specific integration. Several factors may be contributing to the reduction in integration efficiency seen with pGFPCap, including the presence of additional sequence elements or the

proximity of neighboring transcription units (CMV-*GFP*), and this is currently being investigated.

Involvement of the p5-*rep* promoter region in the wt AAV integration event has precedent. Studies by Giraud et al. (29) and Samulski et al. (5) demonstrated that junction fragments of wt AAV integrants into episomal AAVS1 plasmids or chromosomal regions occur predominantly within two AAV sequence elements, the ITRs and the p5 promoter region. More recently, Tsunoda and coworkers used HeLa cells subjected to lipofection to study junctions between the AAV plasmid and the AAVS1 site that formed during site-specific integration. Using a plasmid containing p5-*rep* and Neo^r genes flanked by AAV ITRs, they found that most junctions occurred within the p5 promoter region of the plasmid DNA. These studies suggest that the p5 promoter that contains an RBE might be a hot spot for targeted AAV integration. In addition, Tullis and Shenk (65) showed that a p5-*rep* sequence functions in *cis* to increase the efficiency of AAV replication. Finally, using an in vitro replication system Nony and co-workers recently published a study which suggested that a p5-*rep* sequence between nucleotides 190 and 540 of the wt AAV-2 genome promoted efficient replication of rAAV plasmid vectors (64, 65). Since the p5-*rep* sequence identified by Nony et al. is present in the pGFPCap and pRepGFP constructs, we propose that this *cis*-acting replication element is also functioning as an enhancer of integration.

Further studies will be required to fully understand the relationship between the newly identified enhancer element and the RBE-terminal resolution site of the ITR with respect to the mechanism of integration. It is also likely that the delicate balance of regulated *rep* gene expression that occurs during the life cycle of AAV contributes significantly to the overall efficiency of integration. Vectors that regulate Rep expression in a manner that optimizes integration and yet minimizes unwanted chromosomal disruptions are a critical area that has not been developed. Incorporating these new insights into a variety of gene transfer strategies, including the Ad-AAV chimeric strategy that initiated these studies, should

make a significant contribution toward achieving the long-term goal of site-specific integration of a therapeutic gene.

1.8 Rep Toxicity.

1.8.1 Rep can inhibit PKA and PrKx.

Viral interference is a frequent consequence following infection of an animal cell with more than one related or unrelated virus. Characterization of this interaction during influenza infection led to the discovery of the interferons and their role in viral interference (80).

Classically, viral interference can be either direct or indirect (interferon mediated).

Direct interference occurs when a viral protein or a viral-induced protein disrupts the replication of another virus.

Indirect interference takes place when a virus induces secretion of interferon and other cytokines that protect cells from subsequent infection.

While the molecular mechanisms of interferon-mediated interference are well known (81), mechanisms of direct interference have not been as extensively characterized.

Examples of direct interference include the inhibition of vaccinia (a poxvirus) and vescicular stomatitis virus (VSV) by poliovirus and vaccinia by Frog virus 3 (an iridovirus) (82, 83, 84). Recently, non-interferon-mediated interference was described in patients infected with HIV and the non-lytic virus hepatitis G (85).

A hallmark of the adeno-associated virus serotype 2 (AAV-2) life cycle is its interaction and inhibition of replication of other viruses.

AAV-2 is a dependent virus and requires the presence of a helper virus for productive replication. Helper viruses include adenovirus (Ad) (86), cytomegalovirus (87),

herpesvirus (88), EpsteinBarr virus, varicella virus (89), pseudorabies virus (90), vaccinia virus (91) and papillomavirus (92).

However, during a co-infection, AAV can inhibit both Ad and simian virus 40 (SV40) propagation (93), while expression of AAV Rep proteins is sufficient to inhibit the DNA replication of HSV (94), BPV (95), HPV (96) and HIV (97). In addition to inhibiting helper virus replication, AAV co-infection can also suppress transformation by a number of viruses and viral oncoproteins (98).

In the absence of a helper virus, AAV-2 is able to establish a latent infection by integrating in a locus specific manner on the Q arm of human chromosome 19 (4). The four related viral non-structural Rep proteins (Rep78, 68, 52 and 40) are essential for both aspects of the AAV-2 life cycle.

It was described that a stable interaction takes place between the unspliced Rep proteins, Rep78 and Rep52, and the cAMP-dependent protein kinase A (PKA) and its novel homolog PrKX (62, 63). This interaction resulted in the inhibition of PKA kinase activity. No interaction was detected with the spliced Rep proteins, Rep68 and Rep40. A biological effect of Rep78 inhibition of PKA and PrKX activity is the decreased expression of cAMP responsive genes in Rep78-transfected cells (62). The interaction between Rep78/52 and PKA was found to have a physiologically relevant dissociation constant of 320 nM (62) and additional studies using steady state kinetic analysis and mutagenesis of Rep78 demonstrated it could act as a competitive inhibitor with respect to a peptide kinase substrate (41).

In addition to its role in cellular signal transduction, the PKA pathway also has a role in viral infection. cAMP-responsive elements (CRE) regulate the expression of numerous viral genes. Recently, Ad has been shown to require cAMP-dependent protein kinase activation to facilitate its transport to the nucleus (99). In addition, the E1a, E3 and E4 promoters of Ad contain CREs and are PKA responsive (100).

Thus, like their cellular homologs, viral genes also may be affected by Rep78 inhibition of PKA and PrKX activity. It was hypothesized that during an AAV-2/Ad coinfection, Rep78 inhibition of cellular PKA and PrKX activities could result in both the down-regulation of specific Ad genes and an inhibition of Ad replication.

AAV-2 Rep78/52 proteins contain an inhibitory domain similar to that of the heat-stable PKA inhibitor PKI (101). This domain, while not directly necessary for AAV replication and packaging, is necessary for AAV-2 Rep78/52 inhibition of PKA and PrKX. Furthermore, mutated AAV-2 genomes lacking this region fail to inhibit Ad replication, suggesting that modulation of PKA activity is a mechanism by which AAV-2 interferes with helper virus replication. Finally, AAV-2's ability to inhibit Ad replication via modulation of PKA activity is necessary to preserve its replication fitness during an Ad co-infection.

1.8.2 Other causes of Rep-mediated cell death.

Apoptosis, or programmed cell death, is a highly regulated cellular suicide process. It is involved in normal tissue development as well as in the response of the cell to stress, growth factor deprivation, and DNA damage. Morphological changes typical for apoptotic cells include nuclear and cytoplasmatic condensation, which is followed by the fragmentation of the cell into apoptotic bodies. In vivo, these cell fragments are consumed by macrophages without the elicitation of an inflammatory response (102, 103). Biochemical characteristics include fragmentation of DNA, partial loss of plasma membrane asymmetry, and reduction of the mitochondrial transmembrane potential. Apoptosis can be triggered by external or cellular signals. Stimuli from both pathways are integrated and amplified by a family of cysteine proteases with aspartate specificity, referred to as caspases. Caspases are expressed as zymogens, inactive proenzymes which are proteolytically activated during the transduction of death signals. Caspases by proteolytically cleaving vital cellular proteins, are also involved in the execution of cell

death. Among the caspase targets are actin, lamins, and poly(ADP-ribose) polymerase (4, 104).

The majority of experiments analyzing the cytotoxicity of Rep78 have been done with inducible stable cell lines which either require a toxic heavy metal for induction of expression (105, 106) or have shown low-level expression (32).

The observed effects of Rep78 on cell survival and cell cycle progression in this transient system differ from the data obtained with stable Rep-inducible cell lines. Holscher et al. (32) described a stable HeLa cell line expressing Rep under the control of the glucocorticoid-responsive mouse mammary tumor virus promoter. Upon induction, no cytotoxic or antiproliferative effect of Rep was detected. Yang et al. (105) described 293-based cell lines that express the AAV Rep proteins under the control of an inducible mouse metallothionein transcription promoter. Upon induction with heavy metals, an accumulation of Rep-expressing cells in S phase was observed, but no toxicity was reported. However, Rep enhanced the toxicity of UV irradiation and incubation with cadmium (106). These differences in the effect of Rep on the cell may be due to the cell types used for the studies, expression efficiencies of the *rep* gene, and adaptation of the cell lines to background levels of Rep expression or alterations in the genomic *rep* gene. 293 cells contain a colinear segment from human adenovirus type 5, from nt 1 to 4344, which is integrated into chromosome 19 (19q13.2) (107). This segment contains the E1A-E1B region of the adenovirus genome.

The E1A gene products bind to key elements such as members of the pRB family, inducing unscheduled cell cycle progression.

The E1B-55K protein was shown to bind and inhibit p53, while E1B-19K acts as a Bcl-2 homolog in inhibiting apoptosis (82).

HeLa cells are a cervical-carcinoma-derived cell line containing multiple copies of integrated human papillomavirus (HPV) type 18 DNA. HPV type 18 encodes regulators of cell cycle progression and apoptosis which act similarly to the adenovirus-encoded E1

proteins (108). The viral gene products of both cell lines are likely to modulate the effect of Rep on the cell cycle and apoptosis and may explain the differences observed in the different systems.

In addition, an effect of the inducers of the stable Rep-expressing cell lines on cell growth and death is possible. Yang et al. used zinc and cadmium to induce Rep expression. Cadmium is a highly toxic heavy metal that has been shown to induce distortion of the cell cycle (109) and apoptosis by causing oxidative stress and DNA damage (110); zinc, in contrast, is efficient at inhibiting apoptosis (111). Interesting analogy between the effects of AAV-2 Rep78 and the nonstructural protein (NS-1) of the autonomous parvoviruses on the cell. Both proteins possess cytostatic and cytotoxic potential. Cell death caused by NS-1 expression was induced by apoptosis (112) which was mediated by and dependent on caspase-3. The cytostatic potential of NS-1 correlated with an accumulation of cells in G_2 and a block in cellular DNA replication which was proposed to be a consequence of NS-1-induced DNA damage (113).

1.9 Adenoviruses.

1.9.1 Structure.

Vectors based on different viruses have been developed to embrace a wide range of strategies for the gene therapy of a variety of diseases. Evaluation of many of these approaches has revealed a number of fundamental problems. These limitations are driving vector technology efforts toward a further evolution of the present systems and the generation of new classes of vectors that combine the best features of different viruses (114, 59).

The modification of Ad vectors is an example of vector engineering directed to solving problems identified by preclinical studies. Ad is considered an attractive vehicle for several

reasons. The viral life cycle is well characterized, its genome is easy to manipulate, and the resulting vector can be grown to high titers (115).

All Adenovirus particles are similar: non-enveloped, 60-90nm diameter. They have icosahedral symmetry easily visible in the electron microscope by negative staining and are composed of 252 capsomers: 240 "hexons" + 12 "pentons" at vertices of icosahedron.

The hexons consist of a trimer of polypeptide II with a central pore; VI, VIII and IX are minor polypeptides also associated with the hexon, thought to be involved in stabilization and/or assembly of the particle. The pentons are more complex; the base consists of a pentamer of peptide III, 5 molecules of IIIa are also associated with the penton base.

The pentons have a toxin-like activity.

A trimeric fibre protein extends from each of the 12 vertices (attached to the penton base proteins) and is responsible for recognition and binding to the cellular receptor. A globular domain at the end of the adenovirus fiber is responsible for recognition of the cellular receptor. (Fig. 1.8)

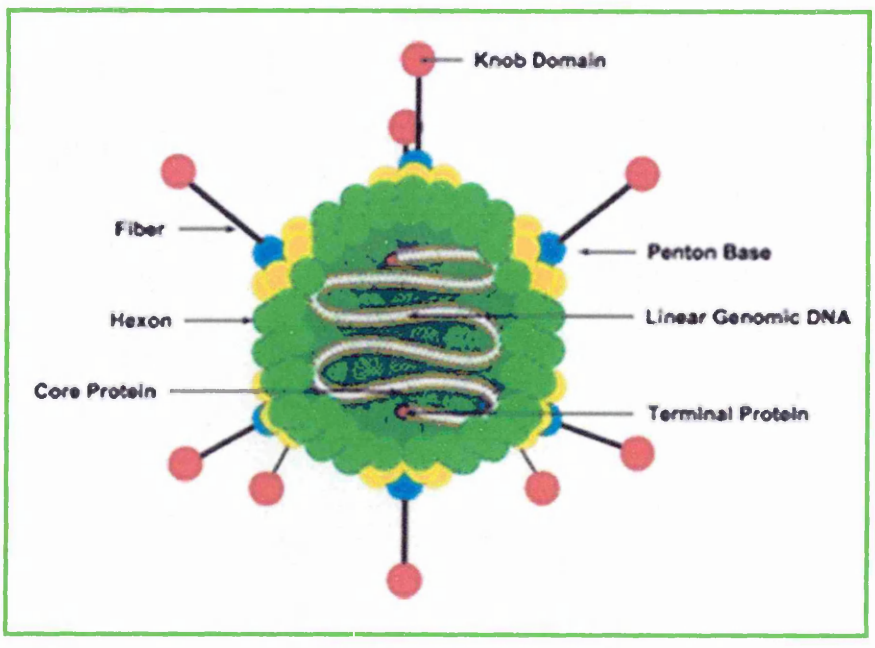

Fig. 1.8 Schematic representation of Ad structure.

While there are over 51 serotype strains of adenovirus, most of which cause benign respiratory tract infections in humans, subgroup C serotypes 2 or 5 are predominantly used as vectors. The life cycle does not normally involve integration into the host genome,

rather they replicate as episomal elements in the nucleus of the host cell and consequently there is no risk of insertional mutagenesis.

1.9.2 Ad genome.

Adenoviruses are non-enveloped viruses containing a linear double stranded DNA genome.

The wild-type adenovirus genome is a linear, non-segmented, d/s DNA, 30-38 kbp (size varies from group to group) which has the theoretical capacity to encode 30-40 genes. The terminal sequences of each strand are inverted repeats, hence the denatured single strands can form "panhandle" structures (100-140 bp). There is a 55 kDa protein covalently attached to the 5' end of each strand. Of the approximately 35 kb viral genomic DNA up to 30 kb can be replaced with foreign DNA (116). The adenovirus particle limits the amount of DNA that can be packaged to ~105% of the genome, only ~1.8 kb more that the wild-type virus genome.

There are four early transcriptional units (E1, E2, E3 and E4), which have regulatory functions, and a late transcript, which codes for structural proteins.

1.9.3 Genome transcription.

The adenovirus genome is transcribed in both directions and alternative splicing allows multiple transcripts to be generated from the same sequence. Any manipulation of the virus genome therefore requires the coding capacity of both DNA strands to be considered.

The E3 gene region is dispensable for adenovirus replication in vitro and can be deleted from both replication-competent and replication-deficient vectors to permit larger inserts.

Adenovirus vectors may be either replication-competent or replication-deficient.

In replication-competent adenovirus recombinants, transgenes are usually inserted in the E3 region and very high levels of expression can be achieved with transcription driven by the late promoter. Replication-deficient adenovirus vectors are usually based on adenovirus

E1-E3 deletion mutants. Deletion of the E1 gene region (both E1A and E1B) permits vectors to accommodate significantly larger inserts, removes a region of the genome associated with cellular transformation and generates a vector that is not only replication-deficient but also cannot activate early phase gene expression. This defect in early phase gene expression generates a vector which can promote efficient transgene delivery and expression in the absence of significant vector gene expression. However, breakthrough to early and late phase gene expression can occur, particularly following infection at high MOI or if the target cell expresses an endogenous "E1A-like" function. Breakthrough expression from the vector genome has been associated with the induction of an immune response following in vivo gene delivery. Replication-deficient adenovirus vectors incorporating additional mutations or deletions have been generated to address this problem. The deletion of additional sequences from the vectors also permits the insertion of larger transgenes.

1.9.4 Ad vectors.

Ad genome was modified to obtain recombinant viral vectors (Fig 1.9).

- Progenitor vectors have either the E1 or E3 gene inactivated, with the missing gene being supplied in trans either by a helper virus, plasmid or integrated into a helper cell genome (human fetal kidney cells, line 293) (118).
- Second generation vectors additionally use an E2a temperature sensitive mutant (119) or an E4 deletion (120).
- The most recent "gutless" vectors contain only the inverted terminal repeats (ITRs) and a packaging sequence around the transgene, all the necessary viral genes being provided in trans by a helper virus (121).

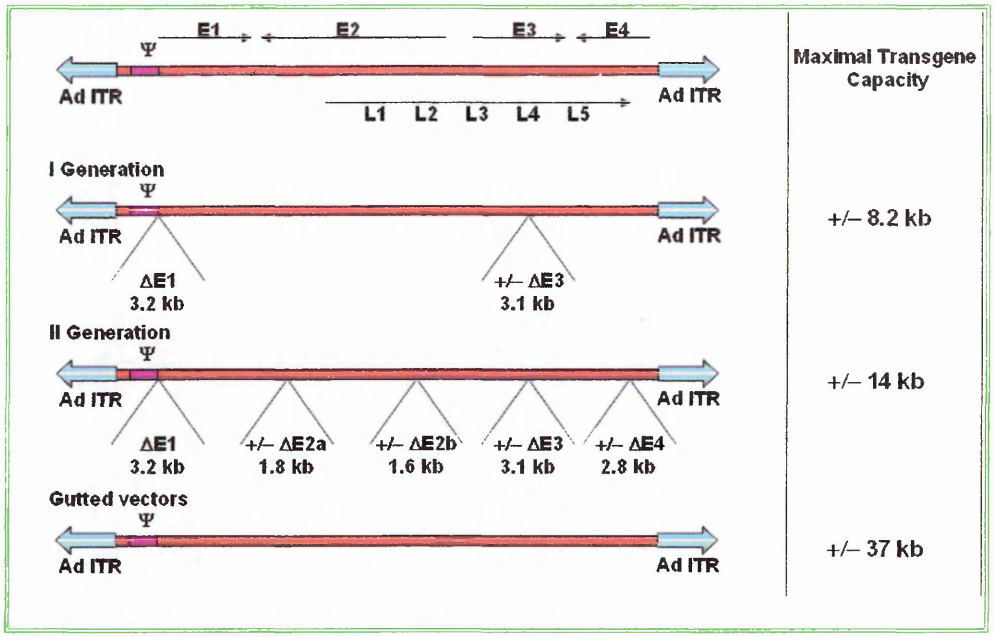

Fig. 1.9 Schematic representation of Ad wt and vector structure.

From the viewpoint of safety, size of transgene insertion and absence of vector gene expression, these so-called 'gutless' adenovirus vectors are attractive. They contain the inverted terminal repeats (ITRs) and adjacent sequences essential for replicating the adenovirus genome, including the cis-acting signal sequence (psi) which directs packaging of adenovirus DNA into virus particles. The gutless vectors require virtually all adenovirus gene functions to be provided for vector propagation and, since this cannot yet be achieved using a packaging cell line, they must be provided using a helper cell. Although their potential is enormous, current gutless vectors are complex and technically difficult to use. However, there are dangers associated with the use of adenovirus vectors, and a few deaths have occurred in clinical trials.

1.9.4.1 Adenoviral vectors of the first generation.

The genome of adenoviruses consists of 30-38 kb of double-stranded linear DNA with inverted terminal repeat (ITR) sequences at each end. Expression of genes occurs in two phases, early and late, defined by the onset of DNA replication (127).

Early genes are encoded by four distinct transcription units, E1–E4, whereas the late gene products are generated from a single promoter. Importantly, proteins encoded by E1 region are indispensable for further viral gene expression and DNA replication (128).

Vector of the first generation is prepared by substitution of a transgene in the place of E1 (or E1 and E3) genes (Fig. 1.9). The resulting construct has a cloning capacity up to 9 kb. An E1-deficient (ΔE1) vector is replication-defective and must be propagated in a permissive cell line, engineered to provide E1 functions in *trans* (129). Substitution for the E3 genes is not necessary, as they are involved in inhibition of host immune antiviral response, not in the replication of the adenoviral genome.

Among the 51 human adenovirus serotypes discovered to date, Ad5 and Ad2 are most commonly used for generation of vectors (128). Adenoviral vectors give the most efficient gene transfer in comparison with other systems (130). Moreover, they can transduce both dividing and post-mitotic cells of nearly all human tissues – including skin, muscle, blood vessel, bone, nerve, and liver (127, 130). They can be also effective in delivering genes into some leukocytes (231). Following delivery, transgene expression is at a very high level. Unfortunately, it decreases rapidly after several days, being low or undetectable after several weeks (130).

Many studies have clearly demonstrated that adenoviral vectors of first generation induce innate and adaptive immune responses *in vivo* against viral capsids and transduced cells (11). Despite the deficiency in the E1 region, the vectors are, in fact, not completely replication defective (132). They deliver the transgene along with the residual viral genes and indeed synthesize some viral proteins. Even low level expression of these leads to activation of CTL and results in destruction of expressing cells, being the major cause of transgene silencing (130).

1.9.4.2 Helper-dependent adenoviral vectors (HdAd).

Helper-dependent adenoviral vector (HdAd), called also "gutless" or "gutted" vector, is created by removing all viral genes and leaving only the ITRs necessary for vector propagation, and the Ψ sequence required for packaging (Fig. 1.9) (12). Any unused space is occupied by a transgene or by noncoding "stuffer" DNA sequence, to build the vector to a size suitable for packaging (Fig. 1.9). This strategy completely eliminates the production of viral proteins in infected cells. Therefore, HdAd elicits only minute or negligible CTL response and is capable of producing long-term gene expression (133). Additional advantage of HdAd is a high cloning capacity, extended up to 37 kb (12). The nature of the DNA backbone can have important effects on the functioning of the HdAd virus, which must be taken into account in the design of vectors. The most commonly used stuffer DNA originates from human hypoxanthine-guanine phosphoribosyltransferase (HPRT). The first step in generation of HdAd constructs is based on ligation of the expression cassette into large plasmids containing the viral ITRs flanking stuffer DNA. This process, although commonly applied, is generally very inefficient. It has been shown, however, that similarly as in the case of the ΔE1 adenoviral vectors, plasmids for generation of HdAd constructs can be obtained by homologous recombination in *Escherichia coli,* which potentially can facilitate the production (134).

A number of systems have been also developed for rescuing HdAd. The most common method for propagation and purification of HdAd utilizes two elements: i) a helper virus (ΔE1/ΔE3) with Ψ sequence flanked by loxP sites (Fig. 1.10), ii) a modified 293Cre cell line expressing Cre recombinase which catalyzes recombination between loxP sequences, excising the packaging site from helper DNA. Such a deletion renders the helper genome un-packagable but leaves all other viral functions intact, retaining the ability to replicate and provide helper functions.

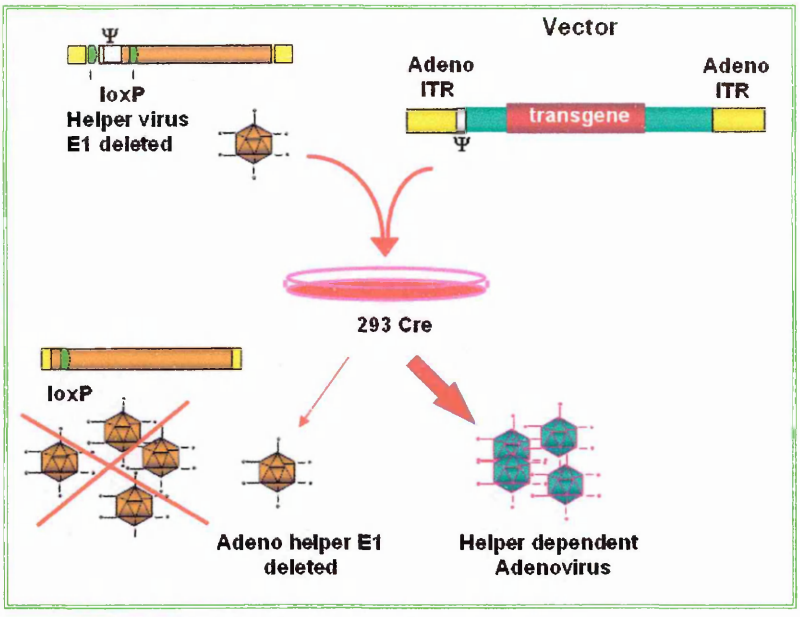

Fig. 1.10 Schematic representation of Hd-Ad virus production.

The efficacy of this technology is sufficient for experimental gene therapy, but is not suitable for production and purification of HdAd vectors at a scale necessary for clinical use (135).

To increase the efficiency of the system, both improved helper viruses and alternative gutless vector producer cell lines are necessary. One of the promising modifications is establishing the cells adapted to serum-free suspension culture, which can allow obtaining high-titer gutless vector preparations by using bioreactor technology (135).

An additional problem to be solved is contamination with helper ΔE1 virus, which may have substantial unwanted effects. Unfortunately, a helper virus, even lacking a packaging signal, still can be packaged, although at a low frequency (about 0.1%) (135). It seems that this level of impurity cannot be further decreased using the Cre/loxP system, as Cre recombinase in 293Cre cells permits some helper viruses to escape packaging signal excision and propagate (136). Thus, the resulting viral stocks must be additionally purified by ultracentrifugation in CsCl, which can produce HdAd stocks with very low (less than 0.01%) helper contamination (Fig. 1.11). This separation step hinders, however, large scale production of clinical-grade HdAd virus.

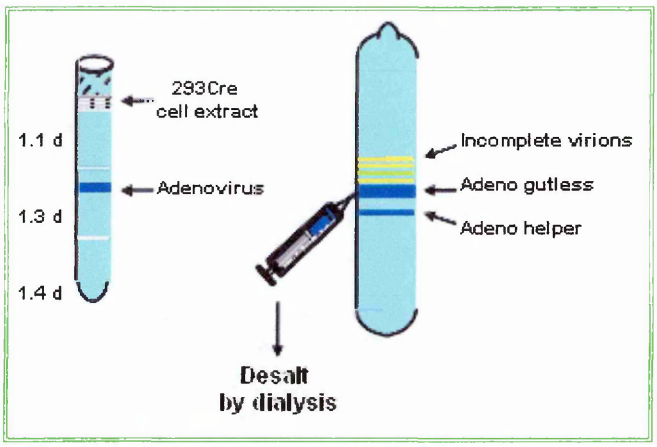

Fig. 1.11 Schematic representation of Ad purification by CsCl gradient.

One of the possible solutions is using a more efficient recombinase, e.g. modified FLP (FLPe), to remove Ψ from the helper virus in the producer cells. FLP has been shown to mediate maximum levels of excision close to 100% compared to 80% for Cre. Thus, it has been postulated that the FLPe-based system may yield HdAd with very low levels of helper virus contamination without the need for ultracentrifugation, which should allow large-scale generation of gutless vectors by means of column chromatography (137). Finally, the safety of the HdAd vectors can be further optimized by using double-deleted ΔE1ΔE2a helper virus.

Gutless adenoviruses can infect a wide range of mammalian tissues, independent of the replicative state of the cells. Like ΔE1 particles, intravenously injected HdAd vectors transport the transgene preferentially to the liver, where infection efficacy may reach almost 100%.

Nevertheless, certain serotypes of adenoviruses have diverse tissue tropisms *in vivo*, and in some tissues, e.g. in skeletal muscles, the efficacy of adenoviral vectors is relatively low. Particularly resistant are some lymphoid cells (138). This is in contrast to the effects of ΔE1 vectors, secretion of pro-inflammatory cytokines was minimal after HdAd vector injection, resulting in reduced numbers of activated microglial cells, astrocytes, and infiltrating macrophages in brain tissue. These findings indicate that HdAd vehicles should provide a safe and effective means to transfer therapeutic genes into the brain (139).

1.9.5 Immunogenicity.

Adenoviral vectors are very efficient at transducing target cells *in vitro* and *in vivo*, and can be produced at high titres ($>10^{11}$/ml). Transgene expression in vivo from progenitor vectors tends to be transient (117). Following intravenous injection, 90% of the administered vector is degraded in the liver by a non-immune mediated mechanism (122). Thereafter, an MHC class I restricted immune response occurs, using $CD8^+$ CTLs to eliminate virus infected cells and $CD4^+$ cells to secrete IFN-alpha which results in anti-adenoviral antibodies (123). Alteration of the adenoviral vector can remove some CTL epitopes, however the epitopes recognised differ with the host MHC haplotype (124). The remaining vectors, in those cells that are not destroyed, have their promoter inactivated (120) and persisting antibody prevents subsequent administration of the vector.

Approaches to avoid the immune response involving transient immunosupressive therapies have been successful in prolonging transgene expression and achieving secondary gene transfer. A less interventionist method has been to induce oral tolerance by feeding the host UV inactivated vector (125). However, it is desirable to manipulate the vector rather than the host. Although only replication deficient vectors are used, viral proteins are expressed at a very low level which are presented to the immune system. The development of vectors containing fewer genes, culminating in the "gutless" vectors which contain no viral coding sequences, has resulted in prolonged in vivo transgene expression in liver tissue (13). The initial delivery of large amounts of DNA packaged within adenovirus proteins, the majority of which will be degraded and presented to the immune system may still cause problems for clinical trials. Moreover the human population is heterogeneous with respect to MHC haplotype and a proportion of the population will have been already exposed to the adenoviral strain (126).

Adenovirus genome is relatively easily manipulated in vitro and the genes coupled to the late promoter are efficiently expressed in large amounts.

1.10 Ad Serotypes.

Human adenoviruses (Ads) are associated with a wide range of tropisms. They have been classified into six distinct subgroups A to F, with at least 51 serotypes (140), on the basis of their genetic variability, oncogenic potential, and G+C content of their DNA (140). A further sub-classification of subgroups B (BI and BII) and D (DI, DII, and DIII) has been made on the basis of differential hemagglutination patterns (141, 142). Ads have the ability to infect a wide range of different tissues and have been identified as causative agents of widely different diseases (140, 143). For example, serotypes Ad 2 and Ad 5 (subgroup C) are associated with upper-airway infections, as is serotype Ad 3 (subgroup B), although the latter appears to infect an anatomically distinct region of the airway (143). Serotypes Ad 8 and Ad 9 (subgroup D) are associated with epidemic keratoconjunctivitis, Ad 4 (subgroup E) is associated with pneumonia, Ad 12 (subgroup A) is associated with cryptic enteric infection, and Ad 40 and Ad 41 (subgroup F) are associated with gastroenteritis (143). Detailed phylogenetic analysis of diverse Ad serotypes has yielded two phenotypic clusters; the gastrointestinal cluster, with subgroups A and F, and the respiratory cluster, with subgroups B, C, and E (144).

It has been suggested that the apparent tropism of different serotypes in different tissues results from virus interactions with distinct cellular receptors. Indeed, it has been shown convincingly that the Ad 2/5 and Ad 3 fiber proteins recognize different cellular receptor proteins (156, 148).

Attachment and uptake into cells of subgroup C Ads occur by separate but cooperative events that result from the interaction of the fiber protein with a receptor for attachment and the penton base protein with a receptor for internalization (Fig. 1.12). The 46-kDa coxsackievirus-adenovirus receptor (CAR) protein mediates fiber-dependent attachment of subgroup C Ad 2 and Ad 5 (145). The C-terminal knob of the fiber protein confers the specificity of the cellular receptor recognition (146, 147, 148). Analysis of the fiber 5 knob

by X-ray crystallography has yielded a model for the structure of this protein and has identified several exposed amino acid residues and structural loops that have been theorized to be involved in cellular receptor recognition (149). Next, in a process that has been shown to be independent of fiber-cell recognition (150, 147), the viral penton base protein binds to cellular α_v-integrins through the RGD loop, a tripeptide motif that protrudes out of the tertiary peptide structure of the penton base, resulting in rapid internalization of the virus particle (151). Through cross-competition experiments, it has been shown that the fibers of Ad 2, Ad 5, and Ad 9, despite their distinct tropisms and classification into the different subgroups C and D (140), recognize the same cellular fiber receptor (148). Ad vectors based on serotype 5 (Ad 5) for an efficient infection with adenovirus requires the presence of coxsackievirus-adenovirus receptors (CAR) and α_v integrins on cells (152).

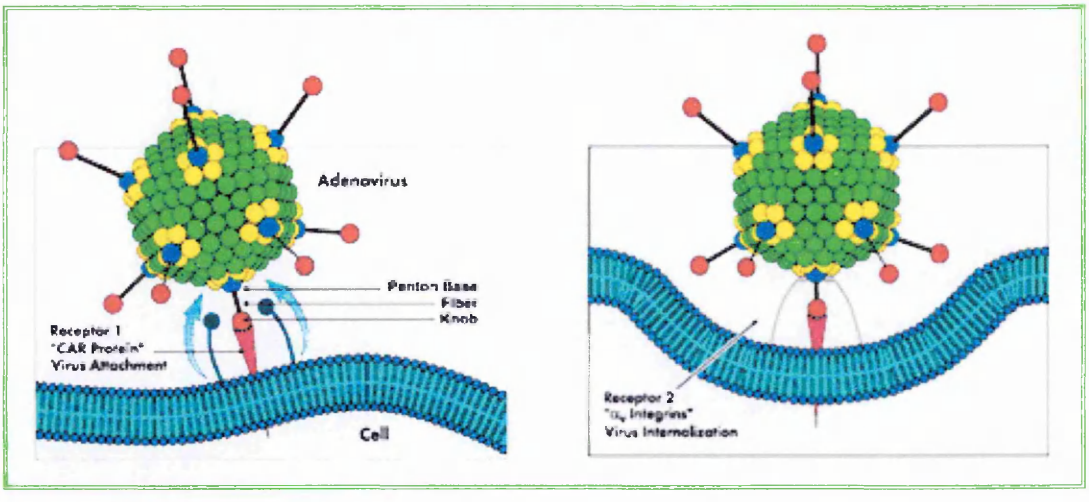

Fig. 1.12 Ad5 uptake and internalization mechanism.

Due to the lack of corresponding primary and/or secondary receptors, Ad 5 gene transfer is inefficient to a number of tissues, such as endothelia (153), smooth muscle (154), differentiated airway epithelia (155), brain tissue (156), and peripheral blood cells. Recently, group B Adenovirus derivates have gained interest as attractive gene therapy vectors because they can transduce target tissue, such hematopoietic stem cells, dendritic cells and malignant tumor cells, that are refractory to infection by commonly used

adenoviral vectors. Since the cell types that can be infected with Ad 5 vectors are restricted by the presence of CAR and α_v integrins, attempts were made to broaden the tropism of Ad vectors. These approaches included complexing Ad with lipids or polycations (157), using bi-specific antibodies directed against Ad fiber and an internalizing cellular receptor (157), and engineering peptide ligands into the fiber (158), hexon (159), or penton (160). Most of these approaches did not abrogate CAR tropism. The most commonly used method to retarget Ad tropism is by swapping part or all of the fiber from one serotype to another (156, 147, 153). The various serotypes of human Ad show differences in tissue tropism and cause different pathologies mostly localized to the gastrointestinal tract, respiratory tract, genitourinary tract, or conjunctiva and cornea (161). Since the nucleotide and amino acid sequences of fibers differ significantly among different Ad serotypes, it has been suggested that they can recognize different receptors (144). This implies that fiber substitution would be sufficient to change virus tropism and has been convincingly shown for Ad 5-Ad 3 chimeras (153), Ad 5-Ad 7 chimeras (162), and Ad 5-Ad 17 fiber chimeras (156). It was shown that it is possible to genetically substitute by heterologous sequences derived from the other serotype the Ad 5 fiber or fiber knob was. Whereas, as told before, may Ad infect cells through the coxsackievirus and adenovirus receptor (CAR), group B adenoviruses use an alternate, attachement receptor. Human CD46 seems to be a cellular receptor for most group B adenoviruses. Serotype 35 emerged as the variant with the highest tropism for $CD34^+$ cells. A chimeric vector (Ad 5/35) which contained the short-shafted Ad 35 fiber incorporated into an Ad 5 capsid was generated. This substitution was sufficient to transplant all infection properties from Ad 35 to the chimeric vector. The retargeted, chimeric vector attached to a receptor different from CAR and entered cells by an α_v integrin-independent pathway (163).

1.11 Collagen VII.

The collagens comprise a family of closely related, yet genetically distinct, macromolecules.

At least 14 different vertebrate collagens have been identified (Fig. 1.13). All collagen molecules consist of three subunit polypeptides, called chains, and there are as many as 25 different genes within the human genome that code for these subunits (164, 165).

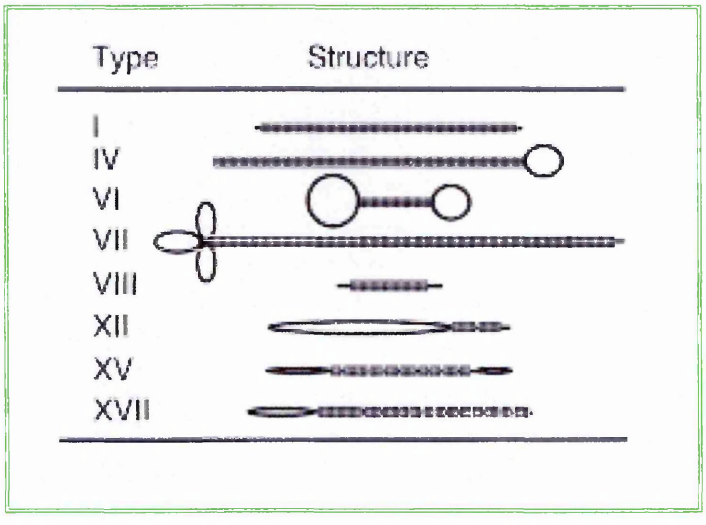

Fig. 1.13 Schematic representation of some proteins of the collagen's family.

The genetically distinct collagens have characteristic tissue distributions. The more abundant collagens, as exemplified by types I and III collagens, have a rather widespread distribution, while some minor collagens have a limited anatomical location. For example, type VII collagen appears to be restricted to the basement membrane zone beneath stratified squamous epithelia. Within the cutaneous basement membrane zone, type VII collagen localizes to the lamina densa and sub-lamina densa areas in the upper papillary dermis (166). More precisely, immuno-localization studies have demonstrated that type VII collagen is the major collagenous component of anchoring fibrils, morphologically distinct structures that extend from the lamina densa and project perpendicularly into the upper papillary dermis (167).

Anchoring fibrils attach the epidermal basement membrane of the skin to the underlying dermal connective tissue (164, 165). As visualized by electron microscopy, anchoring fibrils appear as centro-symmetrically banded elements displaying variable diameters and degrees of curvature.

Anchoring fibrils are seen along the basement membrane, where they appear to originate at the lamina densa and to extend into the stroma where they terminate in anchoring plaques. The anchoring plaques are basement membrane-like, electron-dense regions that contain type IV collagen and perhaps other intrinsic basement membrane proteins. Additional anchoring fibrils originate in the anchoring plaques and then extend further into the stroma, terminating in other anchoring plaques. Anchoring fibrils also originate in the lamina densa, extend into the stroma, and appear to arch back to reinsert into the lamina densa.

Collagen VII is a large homo-trimeric protein with a central triple helix and flanking amino- and carboxyl-terminal globular domains.

Comparisons of the banding patterns of segment-longspacing crystallites of type VII collagen with those of anchoring fibrils indicate that the portion of the anchoring fibril not contained within the basement membrane or the anchoring plaques represents the triple-helical domain.

Type VII collagen (Burgeson, 1987) is a gene located on the p arm of the chromosome 3 (3p21.3) and is constituted by 118 exons translated in a 9 kb c-DNA. Collagen VII is synthesized and secreted as a precursor, thought to be a homopolymer of three pro-α(VII) chains, M.W. 350,000. The aminoacid sequence is very abundant in Gly-Pro-Y motifs (Fig. 1.14).

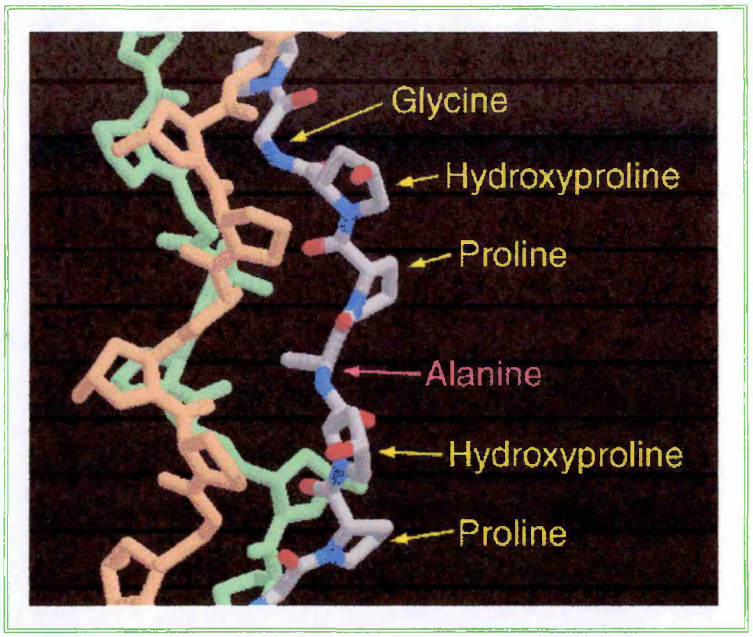

Fig 1.14 Schematic representation of aminoacid distribution in collagen VII.

Approximately one out of every 3 residues is a glycine and the proline content is also high. Stretches of the collagen polypeptide sequence are repeats of Gly-X-Y (X and Y frequently proline and hydroxyproline). In the triple helix, every third aminoacid contacts the center of the structure. This area is so small that only a glycine can fit, which explains why every third amino acid in collagen's structure is a glycine residue (Fig. 1.14). Hydrogen bonding involving hydroxyproline can occur, which further stabilizes the proteins structure.

The N-terminal sequence of α1(VII) contains two vWF-A, ten FnIII repeats, and one sequence of aminoacid homologue to the proteins in the cartilage matrix. This region is folded separately in separates 36 nm arms.

The pro-collagen molecule contains three distinct domains: NC-2, the small amino-terminal non-triple-helical domain (M.W. 95,000); the triple-helical domain (M.W. 510,000); and NC-l, the complex, trident-like carboxyl-terminal globular domain (M.W. 450,000).

The triple-helical domain contains a major discontinuity in that conformation near the center of the domain as detected by sensitivity to pepsin and trypsin digestion (176) which generates the fragments Pl and P2. Additional discontinuities are detected by digestion

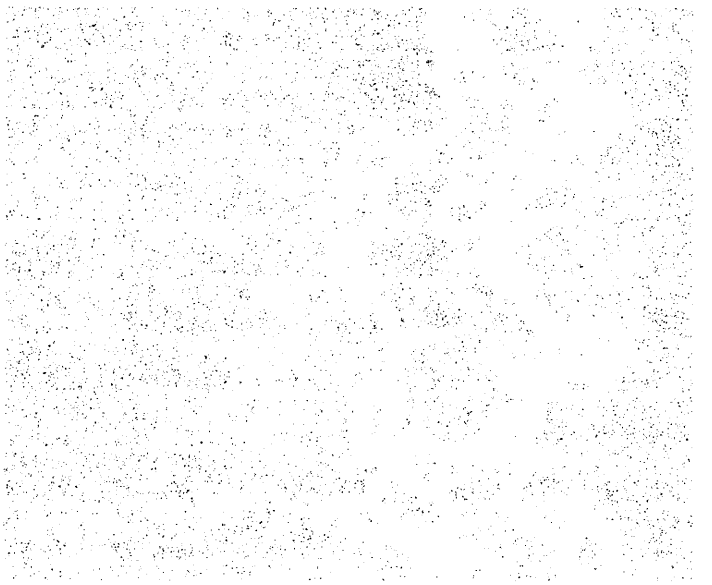

under more severe conditions. These triplex pro-collagen molecules further dimerize through an association of the amino termini such that the triple-helical domains overlap by 60 nm. This overlap may be specified by an interaction of the NC-2 domains with the triple helix and is subsequently stabilized by two or more intermolecular disulfide bonds. The NC-2 domains are then removed, and the dimers assemble into anchoring fibrils by unstaggered lateral associations (177).

After secretion, pro-collagen VII undergoes proteolytic trimming to collagen VII and assembles to polymers (Fig. 1.15) (164).

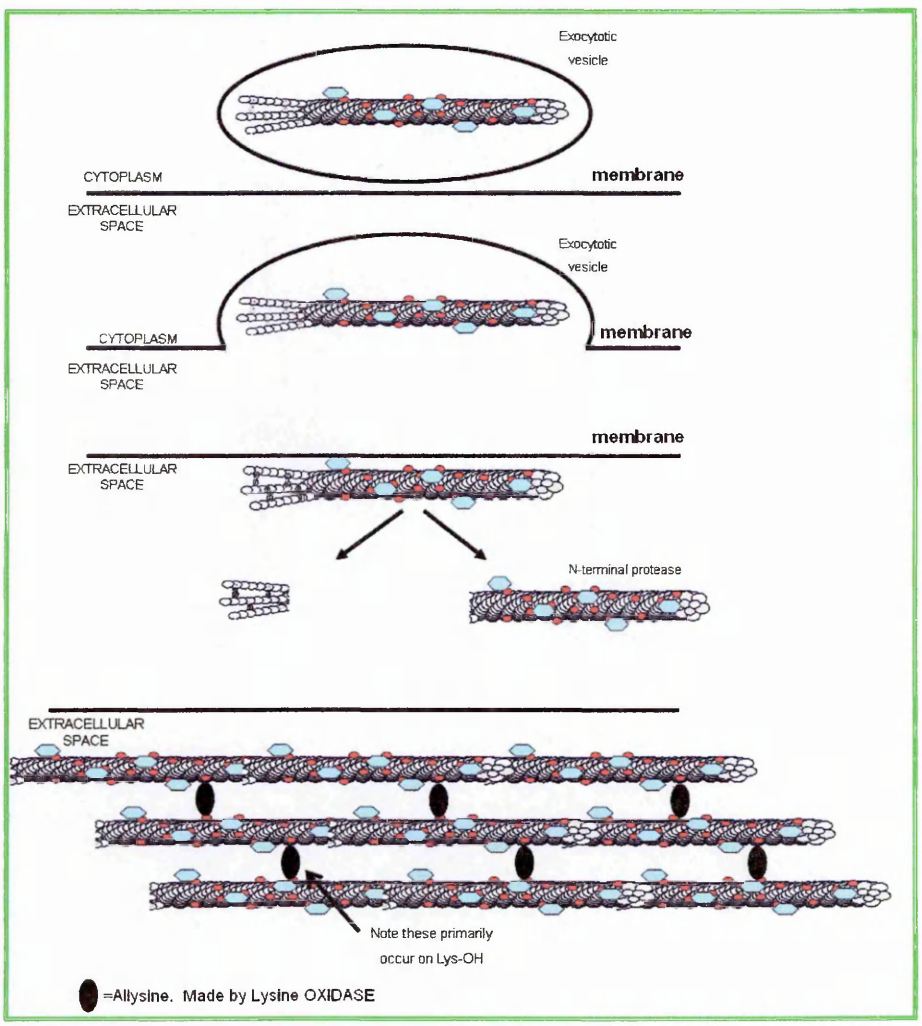

Fig. 1.15 Schematic representation of maturation and secretion of collagen VII. The triplex pro-collagen molecules dimerize through an association of the amino termini such that the triple-helical domains overlap by 60 nm. This overlap may be specified by an interaction of the NC-2 domains with the triple helix and is subsequently stabilized by two or more intermolecular disulfide bonds. The NC-2 domains are then removed, and the dimers assemble into anchoring fibrils by unstaggered lateral associations. After secretion, pro-collagen VII undergoes proteolytic trimming to collagen VII and assembles to polymers.

This is a multistep process during which collagen VII monomers first form di-sulfidebonded antiparallel dimers and then laterally aggregate into anchoring fibrils, which interact with laminin 5 to secure the dermo-epidermal adhesion (164, 166). Further stabilization of anchoring fibrils and presumably of intermolecular aggregates is achieved through cross-linking by transglutaminase-2.

The structure of type VII collagen must account for the apparent flexibility of the anchoring fibrils and for their contact with the lamina densa and the anchoring plaques.

The tortuous shapes of the fibrils seen ultra-structurally are assumed to result from the discontinuities within the triple-helical domain. This assumption is supported by studies of type IV collagen, in which flexible sites correlate well with disruptions in the triple-helical structure known from the primary structure of the type IV chains (Fig. 1.16) (178).

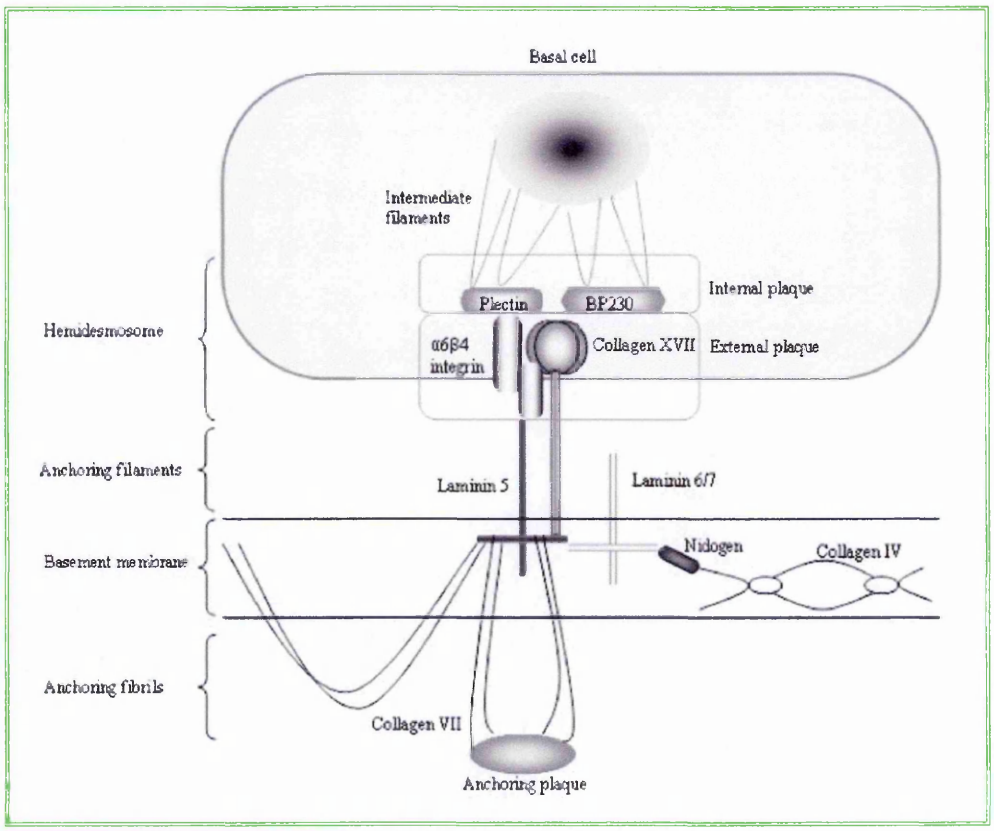

Fig. 1.16 Schematic representation of anchoring plaques.

Anchoring fibrils are functionally deficient in hereditary dystrophic epidermolysis bullosa (DEB) a heterogeneous group of bullous skin disorders (167) with mechanically induced blistering and scarring of the skin. In the most severe forms of the disease, both collagen

VII protein and anchoring fibrils are absent from the skin (168), whereas in milder forms, collagen VII is expressed, but the morphology of the anchoring fibrils may be altered (169).

Mutations in *COL7A1* encoding collagen VII have been disclosed in both recessive and dominant DEB subtypes (170, 171, 172).

In recessive subtypes, homozygous or compound heterozygous mutations leading to premature termination codons underlie very severe skin blistering and scarring (173), whereas homozygous or compound heterozygous missense mutations cause milder phenotypic manifestations.

In dominant DEB (DDEB), only about a dozen mutations have been identified, most of them causing substitution of a glycine in the triple helical domain of collagen VII (172). However, despite a growing number of known collagen VII mutations, the biological consequences of these mutations and the pathogenic pathways from the gene defect to dermo-epidermal tissue separation in the skin have remained elusive.

Glycine substitution mutations in other collagen genes underlie heritable connective tissue diseases, such as osteogenesis imperfecta, chondrodysplasias, certain subtypes of Ehlers-Danlos syndrome, or Alport's syndrome (174, 175). These mutations cause pathologic phenotypes through dominant-negative interference. Therefore, the prediction was that glycine substitution mutations in *COL7A1* had similar effects. Surprisingly, however, molecular genetic analyses of a number of DEB families disclosed several compound heterozygous glycine substitution mutations in *COL7A1* that did not cause a pathologic phenotype in obligate carriers.

Chapter 2

Materials and methods

2.1 Reagents suppliers

2.1.1 Chemicals.

All chemicals were obtained from FLUKA, Sigma Chemicals Co. or Roche.

Others chemicals used during the study were obtained from the following sources:

Agarose for gel electrophoresis	SeaKem LE Agarose Cambrex BioScience Rocland
DNA markers	1 kb Gene Ruler DNA Ladder Fermentas 100bp Ladder Invitrogen
Protein markers	Biorad Rainbow
X-Ray film	Kodak and Amersham
Hydrolysed milk powder	Merck
Nitrocellulose for Western Blot	Protran BA85 Cellulose Nitrate Scheleicher & Schuell
Nylon for Southern/Northern Blot	Stratagene or Hybond
Acrylamide	Applichem

2.1.2 Radiochemicals.

α^{32}P dCTP (Amersham)

2.1.3 Enzymes.

All DNA modification enzymes and buffers were received from either Roche and New England Biololabs (NEB).

2.1.4 Restriction enzymes and buffers.

All restriction enzymes and buffers were obtained from either Roche and New England Biololabs (NEB).

2.1.5 Bacterial strains and growth.

The DH5α strain (F', hsdR17,rk-mk+, recA1, endA1) was used for all transformations, and growth both in Luria Bertani (L.B) or Terrific Broth (T.B) media prepared within the institute.

TOP10 strain (F mcrA Δ(mrr-hsdRMS-mcrBC) ϕ80lacZΔM15 ΔlacX74 recA1 araD139 Δ(ara-leu)7697 galU galK rpsL (Str^R) endA1 nupG) was used for all transformation of TOPO-TA cloning vector following manufacturers instructions.

2.1.6 Plasmids.

Creation of other plasmids are described below (Section 2.5.1). The following were provided by the laboratory of Professor Mavilio.

Human Collagen containing plasmid was provided by Professor Meneguzzi G. INSERM U634, Faculty of Medicine, Nice, France

2.1.7 Solutions and Buffers.

Buffer for flow cytometric analysis (FACS)	PBS 0.1% (w/v) BSA
50x TAE for Agarose gel (1 litre)	242 g Tris base 57.1 ml Glacial Acetic Acid 100 ml 0.5M EDTA, pH 8.0 Water to final volume (1 litre)
Tris-HCl	Trizma Base to the molarity required and HCl to the required pH
100x TBE for Agarose gel (1 litre)	108 g Trizma base 55 g Boric Acid 40 ml EDTA 0.5 M pH 8.0

10% SDS (1 litre)	100 g SDS powder Water to final volume (1 litre)
5 M NaCl (1 litre)	292.2 g Water to final volume (1 litre)
TE Buffer 10x (200ml)	10 ml Tris-HCl pH 7.9 2M (10 mM final) 4 ml EDTA 0.5 M (1 mM final) Water to 200 ml
10 N NaOH (100 ml)	40 g NaOH Water to final volume

2.2 Tissue culture reagents.

2.2.1 Plastic ware.

All standard tissue culture ware (tissue culture flasks, tissue culture plates, tubes etc..) was obtained from Corning Costar and Falcon.

2.2.2 Media.

X-VIVO 10	Biowhittaker
DMEM	Cambrex
IMDM	Cambrex
RPMI	Cambrex

2.2.3 Sera, Supplements and antibiotics.

Fetal Bovine Serum	Hyclone

Trypsin	Cambrex
L-Glutamine	Cambrex
Penicillin/Streptomycin	Biological Industries
HEPES	SIGMA
Doxycicline	SIGMA

2.2.4 Growth factors.

Recombinant human Stem cell factor (SCF)	R&D Systems, and Pepro Tech, England
Recombinant human Flt-3 Ligand (Flt3-L)	Pepro Tech, England
Recombinant human interleukin-3 (rhIL-3)	Pepro Tech, England
Recombinant human interleukin-6 (rhIL-6)	R&D Systems

2.2.5 Other.

Phosphate buffered Saline (PBS) was obtained from Cambrex.

FICOLL was obtained from Limphoprep Fresenius Kabi Norge AS.

Fugene 6 was obtained from Roche.

Effectene Transfection reagent was obtained from Qiagen.

2.3 Antibodies and antisera.

Anti human NGF antibody was obtained from BD (Primary and R-PE conjugated).

Goat Anti mouse IgG (FITC, R-PE conjugated) was obtained from Southern Biotechnology Associates, Inc.

Anti human CD38, R-PE, FITC, or Tricolor conjugated was obtained from Caltag laboratories, U.S.A

Anti human CD34, R-PE, FITC, or Tricolor conjugated was obtained from Caltag laboratories, U.S.A

Anti human Collagen VII Ab-1 (LH7.2) was obtained from Neomarkers.

Anti mouse HRPO was obtained from SIGMA

2.4 Cells.

2.4.1 Stable cell lines:

HeLa	Human carcinoma	From ATCC
293Cre4	Human Kidney	From laboratory of Professor Mavilio
NIH3T3	Murine Fibroblasts	From laboratory of Professor Mavilio
293T	Human Kidney	From ATCC
K562	Human Chronic Myelogenous Leukemia	From ATCC
HEL	Human Herythroleukemia	From ATCC

2.4.2 Primary cells.

Human CD34+ cells.

Were most kindly purified and prepared from umbilical cord blood (UCB) source by myself, by FICOLL density separation followed by magnetic selection based on the Miltenyi MACS kit for cell separation, following the manufacturers recommended protocol. Samples were either used fresh or frozen in FCS containing 10% DMSO, and stored in liquid Nitrogen until required for use.

Keratinocytes

Most of the keratinocytes experiments were done by Dr. Stefano Ferrari (Epithelial Stem Cell Research Centre, Veneto Eye Bank Foundation, Venice, Italy).

2.5 Methods

Methods are divided into 3 sections:

2.5.1 Molecular methods

2.5.2 Tissue culture methods

2.5.3 Gene transfer methods

2.5.1 Molecular Methods

2.5.1.1 Transformation of competent bacteria and small scale bacteria preparations.

DNA to be transformed was mixed with 100 ul of competent DH5α cells prepared specifically for the heat shock mediated transformation method (Maniatis et al. 1982). The mix was incubated 20 minutes on ice, then 1 minutes in watherbath at 42°C, and then returned to ice for further 2 minutes. The mix was then added to 1 ml of SOC media and

incubated at 37°C with agitation for 1 hour. The mix was the plated onto agar plates supplemented with the required antibiotic and placed overnight in a 37°C bacterial incubator. The following day, colonies were picked up and placed into 2 ml of LB media containing antibiotic, and grown overnight with agitation at 37°C. The small bacterial preparations were subjected to small or large scale DNA preparation as required.

2.5.1.2 Small scale (miniprep) preparation of plasmid DNA from bacteria.

Small amounts of plasmid DNA were purified from bacteria, for restriction analysis, following the alkaline lysis method for DNA (Maniatis et al. 1982).

2.5.1.3 Large scale (maxiprep) preparation of plasmid DNA from bacteria.

This method is a scaled up method of the alkaline lysis method, using identical solutions unless stated. Typically 500 ml of an overnight growth of DH5a bacteria in antibiotic containing TB media was used per preparation. The bacteria were pelleted at 6000 rpm for 10 minutes in a Sorvall centrifuge. The residual media was discarded and the centrifuge tube inverted to drain as much media as possible away from the pellet. 20 ml of resuspension solution (Solution I) containing Lysozyme at the final volume of 12.5 ug/ml was added to the pellet, and the pellet was resuspended pipetting and vortexing. The bacterial mix was left at room temperature for 10 minutes. 40 ml of alkaline lysis solution 2 was added, the sample mixed and returned at room temperature for further 10 minutes. 30 ml of ice cold solution 3 was added, the sample again thoroughly mixed, and put on ice for 10 minutes.

The tube was centrifuged at 4500 rpm for 45 minutes, the lysate filtered through medical gauze into 200 ml Falcon tubes (the residual pellet was discarded) and the same volume of isopropanol alcohol was added to precipitate the nucleic acid. The sample was left 10-20 minutes on ice and then the tube was centrifuged at 4500 rpm for 45' minutes at 4°C. The liquid was discarded and the pellet properly drained was resuspended in 10 ml of TE

buffer. Beckman quick seal tubes were prepared as follows. 11 g of Caesium Chloride (CsCl) were measured into 50 ml Falcon tubes to which was added 10ml of resuspended pellet and 300 ml of ethidium bromide (10 mg/ml stock). After CsCl had dissolved, the solution was centrifuged for 30 minutes to 4500 rpm to pellet all the debris. The solution was taken up with a 10 ml syringe and injected into the Beckman quick seal tube, the tubes balanced and then sealed using the Beckman heat sealing device.

Samples were centrifuged in a Beckman NVT 65 rotor at 50000 rpm for at least 14 hours. The tubes were gently removed from the rotor, a hole punched in the top of the tube using a large gauged needle, and a syringe with the needle attached was inserted just below the DNA band which was clearly distinguished from the rest of the gradient due to the intense red colour following the ethidium bromide intercalation. The DNA band was gently removed and injected into 15 ml Falcon tube. 10 ml of butanol CsCl saturated in water was added to the tube, the tube shacked, left to settle and the upper phase discarded (clearly red-pink coloured). This process was repeated several times until no pink colour was visible. The process was then repeated one more time after this to be sure of ethidium bromide removal. Then the samples were loaded into dialysis membrane (MWCO 10000) and dialysed overnight in 4 litres of 1x TE Buffer. The day after dialysed samples were precipitated. Water was added to the tubes to a final volume of 5 ml, 250 ul of 3 M Sodium acetate added, and a further 10 ml absolute ethanol added on top. Tubes were mixed and placed at -20°C for 30 minutes. The tubes were centrifuged 45' 4500 rpm. The pellet obtained was washed twice with 70% ethanol. Purified DNA was resuspended in water and quantified using the standard 260/280 nm absorbance method on a spectrophotometer. DNA was stored at 4°C if required immediately or stored at -20°C for longer use and storage.

GTE (2 litres) Solution I.	18.2 g Glucose (50 mM final) 50 ml 1 M Tris-HCl pH 7.5 (25 mM final) 0.5 M EDTA pH 8.0 (10 mM final)

	Water to final volume
Lysis Solution (40 ml). Solution III.	0.8 ml NaOH 10 N (0.2 M final) 4 ml 10% SDS (1% final) Water to final volume
Neutralisation Solution (2 litres). Solution III.	588.84 g Potassium Acetate 230 ml Acetic Acid Water to final volume
Butanol CsCl saturated	Butanol and water 1:1 (v/v) and CsCl to saturation
1x TE	1:10 (v/v) from 10x TE
3 M Sodium acetate	NaAc in water to the final volume

2.5.1.4 Southern Blot analysis.

Extraction of genomic DNA from cells:

1-10x10^6 cells were lysed in 3 ml of the following buffer:

50 mM Tris HCl pH 8.0
100 mM EDTA
400 mM NaCl
1% w/v SDS

25 ul of proteinase K (10 mg/ml stock) was added and the mix incubated overnight at 37°C or 6 hours at 55°C.

An equal volume of phenol was added to the solution and mixed vigorously. The sample was then centrifuged for 5' at 14000 rpm. The aqueous phase was recovered and an equal volume of phenol/chloroform added. The above step was performed, the aqueous phase taken and an equal volume of chloroform added, the samples mixed and centrifuged as above, the aqueous phase taken and nucleic acid precipitated by the addition of an equal

volume of absolute ethanol 0,3 M Sodium acetate. A glass Pasteur pipette was blunted by inserting it into Bunsen flame and precipitated DNA extracted by dipping the Pasteur and gently pulling. The genomic DNA was clearly visible, it was allowed to air dry briefly, and then the inserted into 300 ul of 70% ethanol, dried and the DNA resuspended in 200 ul of water. It was allowed the DNA to dissolve overnight at room temperature. Nucleic acid concentration was determined using 260/280 nm absorbance measurements on a spectrophotometer.

Probes isolation:

Plasmid DNAs were digested with the opportune enzyme to release the probe fragment. After running in 0.8-1% w/v agarose gel in TAE or TBE buffer, the band corresponding to the required DNA was excised using a scalpel, and the DNA fragment purified using the "crash" method. Concentration was measured running 1 ul sample on 0.8% agarose gel.

"Crash" method for DNA gel extraction:

All the DNA fragment used in this work were purified using this technique. Digested DNA were loaded on agarose gel and run to separate the bands. The band corresponding to the required DNA was excised using a scalpel and the obtained agarose-DNA was crashed using a 1 ml syringe. The gel-DNA mixture was loaded on a glass wool cushion placed into a 1.5 ml eppendorf tube pierced on the bottom. The eppendorf placed over another 2 ml eppendorf tube was centrifuged 30 minutes at the top speed. To the obtained liquid phase was added the same volume of phenol, centrifuged again 2' and traited with phenol and phenol/chloroform. The cleaned aqueous phase was precipitated adding the same volume of absolute ethanol and 1/10 v/v 3 M Sodium Acetate. After precipitation at -20°C for 30' the DNA was centrifuged, the pellet washed twice with ethanol 70% and resuspended in water.

Digestion of genomic DNA and gel electrophoresis:

10-20 ug of genomic DNA was digested with the opportune enzyme (10 U/ug genomic DNA). The digestion generally was performed overnight. The digested DNA was loaded and run on a 0.8-1% agarose gel in TAE or TBE buffer ethidium bromide containing overnight at 40 volts. The gel was photographed.

Southern blotting:

The DNA was denatured by incubating gel in 0.2 M NaOH, 0.6 M NaCl with addiction of thimol blue for 1 hour shacking with one exchange of denaturating buffer. The gel was then neutralised by incubating the gel for 1 hour with 1.0 M TrisHCl pH 7.5, 1.5 M NaCl shacking. Southern blot assembly performed as described (Maniatis et al. 1982) using Duralon-UV Membranes (Stratagene) pre-soaked in distilled water and 10x SSC. Blot was performed overnight in 10x SSC. After blotting the filter was rinsed in 6x SSC and UV crosslinked using Stratalinker.

Hybridisation:

The filter was washed with 0.1x SSC, 0.5% w/v SDS at 65°C for 30 minutes (2 incubation of 15 minutes each) shacking. Followed by 4-6 hours of incubation in pre-hybridisation solution at 42°C rolling.

The prehybridisation solution was removed and replaced with hybridisation solution containing the radioactive labelled probe. The filter was incubated overnight at 42°C followed by 30 minutes room temperature wash shaking in 2x SSC, 0.1% SDS (one change after 15 minutes) and 1 hour wash at 52°C shaking with 0.1x SSC, 0.1% SDS (1 change every 20 minutes). The filter was blot dried and exposed to Kodak autograph film, for various times and the films developed.

Radioactive labelling of probe:

Radioactive labelling was performed using Roche Random primed DNA labelling kit and the quick spin columns, following the manufactures instructions.

100x Denhardt	1 g FICOLL400 1 g Polyvinylpyrrolidone (PVP) 1 g BSA (fraction V) Up to 50 ml with water
20x SSC (2 l)	350.6 g NaCl 176.5 g Citric Acid (trisodium salt) Distilled water up to 2 litres
20x SSCP (1 l)	88.2 g Sodium Citrate (trisodium salt) 140.3 g NaCl 43.7 g Na_2HPO_4 12.7 g $Na_2HPO_4 \cdot H_2O$ Distilled water up to 1 litres
S256 (10x)	16 mg PolyA 16 mg PolyC 400 mg yeast t-RNA 100 mg Salmon Sperm DNA 9 mg E.coli DNA Water to 200 ml
Pre-hybridisation solution (for 20 ml)	5 ml 20x SSCP 1 ml 100x Denhart 10 ml Deionised Formamide Water to 20 ml
Hybridisation Solution (for 20 ml)	6 ml 20x SSC 0.2 ml 100x Denhardt's 10 ml deionised formamide 1 ml 10% w/v SDS 2 g Dextran Sulphate 1 ml S256 + Radioactive labelled probe*

* Note: The radioactive probe is mixed with S256 boiled for 10 minutes and quenched on ice, prior to adding to hybridisation solution. This is to ensure the probe is denatured.

2.5.1.5 Polyacrylamide gel electrophoresis (PAGE) and western blotting.

Different polyacrylamide gel concentrations were made following the published instructions (Maniatis et al. 1982), and assembled on the Biorad miniprotean II gel apparatus following the manufacturers instructions.

1-5x10^6 cell sample were first lysed in 200 ul of protein lysis buffer.

Lysis Buffer	150 mM NaCl 1% v/v Nonidet P-40 0.5% w/v DOC 0.1% w/v SDS 50 mM Tris HCl pH 8.0

The protein samples were mixed with 4x loading buffer β-Mercaptoethanol containing, and loaded into the well of the PAGE using a Hamilton syringe.

4x Loading Buffer (Laemli Buffer) for 5 ml	1 ml 1 M Tris-HCl pH 6.8 1 ml β-Mercaptoethanol 0.4 g SDS 0.02 g Bromo Phenol Blue 2 ml Glycerol Water to 5 ml

Resolving	**7.5%**	**10%**	**12.5%**	**Stack 3.8%**
Acr-Bis	1.25 ml	1.6 ml	2 ml	158 ul
Resolving Buff.	625 ul	625 ul	625 ul	312.5 ul Stacking Buffer
SDS 10%	50 ul	50 ul	50 ul	50 ul
H2O	Up to 5 ml	Up to 5 ml	Up to 5 ml	Up to 5 ml

APS 10%	37.3 ul	37.3 ul	37.3 ul	9.3 ul
TEMED	4.15 ul	4.15 ul	4.15 ul	0.9 ul

The gel was run in Tris-Glycine Buffer (27.9 g glycine, 6 g Trizma base, dissolved in 1 litre of water), containing 0.1% v/v SDS, at 55 mA, until the Bromo Phenol Blue dye had run out of the gel. As a molecular weight marker, 4 ul of Rainbow marker (Biorad) was used.

Blotting:

Nitrocellulose membrane cut to the same size as the PAGE gel were pre-soaked in transfer buffer:

Tranfer Buffer (1 Litre)	3 g Trizma Base 14.4 g Glycine 200 ml Methanol 800 ml Water

Blotting was performed using the Biorad western blotting apparatus and assembled following the manufacturers instructions. Upon assembly the inside of the apparatus was filled up with transfer buffer, and run per 1 hour at 200 volts.

Antibodies staining:

After transfer of the proteins had been performed, the membrane was blocked in PBS containing milk (2.5% v/w) for 1 hour. The primary and secondary antibodies were incubated in PBS 0.1% Tween-100 for 1 hour each. Between one incubation and the other 3 wash were performed in the same PBS 0.1% Tween-100 shaking. After the incubation with the secondary antibodies 2 wash in PBS 0.1% Tween-100 was performed and another in PBS alone before developing with ECL kit (Amersham) following the manufacturers instructions.

Dot blot analysis:

Dot blot analysis was performed for a fast screen of clones human collagen VII producing. Nitrocellulose membrane cut to the same size as vacuum plates apparatus were pre-soaked in PBS. Samples were prepared diluting collagen enriched medium (serum free medium with ascorbic acid used to cultivate cells for 24-48 hours) in PBS to a final volume of 500 ul. Vacuum was not switched off until all the samples were dried. Nitrocellulose was Poinceau stained washed twice in PBS-0.1% Tween-20 and blocked in 5% milk PBS-0.1% Tween for one hour following classical Western blot protocol. All the following steps are the same of western blot.

2.5.1.6 Polymerase Chain Reaction Methods:

2.5.1.6.1 Nested PCR for AAVS1/ITR junctions.

Primers specific for ITR and AAVS1 locus site were obtained from PRIMM, Italy.

Right AAV ITR:16s 5'-GTAGCATGGCGGGTTAATCA-3'

17s 5'-TTAACTACAAGGAACCCCTAGTGATGG-3'.

AAVS1 region: a 5'-GCCCCACTGCCGCAGCTGCTCCC-3'

b 5'-CCGCACAGGCCGCCAGGAACTCG-3'

c 5'-GCGCGQCAGAAGCCAGTAGAGC-3'

d 5'CTGGCTCAGGTTCAGGAGAGG-3'

e 5'-CGCTCAGAGGACATCACGTG-3'

f 5'-GGGACACAGGATCCCTGGAQGG-3'.

All the primers had a melting temperature of 60°C. I round PCR enables amplification of integrated 3' integrated cassette.

dNTPs were obtained from Roche, water was injection grade, while the Taq was the AmpliTaq Gold polymerase (Applied Biosystems, Roche, NJ, USA).

Genomic DNA was extracted following protocols (See Materials and Methods 2.5.1.5).

I Round of PCR mix was obtained as follows:

I Round For primer (3 uM)	5 ul
I Round Rev primer (3 uM)	5 ul
10x Taq buffer	5 ul
Taq polymerase (5 U/ul)	0.5 ul (2.5U)
dNTPs (10 mM)	1 ul
DNA	500 ng
Water	To 50 ul
$MgCl_2$	7 ul

II Round of PCR mix was obtained as follows:

II Round For primer (3 uM)	5 ul
II Round Rev primer (3 uM)	5 ul
10x Taq buffer	5 ul
Taq polymerase	0.5 ul
dNTPs (10 mM)	1 ul
Template 1:100 from I Round PCR	5 ul
Water	To 50 ul
$MgCl_2$	7 ul

The mix was placed in 200 ul Perkin Elmer PCR tubes, and PCR was performed in a Perkin Elmer GeneAmp 9700 termal cycler following the programme below (both for I and II Round):

Denaturation step of 10' 95°C

35 cycles:

Denaturation step of 30'' 94°C

Annealing step of 30'' 60°C

Extension step of 1' 72°C

A final step:

Extension step of 5' 72°C

At the end of II Round amplification PCR samples were mixed with DNA loading dye and run 1.5% w/v agarose gel in TBE buffer, containing ethidium bromide, and visualised on a UV lamp.

Negative control for PCR reaction was water alone.

2.5.1.6.2 PCR for p5 element amplification.

Primers specific for 5' and 3' of p5 element were obtained from PRIMM, Italy in SDS-PAGE purified grade and had the following sequences:

- P5ΔTATAfor:GCTCTAGAGCCGACATTTTGCGACACCATGTGGTCACGCTGG GAAAAAAAGCCCGAGTGA
- P5ΔTATArev:CGCAAGGCCTTCCCCTAGGGCGGCTGCGCGTTCAAACCTCC GCTTCAAAATGGAGACCCTGCTCACTCGGGC

The primers had a melting temperature of 40°C. PCR enables amplification of not overlapping sequence to obtain full length p5 mutated sequence.

dNTPs were obtained from Roche, water was injection grade, while the Taq enzyme was the Amplitaq Gold (Applied Biosystems, Roche, NJ, USA).

In this protocol no template DNA was used, overlapping primers were sufficient to ensure amplification.

PCR mix was obtained as follows:

For primer	5 ul
Rev primer	5 ul
10x Taq buffer	5 ul
Taq polymerase	0.5 ul
dNTPs (10 mM)	2 ul
Water	To 50 ul
$MgCl_2$	5 ul

The mix was placed in 200 ul Perkin Elmer PCR tubes, and PCR was performed in a Perkin Elmer GeneAmp 9700 termal cycler following the programme below:

Denaturation step of 10' 95°C

5 cycles:

Denaturation step of 1' 95°C

Annealing step of 45'' 40°C

Extension step of 1' 55°C

35 cycles:

Denaturation step of 1' 95°C

Annealing step of 45'' 40°C (+0.8°C/cycle)

Extension step of 1' 55°C (+0.5°C/cycle)

A final step:

Extension step of 10' 72°C

PCR samples were mixed with DNA loading dye and run 2.5% w/v agarose gel in TBE buffer, containing ethidium bromide, and visualised on a UV lamp.

Negative control for PCR reaction was water alone.

2.5.1.7 TOPO-TA cloning method.

Cloning of PCR products into TOPO TA vector (invitrogen) were obtained following manufactures instruction.

2.5.2 Tissue culture methods.

2.5.2.1 Maintenance of cell lines.

HeLa, 293 Cre4, 293T, NIH3T3 were maintained in DMEM media supplemented with 10% FCS with penicillin/streptomycin at 25 U/ml, and L-Glutamine at 2 mM. Cells were typically splitted twice a week by washing once in PBS, adding Trypsin solution incubating 5 minutes and then resuspending in fresh media.

All the cells we used were maintained at 37°C in a humidified incubator with 5% CO_2.

Hel, K562 were maintained in RPMI-1640 with 10% FCS with penicillin/streptomycin at 25 U/ml, and L-Glutamine at 2 mM.

All these cells were splitted 1:10 twice a week depending on the experimental requirements.

2.5.3 Gene transfer methods.

2.5.3.1 Generation of Adenoviral stocks.

Viral stocks were prepared by transfecting 293Cre4 cells and co-infecting with helper virus.

DNA tranfection using Calcium Phosphate precipitation method:

1. Seed and incubate $5x10^6$ 293Cre cells in 10 cm dish, approximately 24 hours before transfection in DMEM, 10% FCS, penicillin (25 U/ml), Streptomycin (25 U/ml).

2. Change medium 4 hours before transfection.

3. The plasmid DNA mix is prepared by adding DNA and water to a final volume of 450 ul per dish in a 15 ml Falcon tube. Finally add 50 ul 2.5M $CaCl_2$.

4. The precipitates are formed by adding dropwise of 500 ul of DNA-water-CaCl2 mixture to 500 ul 2xHBS vortexing at full speed. The precipitate should be added immediately to cells. High magnification microscopy of cells should reveal a very small granular precipitate initially above the cells monolayer and after incubation in 37°C incubator overnight, on the bottom of the plate in the space between the cells.

5. The precipitated plasmid DNA should be allowed to stay on the cells for 14-16 hours, after which the media should be replaced with fresh media.

2x HBS (for 50 ml)	5 ml Hepes pH 7.1 (100 mM final) 2.8 ml NaCl (280 mM final) 150 ul Na_2HPO_4 (1.5 mM final) pH 7.1 with HCl
2.5 M $CaCl_2$ (for 100ml)	36.8 g Water to 100 ml

Helper virus co-infection:

Cells after transfection should be infected with helper virus for Adeno production.

Media must be removed and cells washed twice in PBS.

After second wash helper virus at the suitable MOI can be added in PBS and dishes can be incubated for 1 hour in 37°C incubator. After incubation without removing PBS freshly media can be added and cells can be incubated in 37°C incubator.

2.5.3.2 Viral harvest and concentration.

Rescue and amplification of the HD-Ad viruses were carried out by transfection of 293Cre4 and infection with AdH14 first-generation helper virus (Merck, West Point, PA, USA), as previously described (179)

2.5.3.3 Titration of Adenoviral vectors.

1. Plate $5x10^4$ cells per well the day before in a 6-well plate (the day after you will have approximately 10^5 cells/well).
2. The following day, prepare serial ten-fold dilutions of viral stocks in PBS.
3. Titrating the viral stock you should have 500 ul-1 ml of the PBS dilute viral stock per each well.
4. Incubate the Hela cells with PBS dilute virus for 1 hour at 37°C 5% CO_2 incubator.
5. Add fresh medium to 3-4 ml.
6. Incubate 36-48 hours at 37°C 5% CO_2 incubator.
7. Wash well with 2 ml PBS.
8. Add 500 ul of Trypsin to each well. Wait until cells are detached from plates (5' 37°C).
9. Add 2 ml PBS to each well and harvest cells in FACS tubes.
10. FACS samples and calculate the titer.

Notes:

The MOI (multiplicity of infection): TU/ml/n. cells to be infected for the following ranges: 10^{-3} ul-1 ul infection. Efficiency is primarily controlled by vector concentration (TU/ml). MOI should be considered only for certain ranges of concentration of cells (>10^4 cells/ml) and vector (>10^6 TU/ml)

2.5.3.4 $CD34^+$ stem/progenitor cells purification and transduction.

1. Human $CD34^+$ stem/progenitor cells were purified from the FICOLL mononuclear cell fraction of umbilical cord blood by positive selection using the CD34 magnetic cell isolation kit.

2. $CD34^+$ cells were infected with viral stocks at a MOI of 50-300 in serum-free IMDM 20% BIT serum substitute containing, supplemented with 20 ng/ml rhIL-6, 20 ng/ml rhTPO, 100 ng/ml Stem Cell Factor and Flt3-L for 24 hours.

3. Transduced $CD34^+$ cells were washed in IMDM with 10% Fetal Bovine Serum, plated at a density of 1,000 cells/ml in methylcellulose medium containing 4 U/ml rhEpo, 10 ng/ml GM-CSF, 10 ng/ml rhIL-3, 50 ng/ml rhSCF, and scored by light fluorescent microscopy 10 to 14 days after plating.

4. Transduced $CD34^+$ cells were grown in liquid culture in the same medium used for transduction to maintain an undifferentiated phenotype.

2.5.3.5 Transfection techniques.

Stable cell lines were generally transfected using Calcium Phosphate precipitation (See 2.5.3.1 Generation of Adenoviral vectors for details).

HeLa cells were also tranfected with other techniques to obtain higher levels of positivity of bulk population.

FUGENE transfection:

1. Seed and incubate $3x10^5$ HeLa cells in 6 cm dish, approximately 24 hours before transfection in DMEM, 10% FCS, penicillin (25 U/ml), Streptomycin (25 U/ml).

2. Change medium 4 hours before transfection.

3. The plasmid DNA mix is prepared in 1.5 ml eppendorf tubes by adding not supplemented media (100 ul/ug DNA) to the plasmid DNA.

4. The precipitates are formed by adding dropwise 30 ul/ug DNA of FUGENE reagent following the manufacturers instructions. Bubbling was performed using p200 pipette pipetting 4-5 times in the bottom of eppendorf tube. High magnification microscopy of cells should reveal a very small granular precipitate. After precipitate addition cells must be incubated in 37°C incubator overnight.

5. The precipitated plasmid DNA should be allowed to stay on the cells for 14-16 hours, after which the media should be replaced with fresh media.

Effectene transfection:

1. Seed and incubate $3x10^5$ HeLa cells in 6 cm dish, approximately 24 hours before transfection in DMEM, 10% FCS, penicillin (25 U/ml), Streptomycin (25 U/ml).

2. Incubate the cells under their normal growth conditions.

3. Dilute 1 ug DNA dissolved in TE buffer, pH 7.0 to 8.0 with the DNA condensation buffer, Buffer EC, to a total volume of 150 ul. Add 8 ul Enhancer and mix by vortexing for 1''.

4. Incubate to room temperature for 2-5' then spin down the mixture to remove drops.

5. Add 25 ul Effectene Transfection Reagent. Mix by pipetting up and down 5 times or by vortexing 10''.

6. Incubate the samples for 5-10' at room temperature to allow transfection-complex formation.

7. Aspirate medium from cells and wash once with PBS.

8. Add 1 ml growth medium to the tube containing the transfection complexes. Mix by pipetting up and down twice, and immediately add the transfection complexes drop-wise onto the cells in the 60 mm dishes. Swirl the dish to ensure uniform distribution of the transfection complexes.

For 6 cm dishes

DNA ug: 1

Enhancer ul: 3.2

Final Volume DNA in EC Buffer ul: 100

Volume of Effectene ul: 10

Volume of medium to add to cells ul: 1600

Volume of medium to add to complexes: 600

2.5.3.6 Stable cell lines.

1. HeLa cells were maintained in DMEM supplemented with 10% FCS, and transfected/transduced in 6-10 cm Petri dishes as indicated.

2. Cells were kept in culture to lose not integrated plasmids/viruses.

3. Cells were FACS sorted and the enriched bulks were limited diluted. 0.3 cells per well (in 96 wells plates) were plated.

4. Isolated clones were subsequent grow up and expanded in bigger plates, till 10 cm plates.

Chapter 3

Aim of the work

Rationale.

Gene transfer in somatic cells has without any doubt a big potential to treat a number of genetic and acquired diseases. Among the several delivery systems developed, viral vectors derived from retroviruses, moreover murine retroviruses, are the most widely used.

Retroviruses are peculiar in respect to other viruses by two characteristic steps in their life cycle: reverse transcription, resulting in a double strand DNA copy of the viral RNA genome, and integration, leading to the covalent attachment of the viral DNA to host cell DNA.

Integration process is an unequalled, and often indispensable tool to obtain high efficiency and stable gene transfer.

Up to now retroviral and lentiviral vectors are the only available tools to integrate foreign genes into human cells at reasonable efficiency. However their use involves some important problems and limitations:

1. Retroviral vectors (both gammaretroviral and lentiviral) can generally integrate only transgenes with a size limit of 5-7 kb.
2. Independent regulation of multiple transcription units is difficult in a retroviral vector context.
3. Integration of retroviral vectors into the target cell genome occurs randomly, preferentially into active genes. In the last years to this phenomenon has been associated an important risk of insertional mutagenesis and oncogenesis due to the deregulation of gene/s near the genomic region in which the provirus integrates (0).

Alternative to retroviruses are present but at the moment not well studied and developed.

Due to these limitations we decided to explore other viral systems to achieve high efficiency and stable gene transfer. In particular our aims were to obtain a good system to achieve site-specific integration and a vector without stringent limitation in cassette accommodation.

We explored the possibility of other viral systems using a large cassette and trying to target it in a site-specific way.

Due to the know how of our laboratory, we choose to use a new kind of vectors, the Ad/AAV hybrid vectors. In fact they theoretically possess all the requisition we need: large capacity and site-specific integration machinery.

The wild-type AAV genome is a linear, single-stranded DNA filament of 4.7 kb, which contains at both ends a 145-base inverted terminal repeat (ITR) sequence, encoding the origin of replication and the packaging signals, and two AAV-specific genes, rep and cap (31). Rep gene encodes four overlapping proteins of 78, 68, 52, and 40 kDa, generated by alternative splicing of transcripts from two alternative promoters. The ITRs and either Rep78 or Rep68 are sufficient for replication of the AAV genome and mediating its integration into a specific site (AAVS1) on human chromosome 19q13.3–qter (45, 5).

Due to the very limited packaging size of wt AAV particles, recombinant AAV vectors are deleted of all viral genes and have therefore lost the Rep-mediated, site-specific integration property of the wt viruses.

The recombinant AAV vectors maintain only a residual capacity for ITR-mediated integration in some target cells (e.g. liver), although at low efficiency and with virtually no site-specificity (26).

The AAV ITRs and Rep functions have been previously incorporated into hybrid, large-capacity viral vectors, such as baculoviral and HSV-1 amplicon vectors (57, 59), or into a split Ad/AAV vector system, in which an AAV ITR-flanked integration cassette and a Rep78/68 expression cassette were carried by two different HD-Ad vectors (57) (Fig. 3.1).

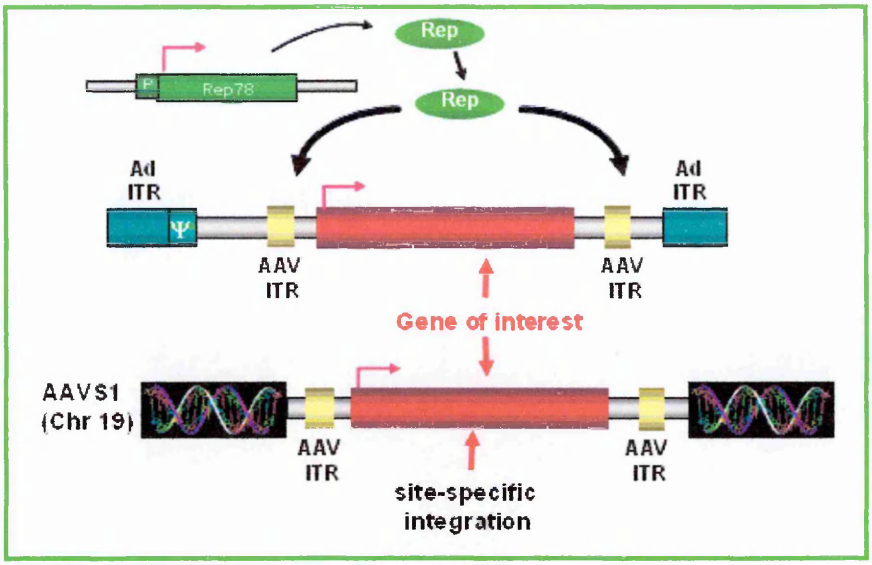

Fig. 3.1 Schematic representation of Ad/AAV integration machinery in a split vector design. In this vector design the integration cassette is contained between the AAV ITRs and subcloned inside the Ad ITRs to be packaged. The Rep78 integration protein is supplied in trans using a non integrating Ad vector. Rep act on AAV ITR and AAVS1 sequences permitting the cassette integration into human Chr19.

In these systems the inhibitory effect of Rep on viral replication prevented or significantly affected the production of Ad and HSV-1 vectors incorporating all the elements of the AAV integration machinery.

Background

Recently in this laboratory it was described the development of a single hybrid Ad/AAV vector (an alternative to the split Ad/AAV system) carrying a double reporter gene integration cassette flanked by AAV ITRs and, outside to the AAV ITRs (into the non integrating region) a tightly regulated, drug-inducible Rep expression cassette (Fig. 3.2). This hybrid vectors were successfully packaged and purified at a titer of 10^9 transducing units/ml. Upon infection at low multiplicity of susceptible human primary cells and cell lines, Rep-dependent, AAVS1-specific integration of the ITR-flanked cassettes of intact size and function was obtained in the absence of any cell selection.

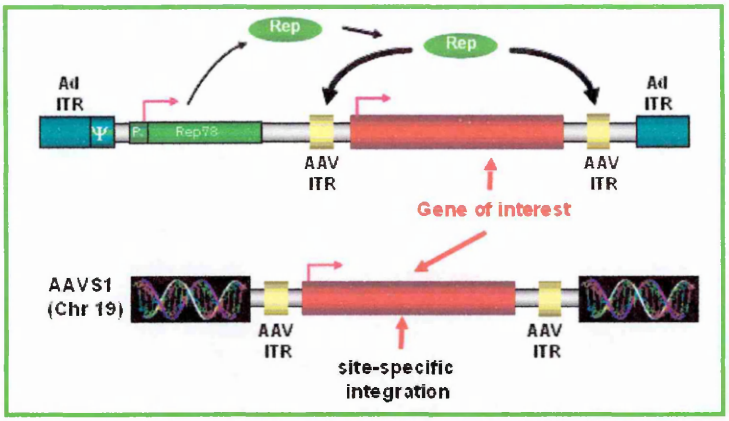

Fig. 3.2 Schematic representation of Ad/AAV integration machinery in a single vector design. In this vector design the integration cassette is always contained between the AAV ITRs and subcloned inside the Ad ITRs to be packaged. Rep78 gene is subcloned in the same vector outside the integrating AAV region.

The Ad/AAV vector system posses two interesting and powerful characteristics that justify our interest on this system:

1. The possibility to integrate in a site-specific way different types of gene expressing cassettes.

2. The possibility to package and target into the target cell a very large DNA fragment (up to 30-35 kb) eventually together with regulatory sequences/elements.

Specific goals.

In this work I tried to explore, characterise and improve all the characteristic of the ITRs-Rep mediated integration of Ad/AAV hybrid vector system in a large cassette contest.

In the hybrid Ad/AAV system the elements responsible for the site-specific integration derive from the AAV virus: ITRs and Rep protein.

The integrating cassette is flanked by the two AAV ITRs and subcloned inside to the Ad vector that permits the accommodation of a very large cassette (Fig. 3.3). A limitation, that we want here to explore was the capacity of AAV integration machinery to integrate such a large gene in respect to its wt genome.

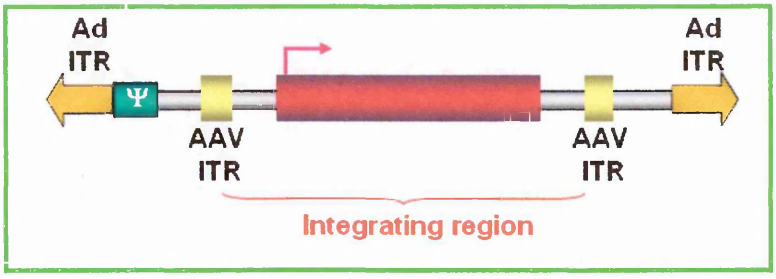

Fig. 3.3 Schematic representation of Ad/AAV vector. The integrating region limited by the AAV ITRs is inserted in the space where was the Adeno genome. In this way there is the possibility to insert very large genes.

Concerning Rep, there are two possibilities to express this protein: subcloning a tightly regulated Rep expressing gene into the non integrating region of Ad/AAV vector (16) (Fig. 3.4 upper panel), or co-transducing cells with both the ITRs flanking cassette and an Ad non integrating vector expressing Rep in a tightly regulated way. (Fig. 3.4 lower panel).

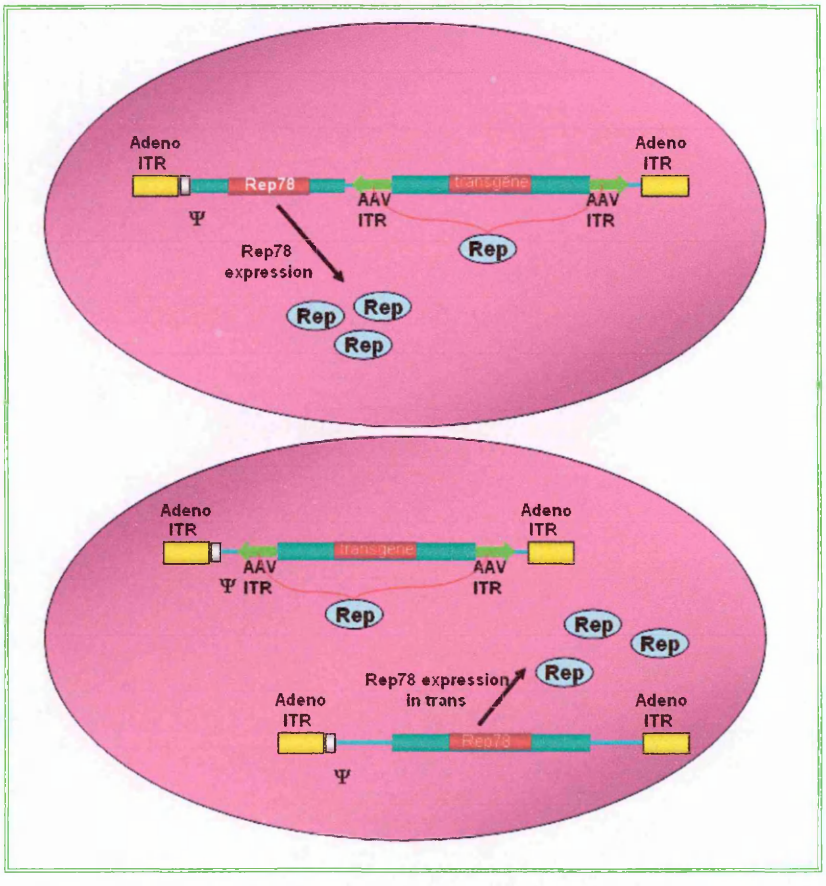

Fig. 3.4 Schematic representation of Rep expression alternatives. Rep can be both administered subcloning it in the non integrating region of an Ad/AAV vector (upper panel) or co-transducing target cells with an Adeno non integrating vector expressing the Rep cDNA (lower panel). The second option can circumvent most of the problems linked to the packaging of the vector in which there is a residual Rep expression.

The development of an efficient integrating, large-capacity viral vector is still an unmet goal of gene transfer technology. The design of helper-dependent (HD), fully deleted Ad vectors has significantly reduced the limitations associated with the first-generation Ad vectors system (e.g. acute toxicity, inflammatory and cytotoxic immune response against the viral proteins) and offers an interesting opportunity to investigate the possibility to transform an Ad non integrating vector into an Ad/AAV hybrid integrating vector.

Chapters 4-7

Results

Chapter 4.

Construction of a large capacity Ad/AAV

4.1 Ad/AAV hybrid vector.

In this first part of my thesis project I decided to design a large capacity Ad/AAV vector to explore the possibility to obtain a high titer virus stock production and compare the efficiency and abilities of the Ad/AAV hybrid vector system in targeting site-specifically an integrating cassette in respect to its size.

In particular I decided to compare the published data regarding the Ad/AAV expressing an integrating cassette constituted by two reporter genes GFP and NGFR (around 4 kb) with a new designed larger ITR-ITR cassette containing the human collagen VII cDNA and the GFP reporter gene (12 kb).

4.1.1 Vector design.

To test the efficiency of Ad/AAV hybrid system as a gene transfer system able to target and integrate efficiently a large expressing cassette into human genome I decided to produce an Ad/AAV viral stock using a Helper Dependent (HD) system.

This system consists of one plasmid expressing the fully deleted Ad vector genome in which we introduced the transgene flanked by the AAV region responsible for integration into the human genome (ITRs).

I decided to subclone inside this kind of vector a constitutively expressed human cDNA collagen VII gene with a second gene, the GPF (Green Fluorescent Protein) as a marker. Collagen VII-GFP represents a very large cassette to be targeted and integrated into a host cell in respect to smaller previously tested vectors (Fig. 4.1 e 4.11).

It is unknown if this system (AAV-ITR + Rep), designed for a genome that is 1/3 of the cassette I tested, was able to integrate such as large transgene, and to do it efficiently and in a site-specific fashion.

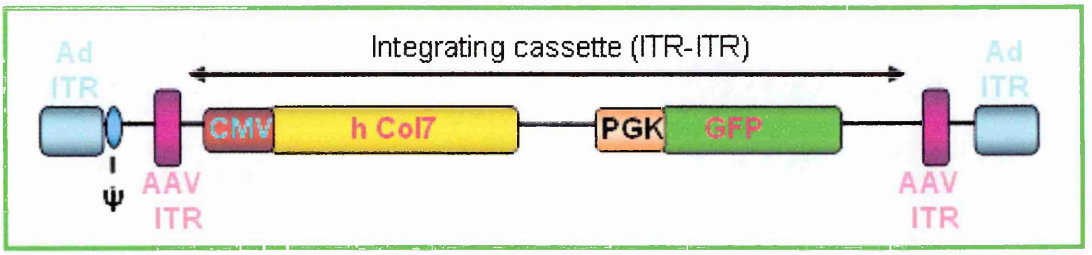

Fig. 4.1 Schematic representation of large integrating vector. The integrating cassette, flanked by AAV ITRs is composed by a large expressing gene (hCol7) under the control of CMV promoter and by a selective marker (GFP) under the control of PGK promoter. In this case Rep is expressed in trans by a non integrating HD-Ad vector.

4.1.2 Large cassette construction.

Cassette was mounted following numerous passages into a pBS SK- plasmid.

First of all the human collagen VII cDNA (from Prof. Meneguzzi G. INSERM U634, Faculty of Medicine, Nice, France) was subcloned as an EcoRI fragment into the EcoRI site of pBS SK- in reverse orientation (pBShcol7REV).

The CMV promoter was recovered as a NruI-EcoRV fragment from the pIRESneo plasmid and subcloned into the EcoRV site of pBS SK- containing human collagen VII (pBSCMVhcol7). The bovine Growth Hormone poly A signal (bGHpolyA) was added to the construct digesting it XbaI and blunting the site. bGHpolyA was obtained from pIRESneo cutting XhoI and XbaI and blunting them.

The cassette was completed (pBSCMVhCOL7pAPGKGFP) introducing to the 3' of CMVhColVIIpolyA the PGKGFPsv40polyA obtained by digesting with EcoRV from pBSPGKGFP. The subcloning was obtained into the EagI blunted site of pBSCMVHCol7PolyA. The two expression cassettes were cloned in the same orientation. The complete large cassette was then extracted by EcoRV digestion from the pBSCMVhCOL7pAPGKGFP vector and subcloned between AAV ITRs. The two ITRs were obtained depriving pBSAAV2 of the whole AAV genome cutting it out with XbaI and filling with klenow to obtain blunt ends.

The ITRs flanking cassette was then cut NotI-ClaI to extract the ITR-flanked cassette and subcloned into the XbaI blunted site of a pBGshuttle vector to perform homologous recombination with the final Ad vector (pΔ28short) (Fig 4.2).

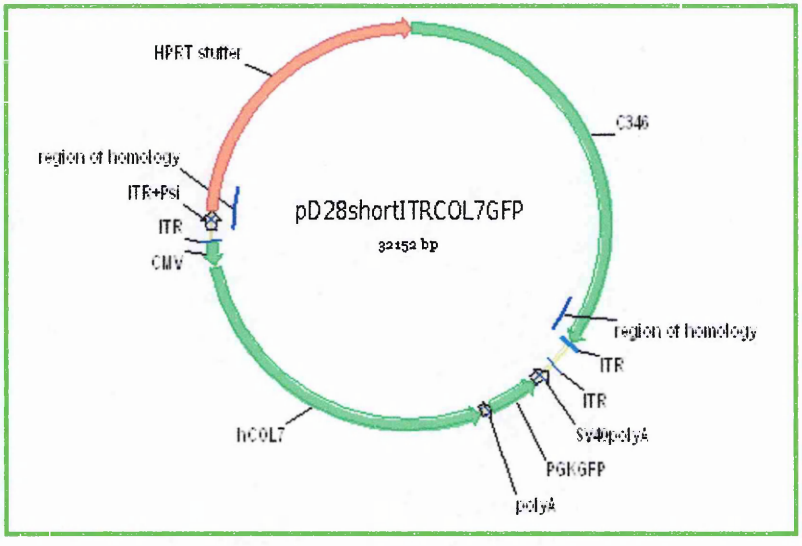

Fig. 4.2 Schematic representation of the large integrating vector.

4.1.3 Homologous recombination.

The final Ad vector was obtained by homologous recombination between the pBG shuttle vector and the pΔ28 vector. The pBGshuttle vector was linearised using the PacI site (Fig. 4.3) to offer free homology regions.

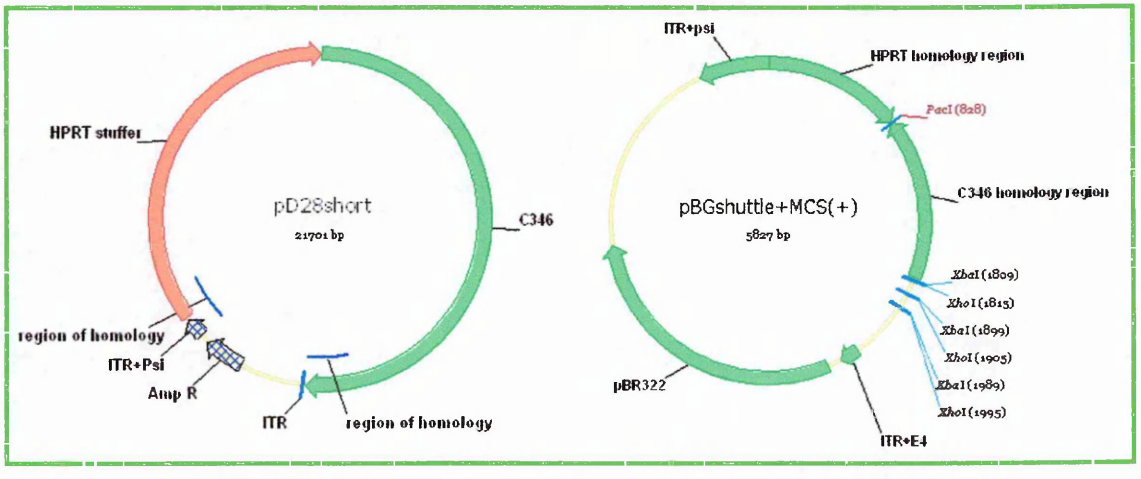

Fig. 4.3 Schematic representation of pD28 vector and pBGshuttle. In the figure the homology regions responsible for the homology recombination event are indicated. On the right panel the XbaI and XhoI cloning site are indicated.

4.2 Vector expression.

Prior to packaging, the Ad/AAV virus vector functionality was tested by transient transfection in 293T and HeLa cells to check for GFP and human collagen VII expression. 293T transfection was done using calcium phosphate method in 10 cm plates. HeLa cells transfection was done using the FUGENE method in 6 cm plates.

Transfection was done with a GFP (pEGFPC3) as a positive control for GFP expression and tranfection efficiency.

Two series of cited cell plates were prepared: one series was analysed by FACS for GFP expression and one series was analysed for human collagen VII expression.

GFP expression:

The day after transfection the cells were washed three times in PBS and 10 ml of fresh medium was added. 24 hours after medium changing cells were detached and analysed by FACS for GFP expressions. Cells were washed twice in PBS and detached with Trypsin. $5x10^5$ cells were resuspended in PBS 1% BSA and analysed by FACS (Fig. 4.4).

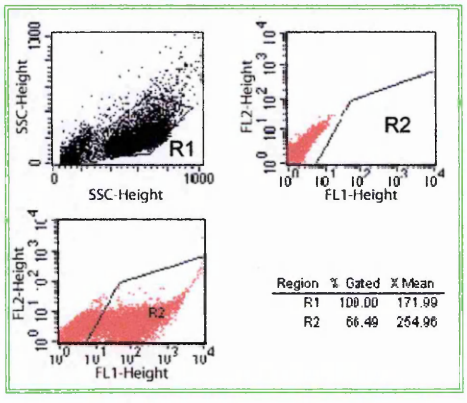

Fig. 4.4 FACS analysis for GFP expression. 293T cells were analysed for GFP expression. R1 gated the living cell population. R2 gated the GFP positive celle population in which there is a FL1 shift. All the transfection demonstrated the correct and efficient expression of GFP by the large capacity Ad/AAV vector.

The vector was able to express correctly GFP.

Human Collagen VII expression:

The day after transfection cells were washed three times in PBS and 5 ml (for 10 cm plates) or 2 ml (for 6 cm plates) of freshly serum free medium containing 50 mg/ml of ascorbic acid. 24-48 hours after medium changing the conditioned medium was harvested and 0.45 um filtered to eliminate debris. 1 ml of the conditioned medium harvested from negative control and hColVII-GFP tranfected cells was dot blotted onto a nitrocellulose membrane. The membrane was treated following a Western blot protocol (See materials and methods) and probed for human collagen VII expression with a monoclonal antibody for human collagen VII (See Materials and Methods) (Fig. 4.5).

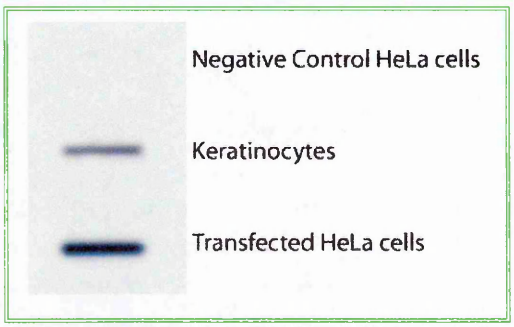

Fig. 4.5 Dot blot analysis for human collagen VII expression and secretion. HeLa cells were analysed for human collagen expression. 1 ml of supernatant from transfected cells was loaded onto nitrocellulose membrane connected to a dotblot apparatus. The samples from transfected cells demonstrated the correct human collagen VII secretion into the medium. Negative control is supernatant from HeLa cells mock transfected. Supernatant from keratinocytesis were used as positive control for human collagen VII expression.

The vector was able to drive correctly synthesis and secretion of human collagen VII into the culture medium.

4.3 Large capacity vector packaging.

Certain of the vector functionality we passed to the HD-Ad virus production.

Ad/AAV virus stock was produced by transfection/infection of the 293Cre4 cell line, as previously described (24).

293Cre4 cells were transfected in 6 cm Petri dishes with pD28shortITRCOL7GFP using calcium phosphate method. The day after cells were washed three times in PBS and 5 ml of fresh medium added. 36-48 hours after transfection cells were co-infected with the helper virus for virus stock production and amplification (as illustrated in Fig. 4.6). 1 ml of PBS containing the helper virus (M.O.I 1) was added to the cells and incubated 30-45' in 5% CO_2 37°C incubator.

All the scale up passages were monitored for GFP expression. Following the increase of GFP positive cells during the scale up passages other helper virus (MOI 1) was added to ensure the constant increase in GFP positive cell number (indicative of Adeno containing transgene amplification). For the scale up process we started from 6 cm dish to end up to 30 15 cm dishes. Cells and supernatants were harvested and processed (See Materials and Methods).

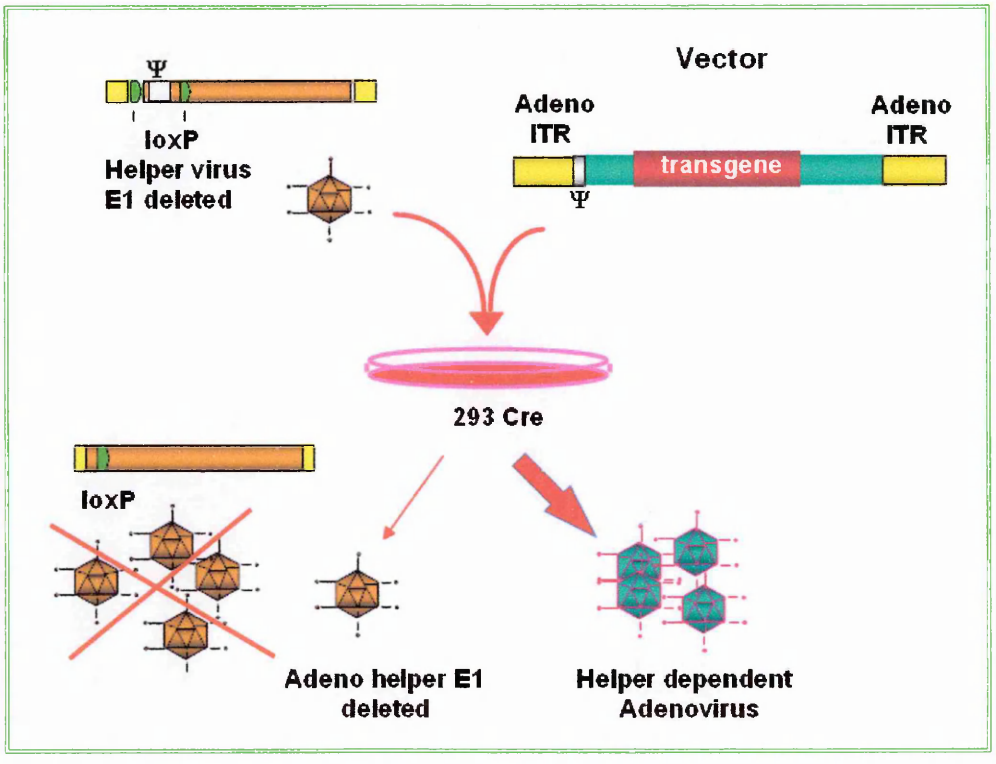

Fig. 4.6 Schematic representation of Adeno Helper Dependent production. Vector plasmid containing transgene is transfected into 293Cre cells. Cells are co-transduced with the helper virus expressing *in trans* all the accessory genes needed for the virus packaging (in our case we utilised MOI 1). The Helper virus has the ψ packaging signal between the two lox p sequences. In presence of Cre recombinase expressed in 293 Cre cells Helper virus can't be efficiently packaged. It is possible to reduce in this way the Helper virus contamination.

4.4 Control of Rep78 expression.

Rep interferes with Ad packaging and is a toxic protein for the host cell, and it is therefore necessary to tightly control its expression (25-27). We decided to use a tet-on control expressing system to administer Rep in a turning on/off system (Fig 4.7).

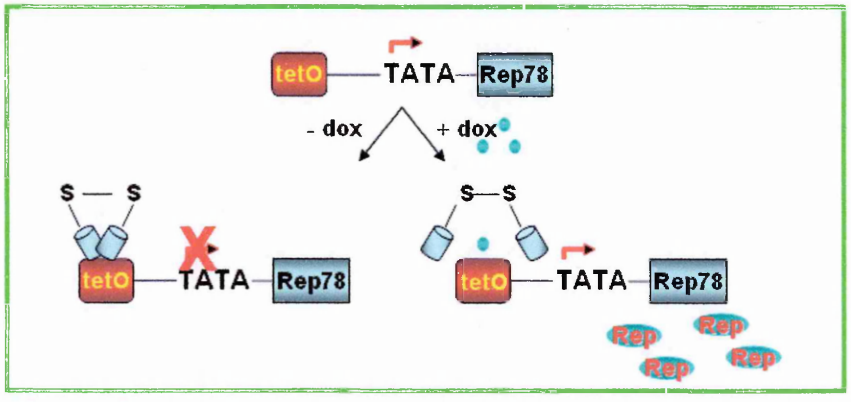

Fig. 4.7 Schematic representation of Tet regulating Rep expression. To overcome or limit the toxic effect in Rep expression we used a tet-on system to switch on/off the Rep production. Rep is expressed in a non integrating Ad and the production was switched on for few days after Ad/AAV transduction adding doxicyclin into the medium.

We tested two kind of vectors for Rep production: CMVRepTS and TKRepTS. The first one containing the transcriptional silencer (tTS) gene expressed under the control of a CMV promoter, while in the TKRepTS vector the Rep78 gene was under the control of the minimal promoter (-81) of the HSV-1 thymidine kinase gene (TK) linked to the tetO element (tetOTK) (Fig. 4.8).

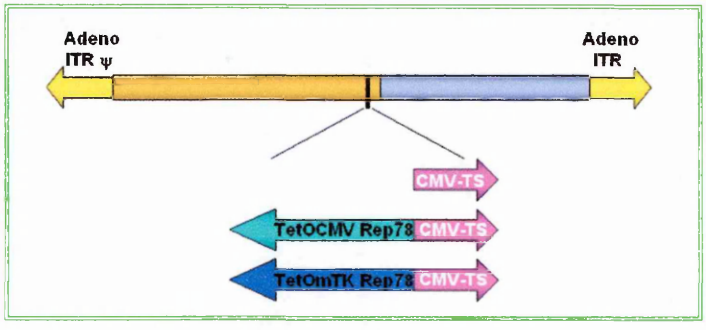

Fig. 4.8 Schematic representation of vector structures. Expression cassettes were inserted into the pSTK120 (25.8 kb) or pSTK119 (23.3 kb) The CMVRep vector contains an AAV Rep78 ORF under the control of the CMV immediate-early enhancer/promoter (-675). In the other vectors an inducible Rep expression cassette is constituted in which the Rep78 ORF is driven by a minimal CMV (-53) or TK (-81) promoter controlled by a bacterial tet operator (tetO) sequence CMVRepTS and TKRepTS.

A control vector, CMVRep, containing only a Rep78 expression cassette driven by the CMV promoter/enhancer in the STK-120 backbone was used to measure the Rep expression level.

Basal Rep78 expression was very well controlled and induced by Dox 48 hours post-transfection at levels comparable to those obtained by an unmodified CMV promoter (Fig. 4.9).

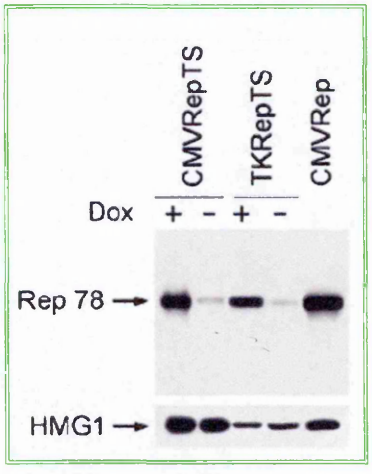

Fig. 4.9 Western blot analysis of Rep expression in 293T cells. The CMVRep vector contains an AAV Rep78 ORF under the control of the CMV immediate-early enhancer/promoter (-675). In the other vectors an inducible Rep expression cassette is constituted in which the Rep78 ORF is driven by a minimal CMV (-53) or TK (-81) promoter controlled by a bacterial tet operator (tetO) sequence CMVRepTS and TKRepTS. 50 ug of protein extract was loaded after measurement by the Bradford method. This Western blot show clearly the possibility to induce Rep in presence of Dox, limiting the Rep expression and cellular toxicity. HMG1 was utilysed as loading control.

To express Rep78 protein we chose to use the CMVRepTS vector.

4.5 Packaging of the Rep78 expressing vectors.

We produced the HD-Ad expressing Rep (CMVRepTS) vector by transfection/infection of the 293Cre4 cell line, as previously described (12 and Fig. 4.6).

The approach in viral amplification in this case, without a marker gene, was different. After five serial passages of viral amplification, the integrity of the episomal Ad vectors

was controlled by Southern blot analysis of Hirt DNA extracted from crude lysates of the packaging cells. Both the CMVRepTS and TKRepTS viruses yielded the predicted restriction fragments when grown in the absence of Dox, while they rearranged when grown in the presence of Dox (results not shown). This data confirmed the known problems of Rep interference with Ad packaging.

Rep production:

6 cm Petri dishes transfected with CMVRepTS and TKRepTS were analysed for Dox Rep induction. After precipitate were washed out one plate per vector type was cultivated in presence of Dox and the other one without. Cells were harvested 24 or 48 hours. Nuclear extracts were analysed by Western blotting using a rabbit anti-Rep polyclonal antiserum. Basal expression level of Rep78 (without Dox) was low from the tetO-CMV promoter and virtually undetectable from the tetO-TK promoter (Fig. 4.10).

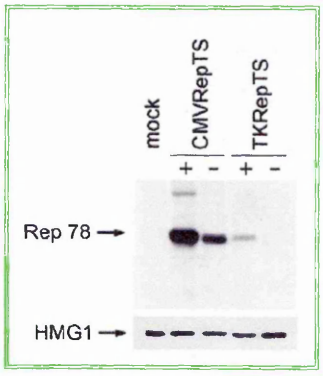

Fig. 4.10 Western blot analysis of Rep expression in 293Cre cells. Cells in which were transfected the two constructs were monitored for Rep expression during virus growth. + and – stand for dox or not dox added. 50 ug of protein extract was loaded after measurement by the Bradford method. HMG1 was utilysed as loading control to normalize the expression of Rep.

4.6 Description of Ad/AAV control vector.

The prototype of integrating vector contained an AAV ITR-flanked integration cassette with two different reporter genes, the green fluorescent protein (GFP) and a truncated

version of the p75 low-affinity nerve growth factor receptor (ΔLNGFR) under the control of the phosphoglycerokinase (PGK) and the SV40 early promoter, respectively, cloned into the STK-120 HD-Ad backbone (Fig. 4.11). In respect to the described large capacity vector this vector possesses the Rep expressing cassette in the non integrating region of the virus. The ITRGNCMVRepTS vector contained only the tTS gene under the control of a CMV promoter, while in the ITRGNTKRepTS vector the Rep78 gene was under the control of the minimal promoter (-81) of the HSV-1 thymidine kinase gene (TK) linked to the tetO element (tetOTK) (Fig. 4.11). The control vector, CMVRep, contained only a Rep78 expression cassette driven by the CMV promoter/enhancer in the STK-120 backbone (Fig. 4.11).

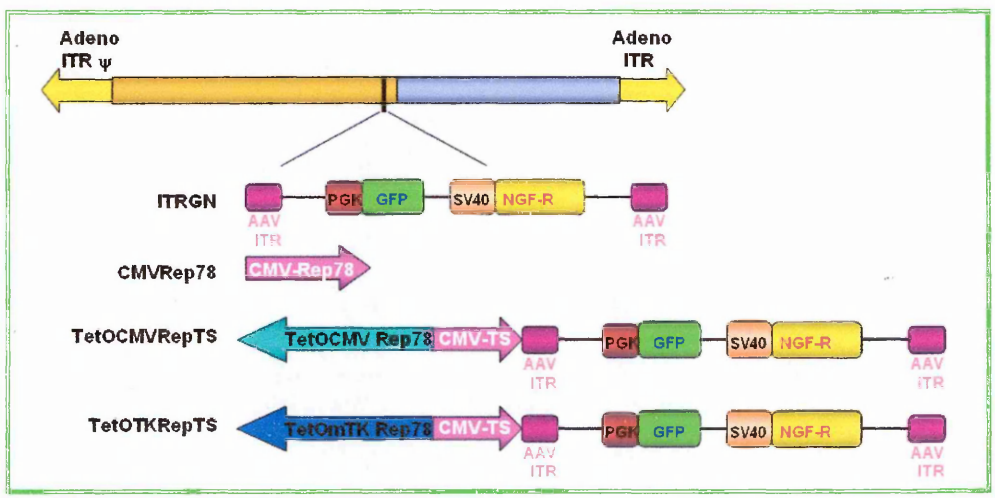

Fig. 4.11 Schematic representation of splitted and single vectors ITR-ITR integrating cassette. In the single vector model Rep is in the non integrating region.

4.7 Viral titration.

Titration to determine the number of transducing units (TU)/ml in the viral vector stock consists of testing serial dilutions on appropriate target cells. The method and time it takes to determine the titer depends on the particular marker gene encoded in the transfer vector and, of course, on the type of transcriptional regulation of the marker gene. For example, vectors with GFP or luciferase markers, under transcriptional control of a constitutive

promoter, can be harvested about 2-3 days post-infection, while for vectors with drug resistant markers it takes approximately two weeks for drug-resistance colony formation.

For vectors in which the marker gene is regulated in a cell-lineage specific fashion, the use of the appropriate cell target is needed. For example, viral titers of vectors with erythroid-specific expression of the marker gene should be calculated by transduction of an erythroblastic cell line.

However, under normal conditions, the most common target cells used to determine viral titers are HeLa and 293T cells.

In our case, viral supernatant titers were determined by transduction of HeLa cells. A fixed number, generally $1x10^5$, of HeLa cells were transduced with serial dilutions of the viral stock preparations. Dilutions of viral supernatant started from 10^{-1} up to 10^{-3}. HeLa cells were transduced with diluted supernatant in PBS for one hour in 37°C 5% CO_2 incubator (See materials and methods).

Transduction efficiency was determined by FACS analysis for GFP expression. Viral titers are usually calculated at that dilution where there is a linear regression of GFP expression and are expressed as transducing units per ml (TU/ml) of viral stock. This is a conventional unit calculated by dividing the number of GFP-expressing cells to the dilution of viral preparation used to transduce cells.

4.8 Large cassette expression after keratinocytes transduction.

Immortalised collagen VII deficient human keratinocytes were transduced at different MOI to test Ad stock proteins production.

Cells were transduced in serum free DMEM for 5 hours in 37°C 5% CO_2 incubator. 10% FCS (final concentration) was supplemented and cells were incubated for 72 hours in 37°C 5% CO_2 incubator prior to gene transfer analysis. 3 MOI were tested 50, 100 and 200.

Control for GFP expression was obtained transducing at MOI 200 with Ad GFP human keratinocytes in the same conditions.

GFP expression:

72 hours after transduction cells were monitored for GFP expression by FACS analysis. Cells were washed twice in PBS and harvested with trypsin. $5x10^5$ cells were resuspended in PBS 1% BSA and FACS analysed (Fig. 4.12)

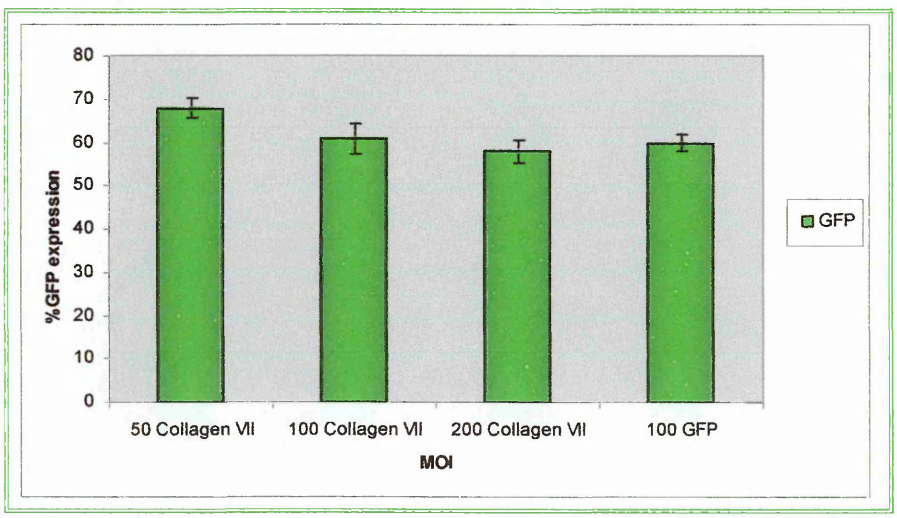

Fig. 4.12 Graphic representation of GFP positive keratinocyte 72 hours after transduction. Keratinocytes were FACS analysed 72 hours after transduction with Ad/AAV expressing human collagen VII and GFP. 3 MOI were tested for Ad/AAV and one (MOI 100) for GFP control to see the expressions of the entire cassette.

Good levels of GFP expression were obtained with GFP control and AdCol7GFP. Raising MOI did not increase the percentage of GFP positive cells, but not toxic effect was observed.

Human collagen VII expression:

72 hours after transduction cells were washed three times in PBS and 10 ml of freshly serum free medium supplemented with 50 mg/ml of ascorbic acid added.

48 hours after medium changing the conditioned medium was harvested and 0.45 um filtered to eliminate debris. All the medium harvested from control GFP and AdCOL7GFP

transduced cells was concentrated by centrifugation in 100 MWCO Amicon columns. Concentrated supernatant was measured by the Bradford method in the spectrophotometer and 30 ug of proteins were loaded on SDS PAGE gel (Fig. 4.13). Western blot was performed following a standard protocol (see Materials and Methods).

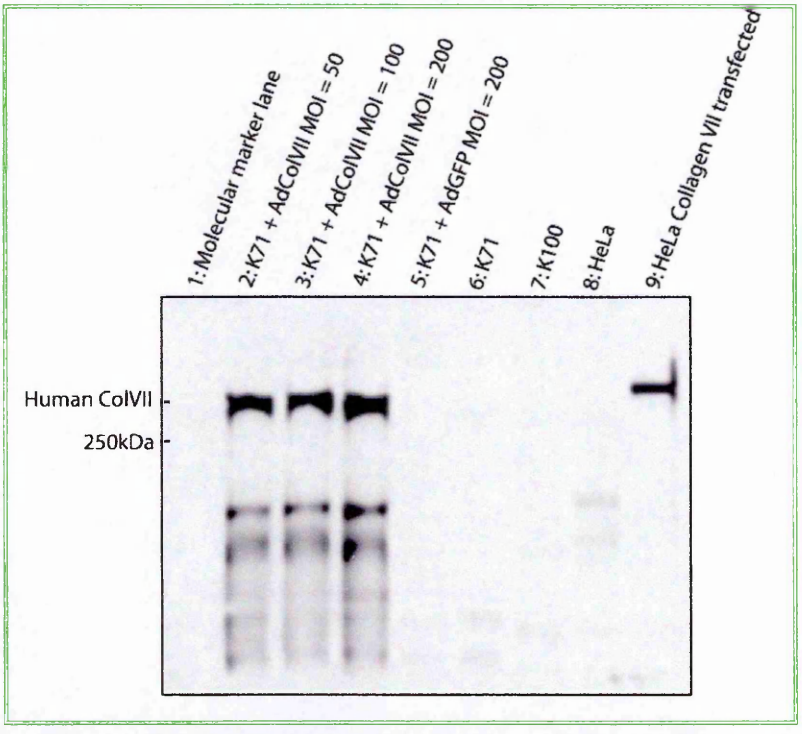

Fig. 4.13 Western blot on transduced keratinocytes concentrated supernatant. Transduced keratinocytes collagen VII deficient were cultived in FCS free medium with 50 mg/ml of ascorbic acid. After 48 hours medium was harvested and concentrated on Amicon 100 MWCO colums. 30 ug of proteins (measured by Bradford method) were loaded on SDS PAGE gel and revealed with anti human collagen VII antibody. K71 and K100 are keratinocytes collagen VII deficient from two different donors. The positive control was represented by HeLa cells transfected with the vector expressing collagen VII.

The vector was able to express correctly human full length collagen VII at very good levels.

Chapter 5

Analysis of Ad/AAV vector integration.

5.1 HeLa cell clones generation.

To compare the efficiency of transgene integration between large capacity (AdITRCOL7GFP) and control (ITRGNRep) vectors we analysed what happened at single cell level.

HeLa cells were transduced with AdITRCOL7GFP and co-transduced with CMVRepTS at MOI 20 for both viruses.

HeLa cell bulk cultures were kept in the presence and absence of Dox to monitor the effect of Rep on overall and site-specific integration.

Bulk culture were monitored for one month for GFP and human collagen VII expression respectively by FACS and dot blot analysis (data not shown).

1.5–2.0% of the cells cultured in presence of Dox, maintained reporter gene expression, while cells cultured without Dox, scored negative already 3 weeks after infection. HeLa cells kept in the presence of Dox maintained GFP expression after one month. After this period HeLa cells were sorted for GFP positivity, and subcloned in 96 well plates at 0.2-0.3 cells/well cell density by limiting dilution (Fig. 5.1).

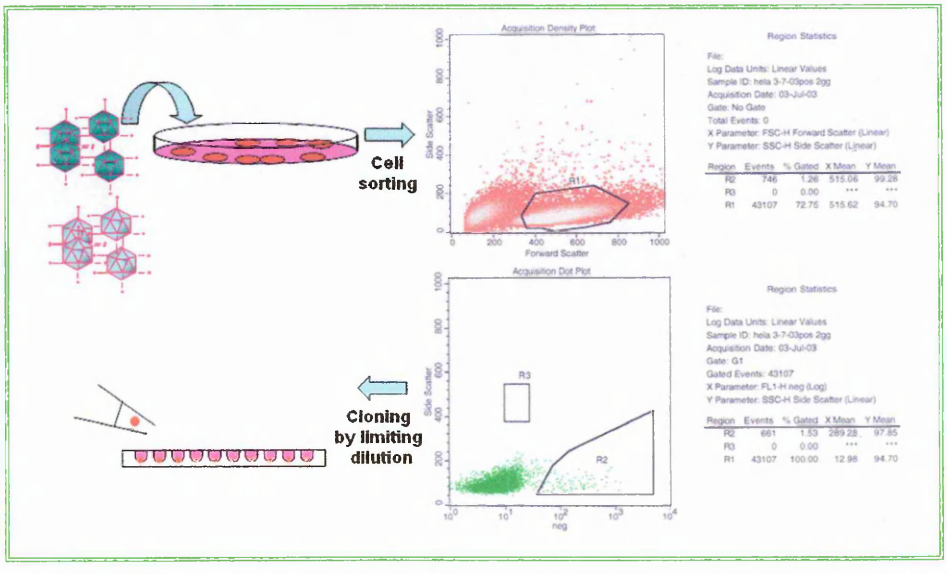

Fig. 5.1 Experimental scheme of clones isolation. HeLa cell clones were transduced with both Rep and collagen + GFP expressing vector. Cells cultured for about a month in presence of Dox were sorted. Sorted HeLa clones were isolated by sorting from the sorted bulk. R1 gated the viable population and R2 gated the GFP population in which there was a shift on X axis.

Single clones were isolated after two weeks of culture and grown for up to one month for further analysis.

More than 50 clones were scored for GFP expression by microscope and FACS analysis (data not shown) and for human collagen VII expression by dot blot (Fig. 5.2). Since the sorted bulk culture was virtually 100% transduced, the vast majority of clones analysed co-expressed GFP and human collagen VII. The presence of GFP and human collagen VII expression was very important because represented a first clue of correct cassette integration.

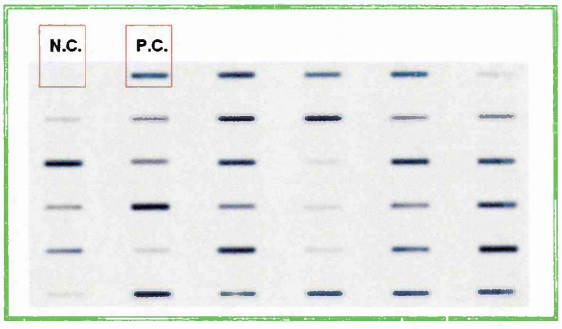

Fig. 5.2 Dot blot analysis for human collagen VII expression and secretion. HeLa cell clones were analysed for human collagen VII expression and secretion. 1 ml of supernatant from transduced cells was dot blotted onto nitrocellulose membrane and recognised following a Western blot procedure with a monoclonal antibody detecting human collagn VII. N.C. is the negative control, 1 ml of supernatant from HeLa cells mock transduced. P.C. is the positive control, 1 ml of supernatant from HeLa cells human collagen VII transfected. Each spot represent a single cell clone.

5.2 Integrity analysis of the integrated ITR-flanked Col7-GFP in HeLa cells.

28 clones were further expanded and genomic Southern blot analysis was performed to determine the integrity of the integrated cassette for each clone. The integrity of the cassette was determined by digestion of genomic DNA with NcoI. NcoI cut twice into the vector releasing a 10 kb fragment encompassing most of the human collagen VII and GFP cDNAs (Fig. 5.3).

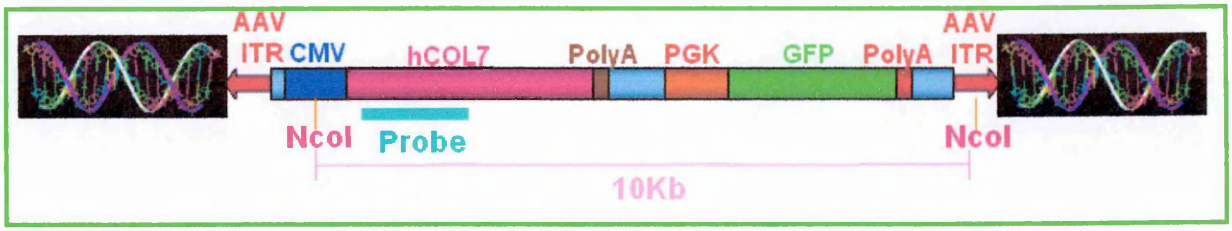

Fig. 5.3 Schematic representation of integrated large cassette. Genomic DNA was digested NcoI to cut the entire cassette from the whole host genomic DNA. NcoI enzyme cut inside CMV promoter and 3' ITR region. Using a human collagen VII specific probe is possible to see a 10 kb band.

This 10 kb DNA fragment can be probed using a human collagen VII specific probe (Fig. 5.3). In all the analysed clones, Southern blot showed no evidence of cassette rearrangement, all the NcoI fragments were of the expected size. This is a very important result. Genome stability of such a large integration cassette was in fact unpredictable, also considering the peculiar nature of its cDNA content. The human collagen VII cDNA sequence has a very repetitive structure, potentially leading to instability and recombination.

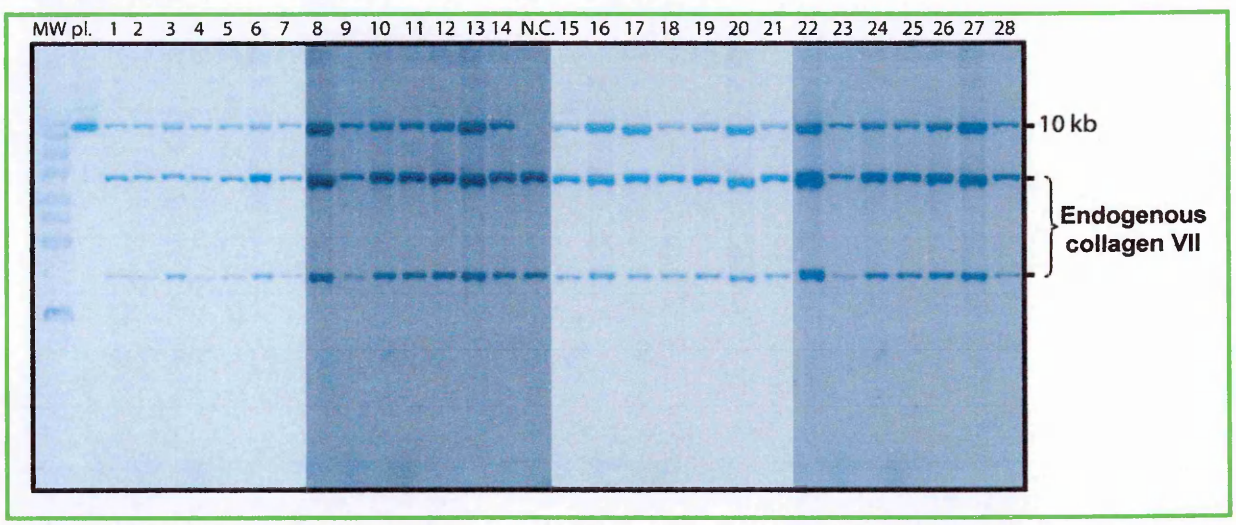

Fig. 5.4 Southern blot analysis of HeLa clones NcoI digested for integrated cassette integrity. pl. stands for plasmid and represent the AdHD plasmid digested with NcoI, N.C. is genomic DNA from Hela cells mock transduced with the virus. 1 → 28 are different HeLa clones. All the 28 HeLa clones showed a 10 kb band corresponding to the correct size of the integrated cassette.

5.3 Human collagen VII expression.

Each positive cell clone was tested by dot blot analysis for human collagen VII secretion (data not shown). $5x10^5$ HeLa cell clones were plated in 6 well plates. The day after plating cells were washed twice in PBS and cells were maintained 24 hours in 2 ml serum free medium with 50 mg/ml of ascorbic acid. 1 ml of the conditioned medium harvested from cells was dot blotted onto a nitrocellulose membrane and probed following the Western blot analysis standard protocol. All the clones analysed expressed human collagen VII. The level of expression was different depending on the clone analysed.

To ensure that what we had seen in dot blot analysis was a correct size protein, we tested by Western blot the clone supernatants.

$5x10^6$ cells of each HeLa clone were plated onto 10 cm Petri dishes. The day after growth cells were washed twice in PBS. 10 ml/plate of serum free medium with 50 mg/ml of ascorbic acid was added and cells were cultivated 24-48 hours in 5% CO_2 37°C incubator. The conditioned samples were collected and 0.45 um filtered to eliminate debris. Supernatants were concentrated with Amicon 100 MWCO columns by centrifugation. Protein-enriched supernatants were measured by the Bradford method and 30 ug of proteins loaded on SDS-PAGE gel. Western blot analysis was performed following standard methods.

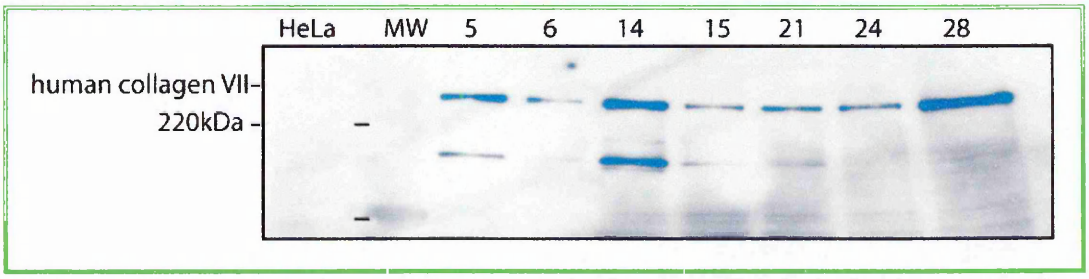

Fig. 4.5 Western blot analysis of concentrated supernatant from HeLa clones. HeLa are wt cells mock transduced, representing the negative control for collagen expression. 5, 6, 14, 15, 21, 24, 28 are AdColVIIGFP transduced HeLa clones selected for analysis. Cells were kept 24 hours in DMEM serum free 50 mg/ml ascorbic acid supplemented. 10 cm plates were incubated 24 hours after transfection with 5 ml media and after incubation time all the medium was 0.45 um filtered and concentrated. 30 ug of total protein sample was run on SDS-PAGE gel. The band under 220kDa is a degraded form of collagen VII.

Western blot analysis confirmed that what we had seen with dot blot screening was effectively a correct human collagen production. Monoclonal antibody we used correctly recognized a band migrating around 300 kDa as expected in all the clones we analysed.

5.4 Site-specific integration of the AAV ITR-ITR large cassette in HeLa cells.

Previously extracted DNA from each HeLa clone was analysed by Southern blotting after restriction with EcoRI, which releases a 9 kb fragment encompassing part of the chromosome 19 AAVS1 site and part of the integrated ITR-ITR cassette (Fig. 5.6). Hybridization with an AAVS1-specific probe and followed by a GFP specific probe showed co-localization in 6 of 23 independent HeLa clones (5 clones after Southern blot analysis revealed the same restriction fragment profile), indicating rearrangement of the AAVS1 region in at least one chromosome 19, in which we obtained site-specific integration (26%).

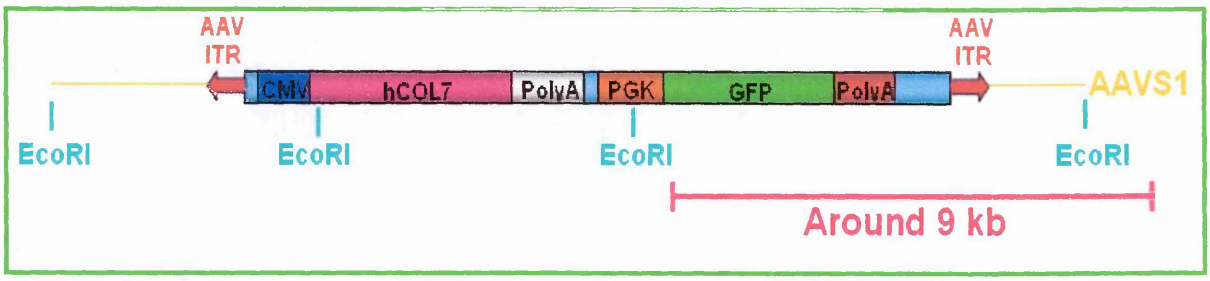

Fig. 5.6 Schematic representation of restriction mapping profile of AAVS1 region with large cassette integration. In the case of AAVS1 site specific integration the vector introduces 2 new EcoRI sites. Co-hybridising Southern blot membrane with both GFP and AAVS1 specific probes is possible to isolate clones with site specific integration.

The same DNA was also digested with AccI which releases a 3.1 kb fragment encompassing most of the chromosome 19 AAVS1. AAVS1 probe showed a size shift of the 3.1 kb band in 16 of 23 independent HeLa clones (70%), indicating rearrangement of

the AAVS1 region in at least one chromosome 19. The rearranged bands hybridized also to a GFP-specific probe in 6 of the 23 clones (26%), indicating the integration of the AAV ITR-flanked cassette in the AAVS1 region.

In 10 clones (43%), the AAVS1 site showed a rearranged band that did not hybridize to the GFP probe, indicating Rep-mediated disruption of the AAVS1 region in the absence of integration. Conversely, 8 of 23 clones showed bands corresponding to intact AAV ITR-flanked cassettes integrated elsewhere in the genome (34%) (Fig. 5.7).

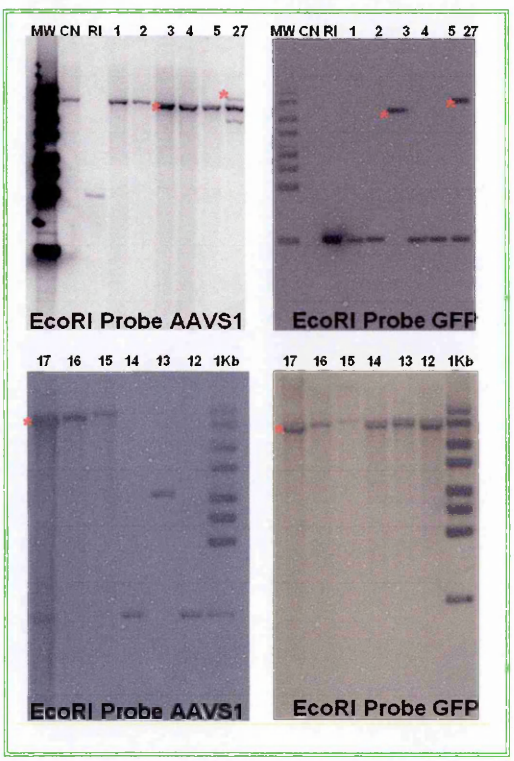

Clone	AAVS1 Rearrangement	Integration
1=2,4,5	Not Present	Random
2=1,4,5	Not Present	Random
3	**PRESENT**	**CHR19**
4=5,1,2	Not Present	Random
5=1,2,4	Not Present	Random
6	Present	Random
7	Present	Random
8=11	Not Present	Random
9	Present	Random

10	Present	Random
11=8	Not Present	Random
12	Not Present	Random
13	Present	Random
14	Present	Random
15	Present	Random
16	Present	Random
17	**PRESENT**	**CHR19**
18	Not Present	Random
19	**PRESENT**	**CHR19**
20	Not Present	Random
21	Not Present	Random
22	**PRESENT**	**CHR19**
23	Not Present	Random
25	**PRESENT**	**CHR19**
26	Present	Random
27	**PRESENT**	**CHR19**
28	Present	Random

Fig. 5.7 Summarising scheme for large cassette integration. Genomic DNA from HeLa clones was digested both with AccI and EcoRI to study the integration of the large cassette into the host genome. In the first panel 2 Soutern blot on the left are hybridised with the AAVS1 probe. Southern blot on the right are the same filters stripped and re-probed with the GFP probe. Site-specific integration was determined when co-hybridisation with AAVS1 probe and GFP probe was present. MW stands for molecular DNA weight, RI is the Adeno plasmid digested with EcoRI, the numbers are single HeLa clones.

5.5 Site-specific integration into human keratinocytes with small cassette vector.

K71 deficient collagen VII keratinocytes were infected with the single vector expressing ITRGN (non integrating vector) alone and with TKRep (expressing the Rep protein able to

integrate the previous vector) at an MOI of 100 and 200. Transduced cells were grown for 5 days in the presence of Dox for Rep expression.

GFP expression:

We tested for GFP expression by FACS analysis 5 days after infection (Fig. 5.8). Cells were washed twice in PBS and harvested with trypsin. $5x10^5$ cells were resuspended in PBS 1% BSA and FACS analysed.

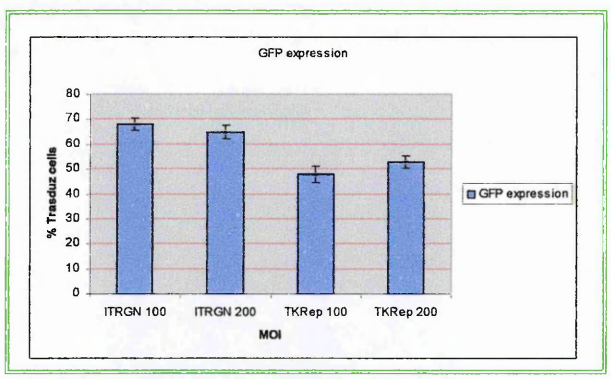

Fig. 5.8 K71 keratinocytes (collagen VII deficient) were transduced with the small cassette vector. ITRGN is the vector without Rep expressing cassette. Two different MOIs were tested. Cells were cultived in presence of Dox for Rep expression where it was present.

Keratinocytes were efficiently transduced with the viruses.

Integrations:

High molecular-weight DNA was extracted from these cells and analyzed it by nested-set PCR with AAVS1- and AAV ITR-specific primers (See Material and Methods).

DNA bands were amplified from keratinocytes transduced by the single vector expressing the ITRGN and TKRep in the presence of Dox.

No signal was detected in cells transduced by the control ITRGN non integrating vector.

We analyzed the distribution of integrants throughout the AAVS1 region by nested PCR using two forward primers on the AAV ITR and three couples of reverse nested primers annealing to different positions within AAVS1 (a and b at nt 526–615, c and d at nt 1175–1349, and e and f at nt 1612–2089, see Fig. 5.9).

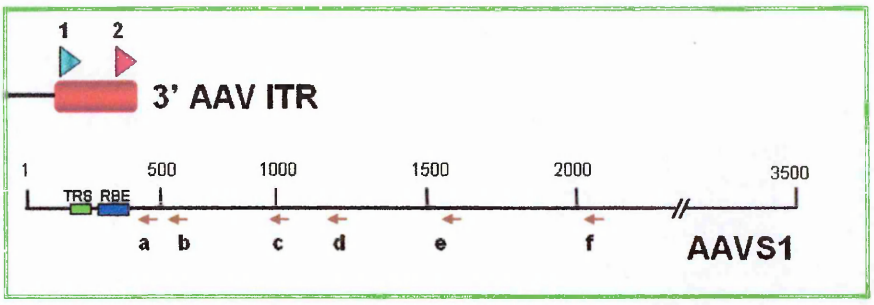

Fig. 5.9 Schematic representation of AAVS1 and AAV 3' ITR nested primers. a-f are 6 primers Rev spanning the AAVS1 region. The For primers are located on the 3' AAV ITR.

Specific DNA bands (200 to 700 bp long) were amplified from all cells only by the c + d and e + f sets of primers (not shown).

To further characterize the integrations, we cloned and sequenced PCR-amplified bands. Analysis of the integration junctions showed that the insertions clustered within a 1 kb region of the AAVS1 (nucleotides 1068 to 2000), downstream of the Rep-binding site (RBS; nucleotides 398–413) (Fig. 5.10).

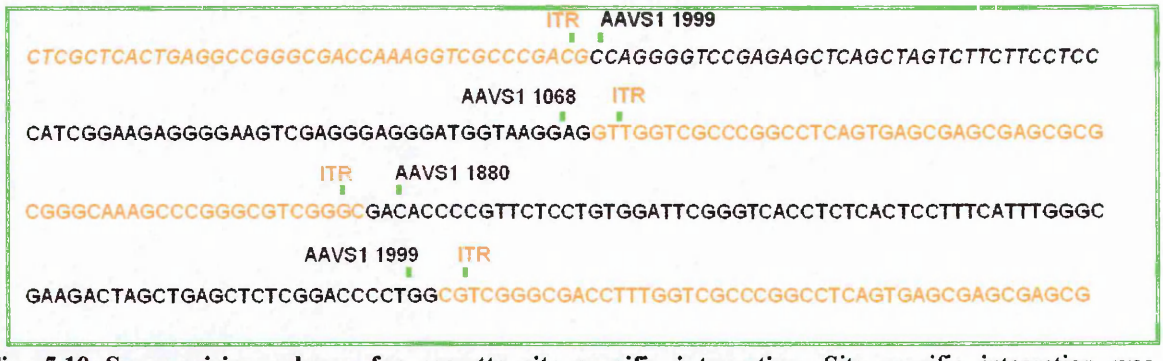

Fig. 5.10 Summarising scheme for cassette site specific integration. Site specific integration was investigated by nested PCR approach and the amplified junctions were sequenced. A clustered insertion point was found within a 1 kb region. Each line represents a different insertion site.

5.6 Site-specific integration into human keratinocytes with the large cassette vector.

K71 deficient collagen VII keratinocytes were infected with the single vector expressing the human collagen VII and GFP alone (non integrating vector) and with TKRep

(expressing the Rep protein able to integrate the previous vector) at an MOI of 100 and 200. Transduced cells were grew for 5 days in the presence of Dox for Rep expression.

GFP expression:

We tested for GFP expression by FACS analysis 5 days after infection (data not shown). Cells were washed twice in PBS and harvested with trypsin. $5x10^5$ cells were resuspended in PBS 1% BSA and FACS analysed (data not shown).

Integrations:

High molecular-weight DNA was extracted from these cells and analyzed it by nested-set PCR with AAVS1- and AAV ITR-specific primers (See Material and Methods).

DNA bands were amplified from keratinocytes transduced by the single vector expressing the human collagen VII and TKRep in the presence of Dox.

No signal was detected in cells transduced by the control ITRCol7GFP non integrating vector.

We analyzed the distribution of integrants throughout the AAVS1 region by nested PCR using two forward primers on the AAV ITR and three couples of reverse nested primers annealing to different positions within AAVS1 (a and b at nt 526–615, c and d at nt 1175–1349, and e and f at nt 1612–2089, see Fig. 5.9).

Specific DNA bands (200 to 700 bp long) were amplified from all cells only by the c + d and e + f sets of primers (not shown).

To further characterize the integrations, we cloned and sequenced PCR-amplified bands. Analysis of the integration junctions showed that the insertions clustered within a 1 kb region of the AAVS1 (nucleotides 1054 to1900), downstream of the Rep-binding site (RBS; nucleotides 398–413) (Fig. 5.11).

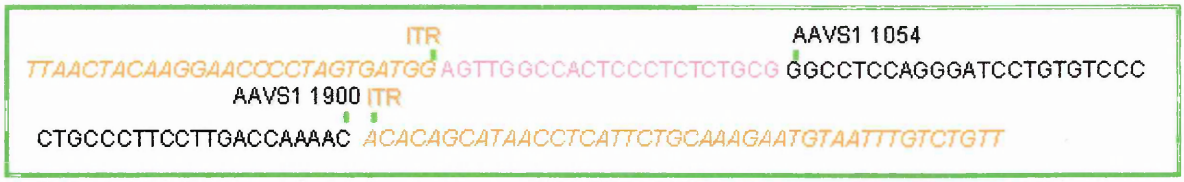

Fig. 5.11 Summarising scheme for cassette site specific integration. Site specific integration was investigated by nested PCR approach and the amplified junctions were sequenced. A clustered insertion point was find within a 1 kb region. Each line represents a different insertion site.

Chapter 6

Optimisation of vector integration.

6.1 p5 element an enhancer on overall and site specific integration?

As we already know Rep mediated integration is extremely inefficient. This inefficiency is worst in a large cassette model.

In my work I tried to find out a system to improve this situation. Two ways were possible to improve the integration efficiency: to act on the integration system, and enhance the transduction efficiency to have more cells with the vectors inside.

Rep-mediated integration of rAAV plasmids is extremely inefficient, with between 0,1 and 1% of transduced cells demonstrating rAAV genome persistence after 6 weeks (48).

In contrast, plasmids that carry the entire AAV genome integrate at efficiencies of greater than 10%. This difference between rAAV plasmids and wt AAV plasmids led to the discovery of a previously unknown cis sequence domain in the left end of the AAV genome that enhances integration efficiency (48). The p5 trs-like motif was identified because it enabled Rep-dependent AAV-2 replication in the absence of the left ITR (132). In addition to its ability to behave as a *cis*-acting replication origin, the p5 region (nucleotides 151 to 289 of wild-type AAV-2) was recently shown to enhance Rep-mediated site-specific integration of plasmid DNA into the human chromosome 19 AAVS1 site (48, 49).

To test the effect of this element in our system we wanted to test a new vector structure/design on overall and site-specific integration percentage re-integrating a mutated form of p5 promoter sequence (p5ΔTATA) into its viral wild-type position, flanking the 5' AAV ITR (Fig. 6.1).

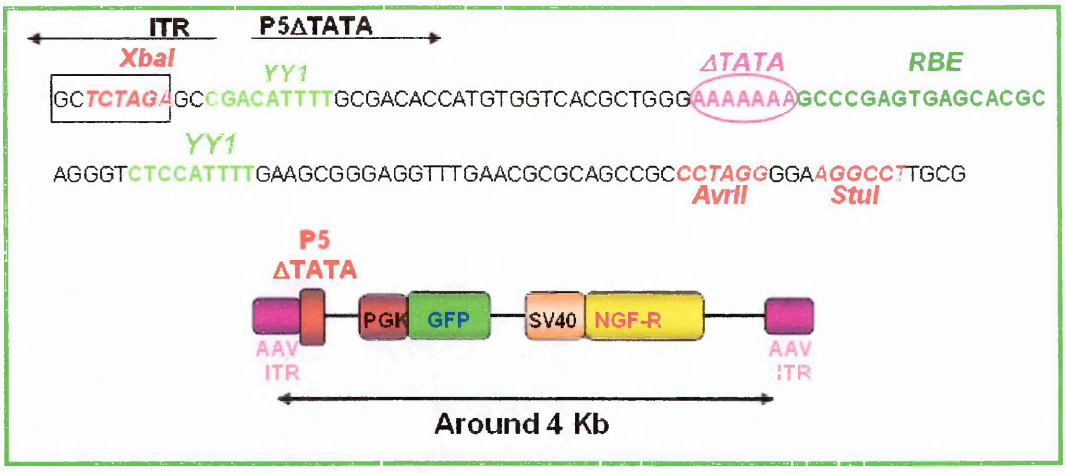

Fig. 6.1 Schematic representation p5 modified sequence. p5 sequence was modified to abolish TATA box by mutating its sequence. The obtained p5ΔTATA was subcloned near the 5' ITR and the ITRp5ΔTATA-ITR was used to flank a two reporter 4 kb integrating cassette.

6.2 ITRp5ΔTATA containing plasmids.

p5ΔTATA promoter sequence was synthesised amplifying two partially overlapping primers into the TATA box mutated region (See Material and Methods). The obtained PCR product was subcloned into a TOPO TA cloning vector. The p5ΔTATA sequence was cut SalI-AvrII blunted and subcloned to the 3' region of 5' AAV ITR into the pBSAAV vector cut XbaI and blunted to obtain pBSAAVp5 (Fig. 6.1).

The 5' unmodified ITR was cut Spe-XbaI and subcloned into a TOPOp5 vector to obtain TOPOp5ΔTATAITR.

The construct pBSITRp5ΔTATAGFPNGFR was obtained digesting the vector pBSITRgfppoliAngfrpoliAinv SalI blunted and XbaI to cut off the 5'ITR and introduce the ITRp5ΔTATA cut DraII blunt and SpeI.

pBSITRp5ΔTATAGFPNGFR was utilised to test the difference in respect to the original construct pBSITRGFPNGFR by transient transfection in HeLa cells co-transduced with the non integrating Ad expressing Rep78 protein. Tranfection experiments were performed in presence and in absence of Dox to switching on/off the Rep production.

$5x10^6$ Hela cells were seeded on 10 cm Petri dishes the day before transfection.

The same amount of the two plasmids (10 ug) was transfected using Calcium Phosphate protocol. HeLa control cells were transfected with a plasmid containing GFPΔNGFR but without ITRs. After an over night incubation of HeLa cells in presence of precipitates cells were washed twice with PBS and fresh medium added for 6 hours and kept at 37°C 5% CO_2. Cells were washed twice with PBS and trasduced with TetRep in PBS (1 ml per 10 cm Petri dish) and incubated for 1 hour at 37°C 5% CO_2. After transduction time 10 ml of fresh medium Dox supplemented was added to PBS containing virus. Transfected transduced HeLa cells were kept in culture one month in presence of Dox to ensure the elimination of non integrated DNA and monitored for GFP expression (data not shown). After this period the GFP positive cells (around 1,5% in the case of wild type ITR and 2,5% for p5ΔTATA) were FACS sorted.

6.3 HeLa cell clones generation.

Cell bulks after FACS sorting were subcloned at 0.2-0.3 cells/well by limiting dilution. Single clones were isolated after two weeks of culture and grown for up to one month for further analysis.

More than 50 clones were scored for GFP expression by FACS analysis (not shown). Since the sorted bulk culture was virtually 100% transduced, the vast majority of clones analysed were GFP positives.

6.4 Site-Specific Integration of the AAV ITR-Flanked Cassette in HeLa cells.

25 clones for pBSITRp5ΔTATAGFPNGFR transfected HeLa and 25 for pBSITRGFPNGFR were further expanded and genomic Southern blot analysis was performed to determine the genome integration of the ITR flaked cassettes for each clone. The site-specific integration of the cassette was determined by digestion of genomic DNA with AccI. AccI cut releases a 3.1 kb fragment encompassing most of the chromosome 19 AAVS1 site.

Southern blot were probed with an AAVS1 and a GFP specific probes.

Unmodified ITR:

In the case of clones obtained from unmodified ITR AAVS1, the probe showed a size shift of the 3.1 kb band in 23 of 25 independent HeLa clones (92%), indicating rearrangement of the AAVS1 region in at least one chromosome 19. The rearranged bands hybridized also to a GFP-specific probe in 16 of the 25 clones (64%), indicating the integration of the AAV ITR-flanked cassette in the AAVS1 region. Further restriction analysis indicated that the AAV ITR-flanked cassette had integrated as a monomer or a dimer in the AAVS1 site and conserved an intact structure in all cases (not shown).

In 7 clones (28%), the AAVS1 site showed a rearranged band that did not hybridize to the GFP probe, indicating Rep-mediated disruption of the AAVS1 region in the absence of integration. Conversely, 2 of 25 clones showed bands corresponding to intact AAV ITR-flanked cassettes integrated elsewhere in the genome (8%). 7 out 25 clones (28%) showed both AAVS1-specific and non-specific integrants (Fig. 6.2).

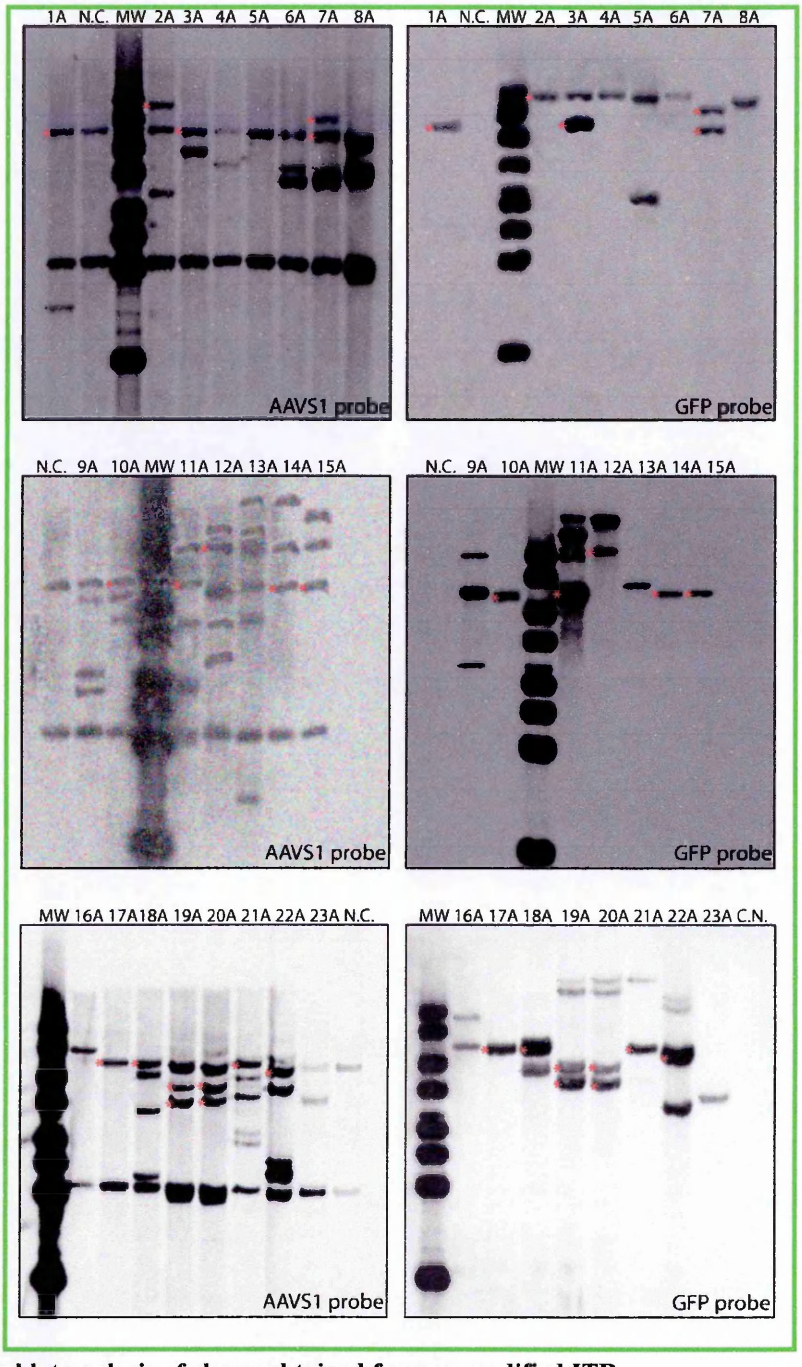

Fig. 6.2 Southern blot analysis of clones obtained from unmodified ITR.

HeLa were transfected with pBSITRGFPNGFR plasmid and transduced with TetRep Ad non integrating vector. 25clones (1A → 25A) were co-hybridised with AAVS1 and GFP specific probes to analyse integrations. Southern blot on the right are the same filters stripped and re-probed with the GFP probe.

p5ΔTATA modified ITR:

In the case of clones obtained from p5ΔTATA modified ITR AAVS1 probe showed a size shift of the 3.1 kb band in 21 of 25 independent HeLa clones (88%), indicating rearrangement of the AAVS1 region in at least one chromosome 19. The rearranged bands hybridized also to a GFP-specific probe in 13 of the 25 clones (52%), indicating the

integration of the AAV ITR-flanked cassette in the AAVS1 region. In 6 clones (24%), the AAVS1 site showed a rearranged band that did not hybridize to the GFP probe, indicating Rep-mediated disruption of the AAVS1 region in the absence of integration. Conversely, 4 out 25 clones showed bands corresponding to intact AAV ITR-flanked cassettes integrated elsewhere in the genome (16%). One clone showed both AAVS1-specific and non-specific integrants (4%).

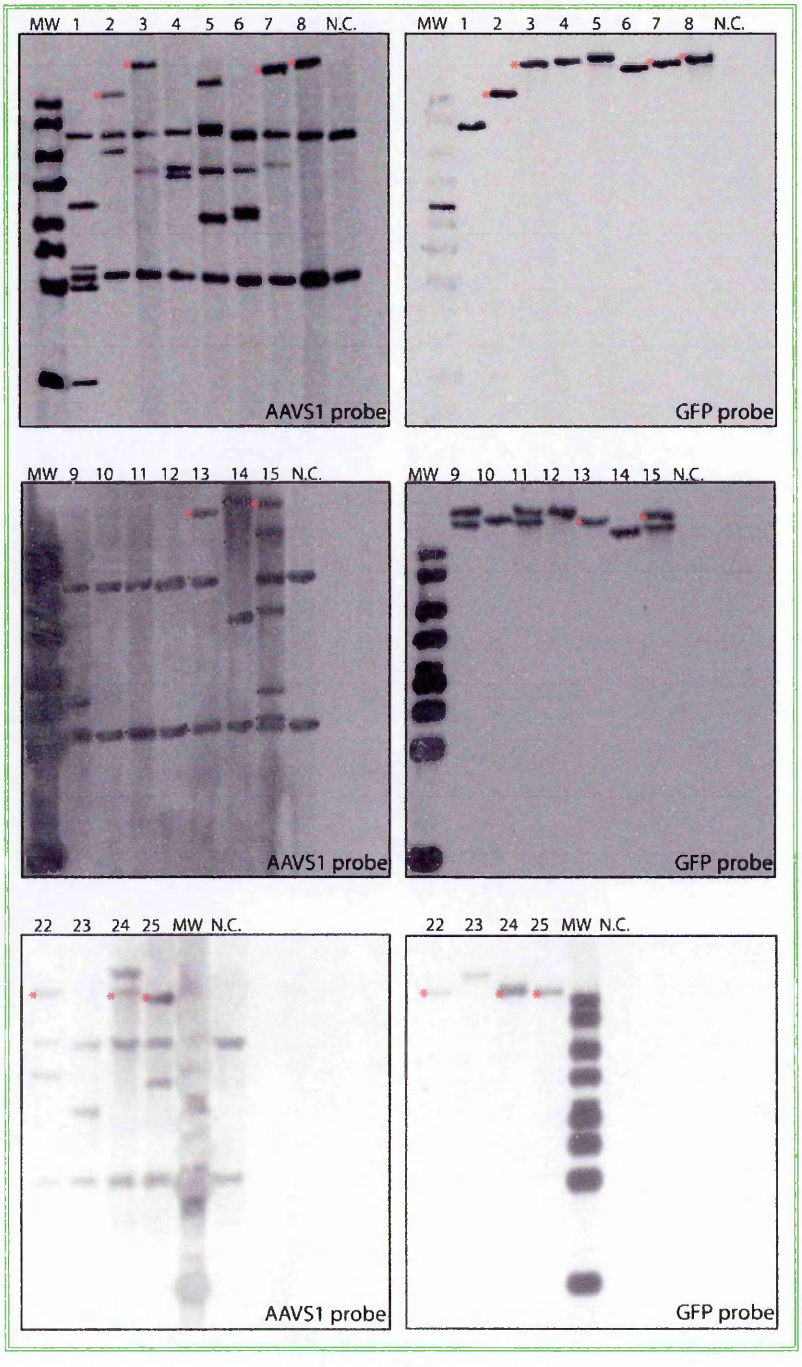

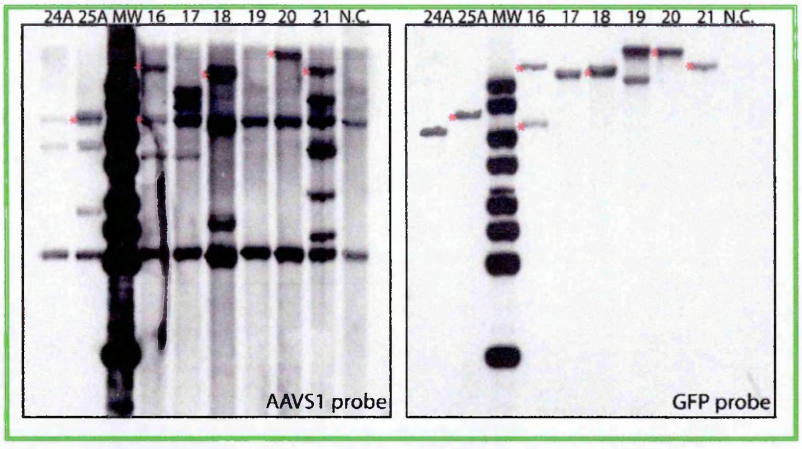

Fig. 6.3 Southern blot analysis of clones obtained from p5ΔTATA modified ITR.

HeLa were transfected with pBSITRp5ΔTATAGFPNGFR plasmid and transduced with TetRep Ad non integrating vector. 25 clones (1 → 25) were co-hybridased with AAVS1 and GFP specific probes to analyse integrations. Southern blot on the right are the same filters stripped and re-probed with the GFP probe.

Analysing the size of the AAVS1 integrated cassette we noticed a big increase in the size of integrated cassette when the cassette is surrounded by the ITRp5ΔTATA. This phenomen is probably due to the integration of multimers of the integration cassette in the AAVS1 locus (Fig. 6.3 and 6.4).

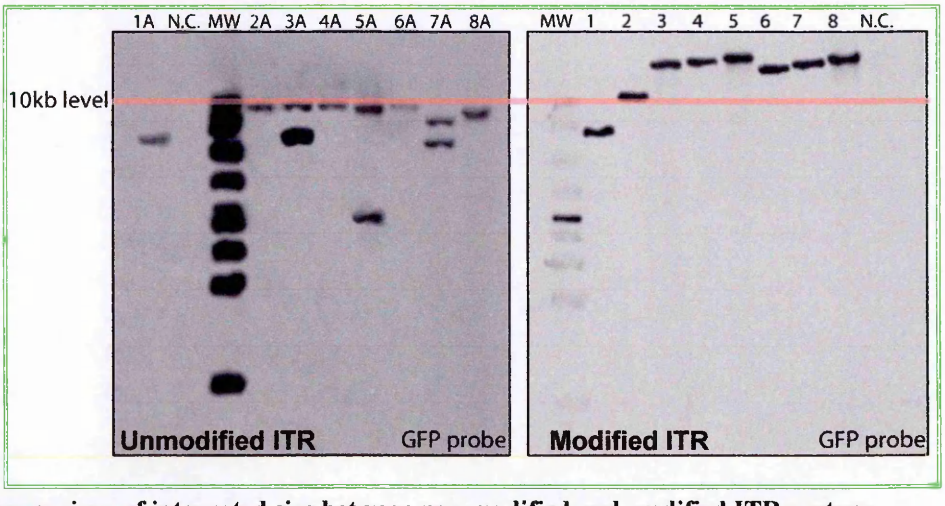

Fig. 6.4 Comparison of integrated size between non modified and modified ITR vectors.

The two vectors are very different in respect to size of the integrated cassette. ITR not modified vector display a classical monomer-dimer integrant, ITR modified vector display a different integration in which are very abundant multimers.

Using this version of the integration enhancer we did not obtaine any important effect on the percentage of overall or site specific integration, but a considerable effect on the copy number in the AAVS1 site. Notably another effect we noticed using ITRp5 is the almost

complete absence of mixed phenomenon (AAVS1 integrants + elsewhere integration) (Fig 6.5).

	ITR	ITRp5ΔTATA
Recombinated AAVS1	24 (96%)	16 (64%)
Site-specific integrations	16 (64%)	9 (36%)
Elsewhere integrations	9 (36%)	16 (64%)
AAVS1 + elsewhere	8 (32%)	1 (4%)
AAVS1 disrupted w/o site-specific integration	8 (32%)	7 (28%)

Fig. 6.5 Summarizing scheme of ITR and ITRp5DTATA integration analysis.

6.5 p5 without ITR which effect?

It seems that a minimal functional p5 element was composed of a 55 bp region (nucleotides 250 to 304 of wild-type AAV-2) containing the TATA box, the Rep-binding site, the trs present at the transcription initiation site (*trs*+1), and a downstream 17 bp region that could potentially form a hairpin structure localizing the *trs*+1 at the top of the loop.

Interestingly, the TATA box was absolutely required for *in vivo* but dispensable for *in vitro*, i.e., cell-free, replication (180).

Rep binding and nicking at the *trs*+1 was enhanced in the presence of cellular TATA binding protein (TBP), and that the over-expression of this cellular factor increased the in vivo replication of the minimal p5 element (180).

Using a series of serials constructs spanning different regions of the p5 region (Fig. 6.6) we wanted to define the minimal elements within the p5 region required for Rep-dependent replication. This aspect could be very important to clarify if the integration phenomenon is dependent on replication of the integrating cassette or if it is possible to obtain site-specific integration independently of this aspect.

Four constructs were generated containing the four p5 regions subcloning this region to the 5' of a double expressing marker construct pBSGFPΔNGFR.

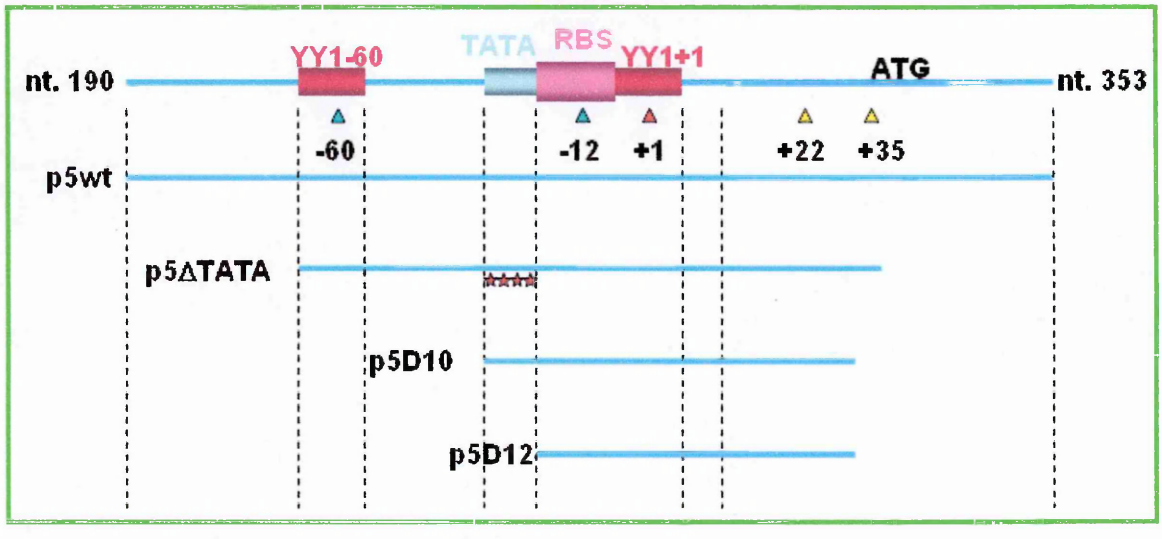

Fig. 6.6 Graphic representation of p5 region mapping. Four different constructs were built to isolate the key region in the p5 element responsible for integration.

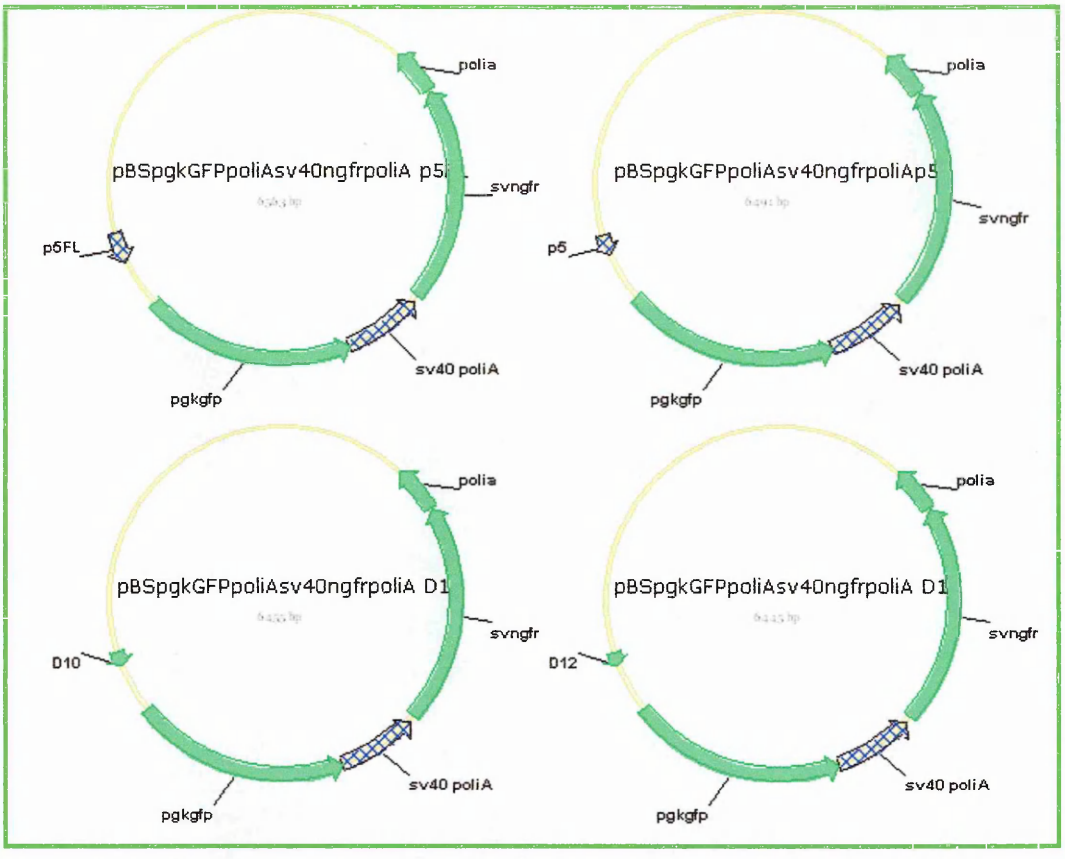

Fig. 6.7 Graphic representation of four constructs used for p5 region mapping. p5 regions were subloned to the 5' of the GFPΔNGFR cassette.

6.5.1 HeLa cell clone generation.

The p5 deleted region constructs were tested in transient transfection in HeLa cells.

HeLa transfection was done using Effectene transfection reagent in 6 cm plates.

The day before transfection $3x10^5$ HeLa cells were seeded on 6 cm Petri dishes. 1 ug of plasmid DNA/dish was transfected.

After over night incubation cells were washed and fresh medium added for 4 hours and kept at 37°C 5% CO_2. Cells were washed twice with PBS and transduced with TetRep MOI 10 in PBS (1 ml per 10 cm Petri dish) and incubated for 1 hour at 37°C 5% CO_2. After transduction time fresh medium Dox supplemented was added to PBS containing virus. Transfected and transduced HeLa cells were kept in culture one month in presence of Dox and monitored for GFP expression.

The same kind of experiment was done co-transfecting 0.2 ug of Rep expression plasmid with the p5 plasmids to study the difference between the two approaches.

Bulk culture were monitored for two weeks for GFP and ΔNGF-R expression by FACS (data not shown).

Bulk cell population was NGF-R selected.

6.6 HeLa cell clones selection.

After another week of culture cell bulks were subcloned at 0.2-0.3 cells/well by limiting dilution. Single clones were isolated after two weeks of culture and grown for up to one month for further analysis.

More than 50 clones for each construct were scored for GFP expression by FACS analysis. Since the sorted bulk culture was virtually 100% transduced, the vast majority of clones analysed expressed GFP.

6.7 Integration analysis in HeLa cells of different p5 region fragments.

25 clones for each p5 fragment plasmids were further expanded and genomic Southern blot analysis was performed to determine the genome integration of the p5 flanked cassettes for each clone. The site-specific integration of the cassette was determined by digestion of genomic DNA with AccI. AccI cut releases a 3.1 kb fragment encompassing most of the chromosome 19 AAVS1 site.

Southern blot were probed with an AAVS1 and GFP specific probes.

Full length p5:

In the case of clones obtained from the plasmid containing the full length wild-type p5 AAVS1 probe showed a size shift of the 3.1 kb band in 23 of 25 independent HeLa clones (92%), indicating rearrangement of the AAVS1 region in at least one chromosome 19. The rearranged bands hybridized also to a GFP-specific probe in 13 of the 25 clones (52%), indicating the integration of the p5-flanked cassette in the AAVS1 region. Further restriction analysis indicated that the p5-flanked cassette had integrated as a monomer or a dimer in the AAVS1 site and conserved an intact structure in all cases (not shown).

In 7 clones (28%), the AAVS1 site showed a rearranged band that did not hybridize to the GFP probe, indicating Rep-mediated disruption of the AAVS1 region in the absence of integration. Conversely, 3 of 25 clones showed bands corresponding to intact p5-flanked cassettes integrated elsewhere in the genome (12%). 3 out 25 clones (12%) showed both AAVS1-specific and non-specific integrants (Fig. 6.3).

p5ΔTATA:

In the case of clones obtained from the plasmid containing the p5ΔTATA sequence AAVS1 probe showed a size shift of the 3.1 kb band in 21 of 25 independent HeLa clones (84%), indicating rearrangement of the AAVS1 region in at least one chromosome 19. The rearranged bands hybridized also to a GFP-specific probe in 10 of the 25 clones (40%), indicating the integration of the p5-flanked cassette in the AAVS1 region. In 6 clones (24%), the AAVS1 site showed a rearranged band that did not hybridize to the GFP probe, indicating Rep-mediated disruption of the AAVS1 region in the absence of integration. Conversely, 5 out 25 clones showed bands corresponding to intact p5-flanked cassettes integrated elsewhere in the genome (20%). No clone showed both AAVS1-specific and non-specific integrants.

p5D10:

In the case of clones obtained from the plasmid containing the p5D10 sequence AAVS1 probe showed a size shift of the 3.1 kb band in 22 of 25 independent HeLa clones (84%), indicating rearrangement of the AAVS1 region in at least one chromosome 19. The rearranged bands hybridized also to a GFP-specific probe in 13 of the 25 clones (52%), indicating the integration of the p5-flanked cassette in the AAVS1 region. In 7 clones (28%), the AAVS1 site showed a rearranged band that did not hybridize to the GFP probe, indicating Rep-mediated disruption of the AAVS1 region in the absence of integration. Conversely, 3 out 25 clones showed bands corresponding to intact p5-flanked cassettes integrated elsewhere in the genome (12%). One clone showed both AAVS1-specific and non-specific integrants (4%).

p5D12:

In the case of clones obtained from the plasmid containing the p5D12 sequence AAVS1 probe showed a size shift of the 3.1 kb band in 18 of 25 independent HeLa clones (72%), indicating rearrangement of the AAVS1 region in at least one chromosome 19. The rearranged bands hybridized also to a GFP-specific probe in 9 of the 25 clones (36%), indicating the integration of the p5-flanked cassette in the AAVS1 region. In 6 clones (24%), the AAVS1 site showed a rearranged band that did not hybridize to the GFP probe, indicating Rep-mediated disruption of the AAVS1 region in the absence of integration. Conversely, 3 out 25 clones showed bands corresponding to intact p5-flanked cassettes integrated elsewhere in the genome (12%). No clone showed both AAVS1-specific and non-specific integrants.

	p5	P5ΔTATA	D10	D12
Site-specific	52	40	52	36
Elsewhere integrations	12	20	12	12
Disruption of AAVS1 w/o site-specific integration	28	24	28	24
AAVS1 + elsewhere	12	0	4	0

Fig. 6.7 Summarizing scheme of integration ability of different p5 constructs.

6.8 Replication analysis in HeLa cells of different p5 region fragments.

The p5 deleted region constructs were transfected in HeLa and 293T cells.

Both transfections was done using Effectene transfection reagent in 6 cm plates.

The day before transfection $3x10^5$ HeLa cells were seeded on 6 cm Petri dishes. 1 ug of plasmid DNA/dish was transfected.

After over night incubation cells were washed and fresh medium added for 4 hours and kept at 37°C 5% CO_2. Cells were washed twice with PBS and transduced with TetRep MOI 10 in PBS (1 ml per 10 cm Petri dish) and incubated for 1 hour at 37°C 5% CO_2. After transduction time fresh medium Dox supplemented was added to PBS containing virus. Transfected and transduced HeLa cells were kept in culture 36-48 hours after medium change in presence of Dox.

The same kind of experiment was done co-transfecting 0.5 ug of Rep expression plasmid with the p5 plasmids to study the difference between the two approaches.

36-48 hours after tranfection cell bulk population was recovered and HIRT DNA extraction was performed.

The DNA recovered from HIRT extraction was digested with DpnI and MboI separately to clarify the replication role (Fig. 6.8). The presence of bands in the MboI digestion is representative of DNA Rep mediated replication.

Southern blot analysis was performed to determine the DNA presence and status of the p5 flanked cassettes for each bulk. Southern blot were probed with a GFP specific probe.

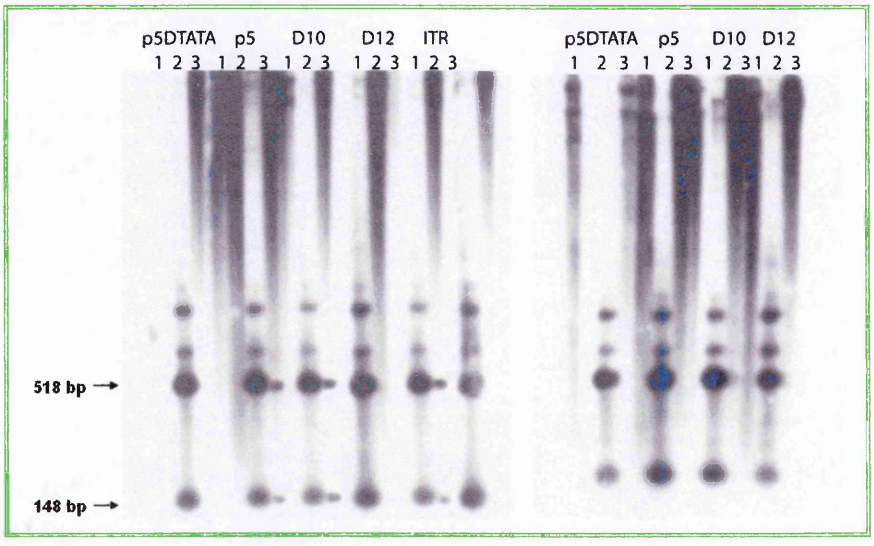

Fig. 6.8. Identification of a minimal p5 element able to replicate in Rep-expressing cells. In vivo replication assay of the p5-containing plasmids. Total DNA extracted 48 h post transfection of HELA and 293T cells cotrasfected or transduced with Rep expressing plasmid or virus (left panel), was undigested (1) digested with either DpnI (2) or MboI (3) and analyzed by Southern blot using a GFP probe. On the right panel the same experiment without Rep. The two expected DpnI digestion products (518 and 148 bp) hybridizing to the GFP probe are indicated by an arrow and are present also in the MboI digestion if replicatio has occurred. The upper bands visible in the MboI-digested samples represent input plasmid DNA. (see Materials and Methods).

With this analysis it is possible to conclude that replication we seen in the case of ITRp5ΔTATA was due to the presence of ITR. In fact p5ΔTATA alone is not able to replicate. The minimal element able to replicate is p5D10, the same construct but without TATA box is not able to replicate. The longer element, p5ΔTATA, in which the TATA box was mutagenised is not able to replicate. It is possible to argue that the TATA box is important for element replication and integration (Fig. 6.9).

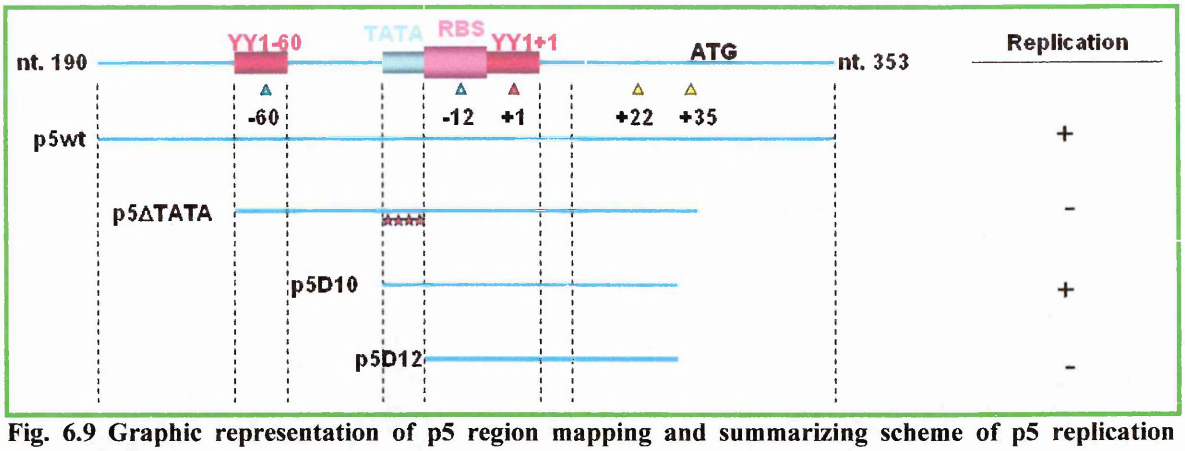

Fig. 6.9 Graphic representation of p5 region mapping and summarizing scheme of p5 replication capacity. Four different constructs were built to isolate the key region in the p5 element responsible for integration and tested for their replication capacity in vivo.

Chapter 7

Expansion of vector tropism.

To obtain a new and flexible vector system it was necessary to expand the vector tropism, to have the possibility to transduce a high number of different kind of cells, and moreover cells relevant for gene therapy.

Efficient infection with Ad vectors based on serotype 5 (Ad 5) requires the presence on cells surface of coxsackievirus-adenovirus receptors (CAR) and α_v integrins (Fig.7.1) (145-154).

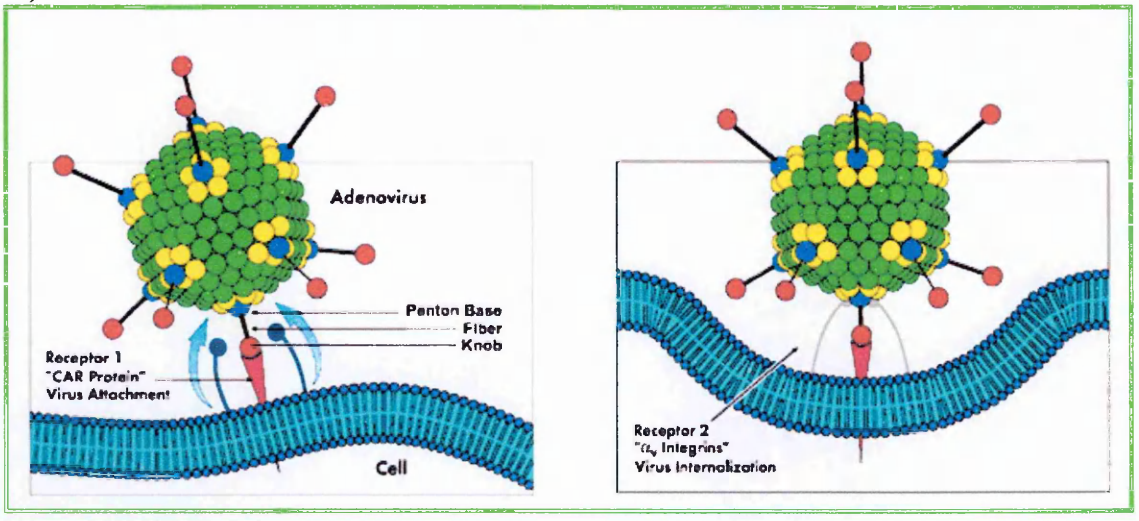

Fig. 7.1 Schematic representation of Adeno 5 serotype mechanism of internalisation. Adeno 5 virus serotype interact with cells via both CAR receptor and α_v integrin co-receptor. The cellular internalization is via endosomes. The endosomal membrane is then lysed in a process mediated by penton base and the content of virions is released in the cytoplasm. Virions partially encoated and DNA are tranported to the nucleus.

The paucity of these cellular receptors is thought to be the limiting factor for Ad gene transfer into different cell types e.g. hematopoietic stem cells.

We screened two different Ad serotypes for interaction with non-cycling human $CD34^+$ cells, HEL and K562 cells on the basis of the level of transduction and transgene stability.

A chimeric vector (Ad 5/35) which contained the short-shafted Ad 35 fiber incorporated into an Ad 5 capsid was generated. This substitution was seen to be sufficient to transfer all infection properties from Adeno 35 (Ad 35) to the chimeric vector. The retargeted, chimeric vector attached to a receptor different from CAR and entered cells by an α_v integrin-independent pathway (Fig. 7.2) (163).

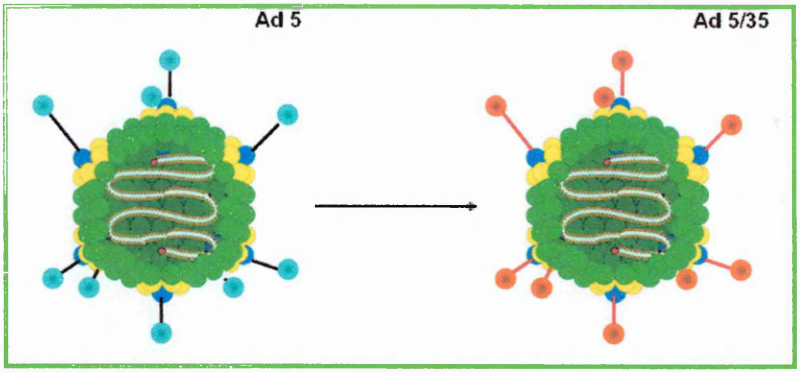

Fig. 7.2 Schematic representation of Adeno 5/35 hybrid serotype generation. The internalisation mechanism differs because Ad 5/35 serotype utilise an alternative internalisation pathway independent from CAR and α_5 integrin co-receptor. The short-shafted Ad 35 fiber was inserted into an Ad 5 capsid to generate a new Ad 5/35 serotype.

Our aim was to test if this was enough to overcome the Ad 5 limited cellular tropism, in particular cells poorly transduced from Ad 5 (like hematopoietic stem cells and hematopoietic derived cell lines).

7.1 $CD34^+$ transduction with Ad 5 serotype.

Human $CD34^+$ stem/progenitor cells were isolated from umbilical cord blood-derived mononuclear cells by immunomagnetic selection of positive cells, using a magnetic beads-conjugated anti-human CD34 (see Materials and Methods).

Cord blood-derived $CD34^+$ cells were cultured for 24 hours in serum free medium containing 20% BIT 9500 serum-substitute in presence of cytokines and transduced with the Ad 5 single vector expressing ITRGN and Rep at different MOI to test the influence of MOI on transduction efficiency.

In particular we used MOI 300. This means that, theoretically 300 TU were used to infect one $CD34^+$ cell.

24 hours post infection cells were analysed by flow cytometry for CD34, CD38 and GFP expression (Fig. 7.3). Under these conditions, more than 98% of cells retain $CD34^+$

phenotype (Fig. 7.3), while about 94% of $CD34^+$ cells were also $CD38^-$, the more immature phenotype of the human HSCs (Fig. 7.3 middle panel). About 12% of total $CD34^+$ cells were transduced as measured by the expression of GFP driven by the internal PGK promoter.

A comparison of the transduction efficiency between $CD34^+/CD38^-$ and $CD34^+/CD38^+$ cells, also shows that the more immature $CD38^-$ subpopulation had a lower transduction efficiency in respect to the double positive subpopulation (11% vs 1%, Fig. 7.3 bottom panel).

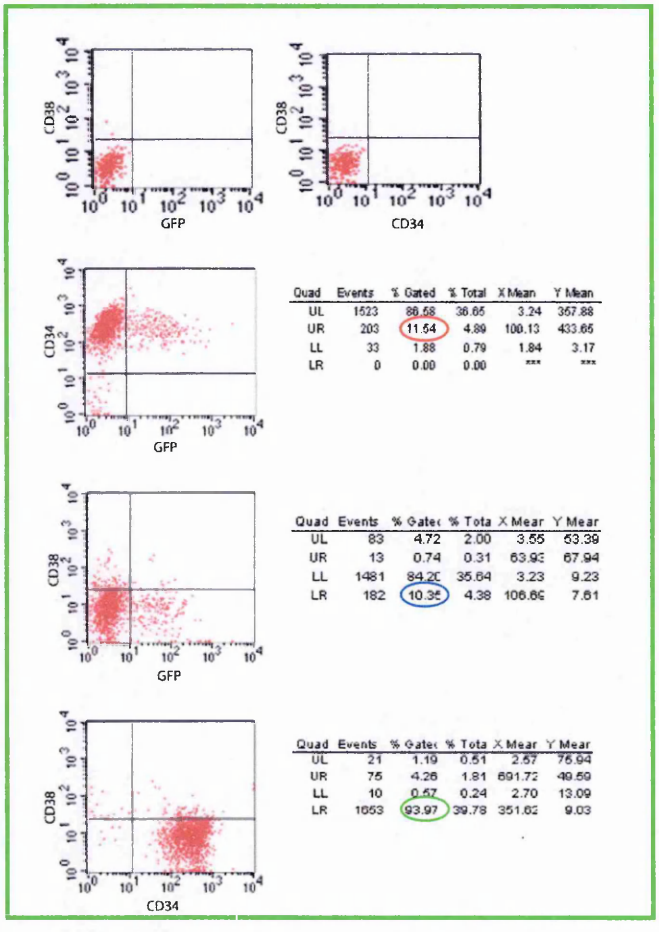

Fig. 7.3 FACS analysis of $CD34^+$ cells transduced with Ad 5. FACS analysis was performed 24 hours after transduction. Cells were labelled with anti CD34 and CD38 and followed for GFP. In the UR region of the second panel is indicated the percentage of $CD34^+$ cells transduced (red oval, around 11%). In the LR region of the third panel is indicated the percentage of $CD38^-$ cells tranduced (blue oval, around 10%). In the LR region of the last panel is indicated the percentage of $CD34^+$ $CD38^-$ cells, the more immature phenotype (green oval, around 94%).

To analyse transgene expression at the level of single colonies, $CD34^+$ transduced cells were plated in methylcellulose to perform the colony forming cell *in vitro* (CFC or CFU) assay. MOI 300, 500 e 1000 in presence of Dox were utilised. Between 10 and 14 days after plating, methylcellulose clonal culture were scored for GFP expression by fluorescence microscopy. No colonies were scored for each group.

In summary, these results shown that high titer Ad/AAV viral stocks were generated using a HD system and the Ad 5 serotype is able to infect quiescent HSCs at a very low efficiency and no colonies were identified.

7.2 $CD34^+$ transduction with Ad 5/35 serotype.

Human $CD34^+$ stem/progenitor cells were isolated from umbilical cord-blood-derived mononuclear cells by immunomagnetic selection of positive cells, using a magnetic beads-conjugated anti-human CD34 (see Materials and Methods). Cord blood-derived $CD34^+$ cells were cultured for 24 hours in serum free medium containing 20% BIT 9500 serum-substitute in presence of cytokines and transduced with the ITRGN vector at different multiplicity of infection (MOI) to test the influence of MOI on transduction efficiency. In particular we used MOI 300.

After 24 hours post infection cells were analysed by flow cytometry for CD34, CD38 and GFP expression (Fig. 7.4). Under these conditions, about 98% cells retain $CD34^+$ phenotype (Fig. 7.4), while about 86% of $CD34^+$ cells were also $CD38^-$, the more immature phenotype of the human HSCs (Fig. 7.4). About 28% of total $CD34^+$ cells were transduced as measured by the expression of GFP driven by the internal PGK promoter.

A comparison of the transduction efficiency between $CD34^+/CD38^-$ and $CD34^+/CD38^+$ cells, also shows that the more immature $CD38^-$ subpopulation had a higher transduction efficiency in respect to the double positive subpopulation (26% vs 2%, Fig. 7.4). This

observation suggests that Ad/AAV vectors are able to transduce quiescent human HSCs at a high efficiency, even more than cycling progenitor cells.

To analyse transgene expression at the level of single colonies, $CD34^+$ transduced cells, were plated in methylcellulose to perform the colony forming cell *in vitro* (CFC or CFU) assay. MOI 300, 500 and 1000 in presence of Dox were utilised. Between 10 and 14 days after plating, methylcellulose clonal culture were scored for GFP expression by fluorescence microscopy. Again no colonies were scored for each group.

In summary, these results shown that high titer Ad/AAV viral stocks were generated using a HD system and the Ad 5/35 serotype is able to infect quiescent HSCs at a good efficiency in respect to Ad 5 serotype but again no colonies were identified.

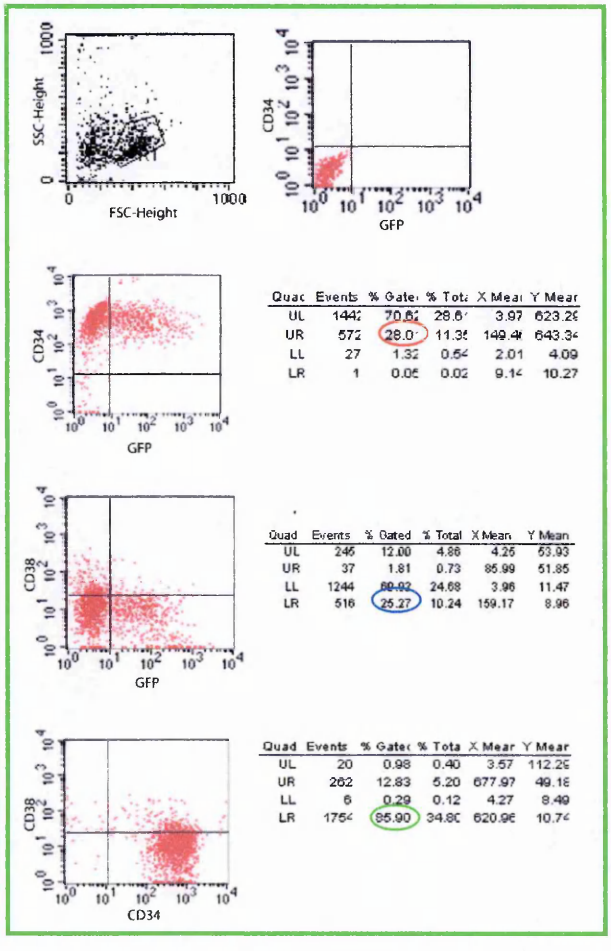

Fig. 7.4 FACS analysis of $CD34^+$ cells transduced with Ad 5/35. FACS analysis was performed 24h after transduction. Cells were labelled with anti CD34 and CD38 and followed for GFP. In the UR region of the second panel is indicated the percentage of $CD34^+$ cells transduced (red oval, around 28%). In the LR region of the third panel is indicated the percentage of $CD38^-$ cells tranduced (blue oval, around 25%). In the LR region of the last panel is indicated the percentage of $CD34^+$ $CD38^-$ cells, the more immature phenotype (green oval, around 86%).

7.3 Hematopoietic derived cell lines transduction with Ad 5 and Ad 5/35 serotypes.

K562 and HEL cells were transduced with ITRGN Ad 5 serotype virus and with Ad 5/35 version of ITRGN without Rep. Cells were transduced at different MOI 50, 100, 300, 500 and 1000 to investigate the role of virus particles in transduction efficiency. The day before transduction $5x10^5$ cells/well were plated in 6 wells plates and incubated all night in RPMI 10% FCS antibiotic and L-Glutamine supplemented.

The day of the transduction media was sucked off and transductions were managed in 500 ul serum free RPMI diluted viruses. Cells were incubated one hour at 37°C 5% CO_2 incubator. After transduction 10% serum (final concentration) was added to RPMI containing virus. Cell bulks were monitored 24 hours post transduction for one month for GFP expression by FACS analysis every three-four days (Fig. 7.5).

Cells harvested for GFP FACS scoring were also stained with trypan blue to investigate if MOI had influences in cell viability (data not shown). No evidence was seen regarding MOI/cell viability.

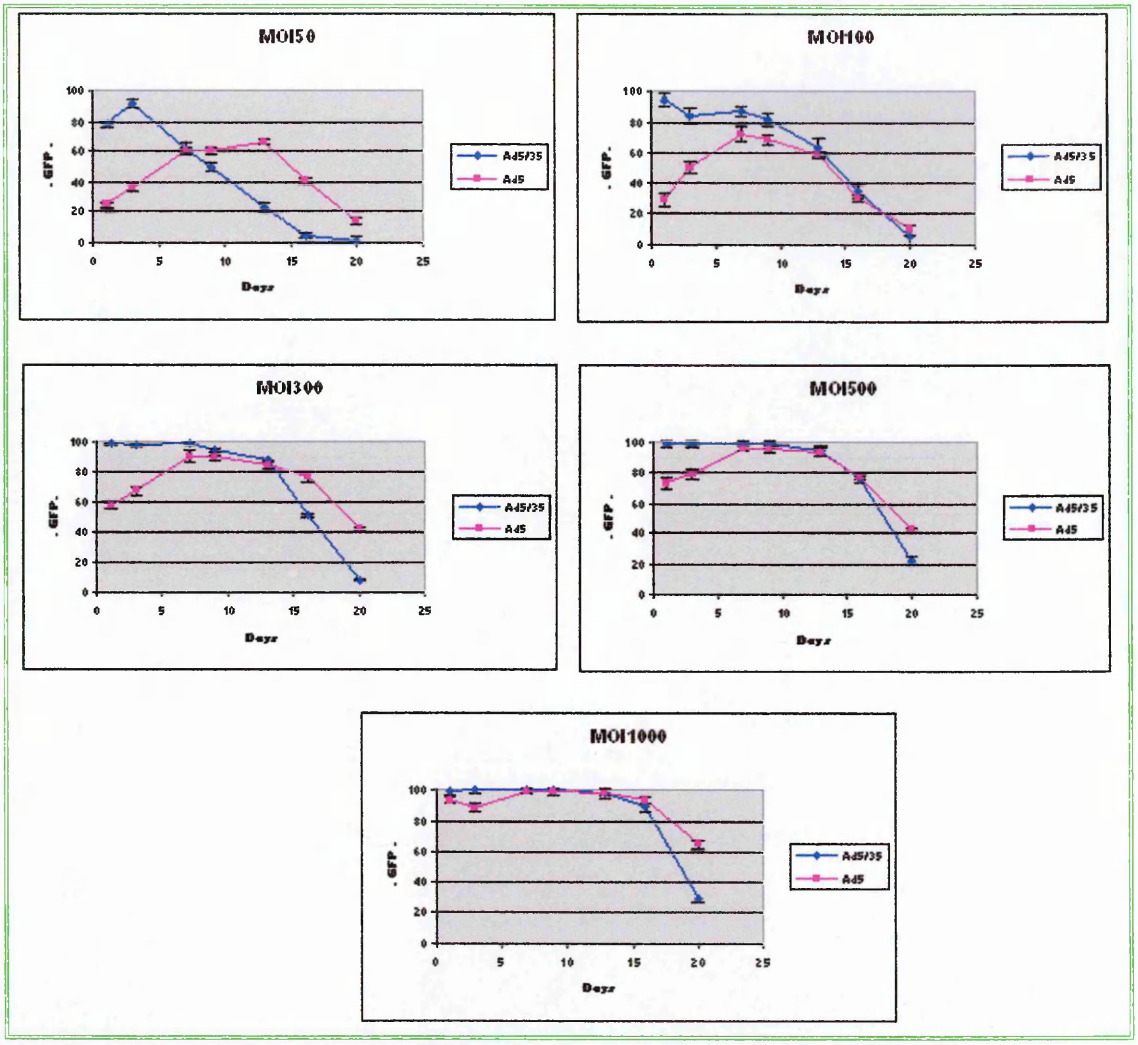

Fig. 7.5 Graphic representation of HEL cells transduction with both Ad 5 and Ad 5/35 serotypes.
HEL were transduced with Ad non integrating vector ITRGN of two serotypes (Classical Ad 5 and Ad 5/35 hybrid serotype) at various MOI and followed for one months for GFP expression and cell death. Plotted data showed that at lower MOI Ad 5/35 is the best transducing serotype in respect to Ad 5. Raising MOI a trend more similar between Ad5 and Ad 5/35 was obtained. Ad 5 seems to be more stable, there are more cells maintaining GFP expression along the time in the middle phase of transduction. Ad 5/35 shows a precocious pick at the beginning of infection in correspondence of which a higher number of cells were transduced with GFP but this pick dropped down in the middle phase following a constant reduction along the time. This phenomenon was not influenced by the cell death. The experiments were reproducted 3 times.

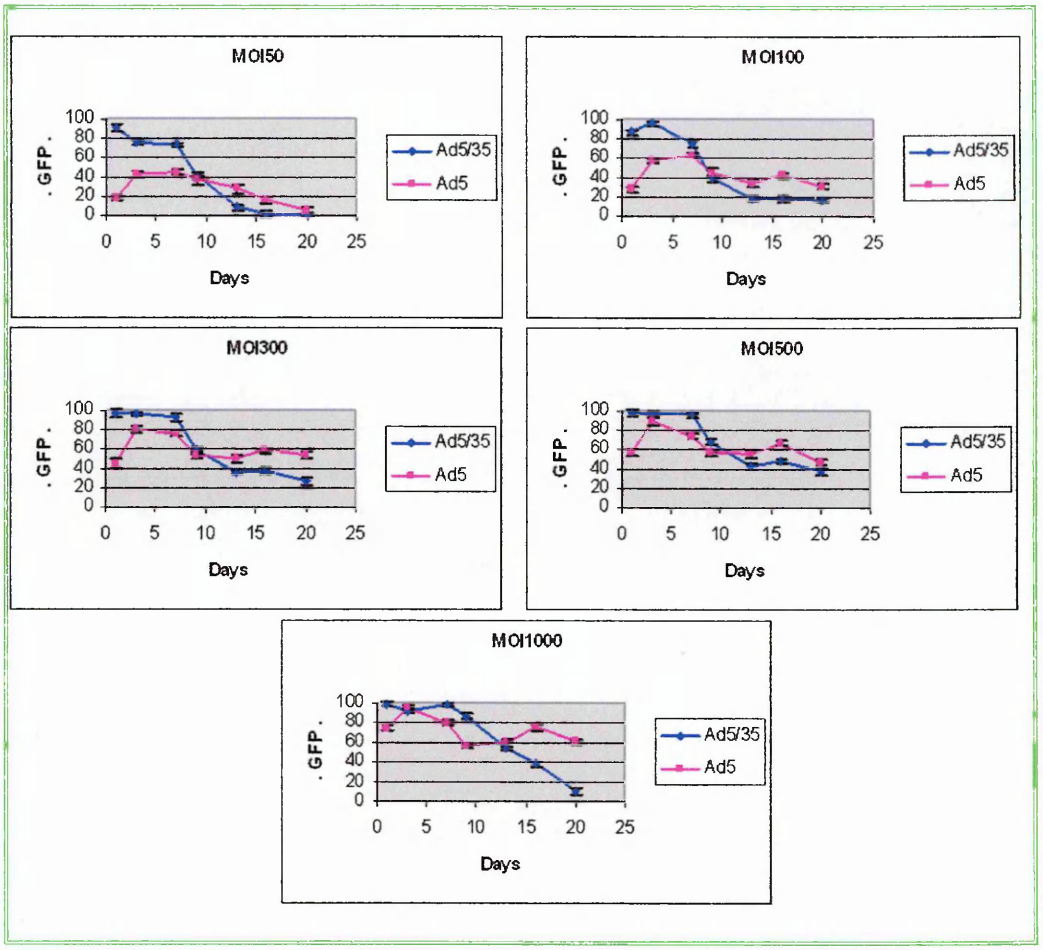

Fig. 7.6 Graphic representation of K562 cells transduction with both Ad 5 and Ad 5/35 serotypes. K562 were transduced with Ad non integrating vector ITRGN of two serotypes (Classical Ad 5 and Ad 5/35 hybrid serotype) at various MOI and followed for one months for GFP expression and cell death. Plotted data showed that at lower MOI Ad 5/35 is the best transducing serotype in respect to Ad 5. Raising MOI a trend more similar between Ad 5 and Ad 5/35 was obtained. Ad 5 seems to be more stable, there are more cells maintaining GFP expression along the time in the middle phase of transduction. Ad 5/35 shows a precocious pick at the beginning of infection in correspondence of which a higher number of cells were transduced with GFP but this pick dropped down in the middle phase following a constant reduction along the time. This phenomenon was not influenced by the cell death. The experiments were reproducted 3 times.

Plotted data demonstrated that at lower MOI Ad5/35 is the best transducing serotype in respect to Ad5. In my hands it was possible to obtain a 2-3 fold increase of GFP transduced cells using Ad5/35 in respect to what I obtained with the same virus in a Ad 5 context. Raising MOI we obtained a trend more similar between Ad 5 and Ad 5/35 both in HEL and K562. In all cell lines we tested in particular at low MOI Ad 5 seems to be more stable, there are more cells maintaining GFP expression along the time in the middle phase of transduction. Ad 5/35 shows a precocious pick at the beginning of infection in

correspondence of which a high number of cells were transduced with GFP but this pick dropped down in the middle phase following a constant reduction along the time. This phenomenon was not influenced by the cell death. The number of dead cells was practically the same between Ad 5 and 5/35. This phenomenon can be explained with a different internalisation mechanism. It seems that Ad 5/35 can transduce more cells at the beginning, but the internalisation system seems to influence DNA stability. For our purpose this doesn't seem a great problem. For our model it is important to have a great amount of virus in the nucleus in the few hours after transduction.

Both virus serotypes stop to be expressed/present around twenty days after transduction.

Chapter 8

Discussion

Gene targeting and homologous recombination technology underwent spectacular development in the last couple of decades, leading to the routine generation of transgenic animals with precise gene modifications by genetic manipulation of embryonic stem cells. However, the efficiency of this technology is still exceedingly low for clinical gene transfer, which almost invariably involves substantial numbers of rare and poorly cultivable cells (e.g., somatic stem cells). For clinical applications, the only available options are either extra-chromosomal expression or uncontrolled genomic insertion of therapeutic genes by means of a virus-derived gene transfer vector. Integrating vectors derived from murine oncoretroviruses (e.g., the Moloney murine leukemia virus, or MLV) have been used in hundreds of gene therapy trials since 1991 (197). Despite the known oncogenic potential of the parental viruses (198), retroviral vectors were considered relatively safe until lymphoproliferative disorders were reported in three patients treated with retrovirally-transduced hematopoietic progenitor cells for X-linked severe combined immunodeficiency (X-SCID). In all three patients, the vector inserted into, and activated, the T-cell proto-oncogene LMO-2, thereby contributing to the establishment and/or progression of the malignancies (199). These events indicated that insertional oncogenesis is an actual "genotoxic" risk associated to the use of retroviral vectors, which may severely limit a wider application of this type of technology. Another problem of these kind of vectors is the relatively small cassette size they can contain. Both retroviral and lentiviral vectors have an insert size limitation of 7-8 kb and moreover this kind of vectors do not easily accommodate introns or complex regulatory elements.

There are several possible solutions to the genotoxicity problem, which range from improving the current retroviral vector design to developing entirely new technology.

An ideal gene transfer vector should be capable of inserting a therapeutic transgene at a precise location into human DNA, where it can be efficiently expressed without perturbing the homeostasis of the rest of the genome and should be so versatile to target also big inserts in a safe way.

For gene therapy applications, the development of vectors that target transgene integration to specific sites in the host genome is a major focus.

Indeed a virus that posses these properties does exist, and that is the wild type AAV (4, 5). AAV genome is a linear, single-stranded DNA filament which contains at both ends a 145-base inverted terminal repeat (ITR) encoding the origin of replication and the packaging signal (31), and two AAV-specific genes, *rep* and *cap*. The ITRs and the Rep protein are sufficient for replication of the AAV genome in the presence of Ad or herpes simplex virus (HSV) helper functions (AAV is incapable of completing its life cycle without a helper virus) (21). In the absence of helper functions, the same elements are sufficient to mediate the integration of the AAV genome into a 3-kb specific site on human chromosome 19q13.4qter (21). This site, called AAVS1, has been mapped to the first exon of myosin binding subunit 85 of protein phosphatase 1 (28). The AAVS1 site appears to be in an open chromatin conformation in the cell lines tested (74), which is thought to help AAV integration and viral gene expression. Integration into this site is mediated by the large AAV Rep proteins Rep68 or Rep78. Rep68/78 demonstrate sequence-specific endonuclease activity and ATP-dependent helicase activity, and can mediate rescue/excision of DNA flanked by AAV ITRs in the presence of Ad super-infection (21). Rep mediated rescue requires the presence of both a Rep binding site (RBS) and a terminal resolution site (*trs*) within the virus AAV ITR and genomic AAVS1 site, whereby the secondary structure of these sites appears to be crucial for Rep68/78-mediated DNA nicking. Rep-mediated rescue of a cassette flanked by AAV ITRs from ds DNA substrates and nicking within the AAVS1 site creates free DNA ends which allow for virus integration via non-homologous end-joining (NHEJ). It is therefore thought that rescue from incoming ds DNA is a prerequisite for integration (45, 48, 49, 50).

The ability of Rep68/78 to mediate integration into AAVS1 has been harnessed for site-specific integration of transgenes from co-transfected ds DNA plasmids. The frequency of AAVS1-specific integration by these plasmid-based methods has differed among studies

from 20 to 50%, whereby integration frequency was measured upon drug selection (19, 16, 14, 53, 18). However, plasmid transfection is not an efficient method for gene transfer. The production of Rep-expressing viral gene transfer vectors (based on adenovirus or HSV-1) is also problematic, because expression of Rep in packaging cells has been shown to severely reduce vector production (189). The vector yield could be increased by placing the *rep* gene under the control of promoters with low activity in packaging cells or by using tet or Cre/lox inducible gene expression systems (190).

There are a series of limitations in using Rep-based hybrid vectors.

Retroviral vectors, particularly the last generations derived from HIV, have a large tropism, and transduce >50% of their target cells (hematopoietic stem/progenitor cells, keratinocytes, neurons, hepatocytes) with negligible toxicity. High efficiency is mandatory for clinical application.

Rep-based hybrid vectors transduce relatively efficiently stable cell lines (10 to 20%) but much less primary cells, either in culture or *in vivo* (1-5%). Most of the papers published on the issue did not even try to address the issue of gene transfer in targets of clinical relevance.

Increasing Rep-mediated gene transfer efficiency appears very difficult. The wild-type AAV uses Rep to replicate as well as integrate, and 15% integration efficiency is probably the best compromise evolution has found between propagation and latency. Improving nature is going to be a tough task, and will probably require some serious protein engineering.

A second hurdle is the proportion of site-specific *versus* non-specific integration. Getting rid of non-specific integration is the reason why we are trying to use Rep or other sequence-specific integrases in the first place (191, 192). If 30-50% of the integrations are still random, the genotoxic risk for the target cells would diminish only by a factor of two or three compared to retroviral vectors, not really enough to make a difference in the real world – hundreds of millions to billions of cells are transduced and administered in a

typical gene therapy protocol. This is true unless the non-specific integrations have a substantially better safety profile compared to those of retroviral vectors, which prefer to integrate into active genes and around transcription start sites (193). Data on this point, however, are scattered and inconsistent. Some authors reported that AAV vectors tends to integrate into active genes (194), while others showed that non-specific, Rep-mediated integration of AAV-based cassettes targets essentially intergenic regions (195). Overall, there is not enough data to reach a conclusive answer on this crucial point. Paradoxically, in a system with only 50% site specificity, the nature of the non-specific events is going to be more important than site specificity itself.

Finally, there is an issue of integration-independent genotoxicity. Significant progress has been made also with other types of proteins, such as transposases or bacteriophage-derived integrases (191, 196). Integrases and transposases introduce, at variable extent, single and double-strand breaks into mammalian genomes. These breaks are potentially recombinogenic, and could cause mutations or genomic rearrangements as dangerous, if not more dangerous, than those caused by random vector insertion. The genotoxicity of recombinases, including that of Rep, has not been studied thoroughly enough to make reliable predictions about the safety of their use in humans. Appropriate regulation of their expression is clearly a crucial variable, but may not be the only one.

Large capacity Ad/AAV.

In this study we showed that a helper-dependent Ad 5 vector expressing Rep78 under the control of a doxicyclin-inducible system for site-specific transgene integration can be used to integrate a large expressing cassette flanked by AAV ITR expressed by another vector into the human genome in a site-specific way. Moreover we speculate that clones with high level Rep78 expression died off due to Rep-mediated toxicity. This is supported by the fact

that the total number of clones that developed was 2 to 3 fold lower for Ad-Rep78 infected cells than in settings with AdhCol7 alone. Furthermore, the percentage of GFP expressing cells in all surviving clones was constant over time, underscoring that these cells did not have a proliferative disadvantage.

This study is a proof of principle that targeted integration of a 12-kb transgene can be achieved at high frequency. Though the inaccuracy of integration and genomic rearrangements are a concern, epidemiological studies show widespread wt AAV infection (80% of humans are AAV seropositive), while no known pathologies, including neoplastic malignancies, have been reported (21).

In my thesis work I studied a new generation of hybrid DNA vectors that combine the large capacity and infectivity of adenoviral vectors with the ability of the AAV Rep protein to direct the integration of AAV ITR-flanked sequences at specific sites into the human genome. In particular I focused my attention on testing the ability of Rep protein to integrate very large transgenes in respect to AAV genome size, on test new methods to improve this system both in transduction efficiency and in integration capacity. Because transduction of primary cells, particularly primary hematopoietic stem cells, with first-generation E1/E3 deleted recombinant Ad vectors is associated with toxicity due to viral gene expression (118), we used in our studies a helper-dependent (HD) Ad vectors, which are devoid of all viral genes (121).

A major difficulty in building viral vectors containing Rep expression cassettes is the negative effect of Rep on viral replication (23), which prevents packaging or reduces titers to values unacceptably low for practical use. To overcome these problems, I used a system developed in my lab in which a tight, drug-inducible transcriptional regulation system based on a minimal promoter under the control of the tetO element and a constitutively expressed tTS suppressor. This combination allowed efficient packaging of a HD-Ad vector containing Rep. Drug-induced activation of Rep allowed a good protein production control.

The vector I developed was three times bigger than those previously developed in the laboratory, and the first concern was to understand whether this system was able to work in this situation. In particular, whether the Rep protein was able to integrate intact copies of the ITR-flanked cassette into the AAVS1 site in stable cell lines without recombination, in the absence of selective pressure and possibly with a good efficiency.

In all GFP expressing clones that were used for integration studies we did not detected Rep78 expression by western blot.

The efficiency of AAVS1-specific integration was a bit lower that what we obtained with the smaller cassette.

With this dual vector system, hCol7-GFP transgene integration into AAVS1 was seen in 30% of analyzed integration sites, whereby transgenes integrated into AAVS1 expressed GFP at high and stable levels. In our study we obtained ~43% of stably transduced HeLa clones in which the AAVS1 locus is rearranged even in the absence of an integrated cassette. This is probably due to the ability of Rep to bind to the RBS in AAVS1, induce nicking at the nearby *trs*, and start unscheduled DNA replication before binding to, replicating, and eventually integrating an ITR-containing genome. The higher percentage obtained with respect to previous studies using a smaller cassette could be due to the cassette dimension, maybe due to abortive events and probably to the use of CMV promoter to ensure a higher Rep expression.

In the presence of exceedingly high or prolonged synthesis of Rep, the AAVS1 site could become a hot spot of chromosome fragility or genetic recombination in transduced cells, an obviously undesirable side effect of a Rep-based integration system. Drug-controlled Rep expression is expected to reduce these potential genotoxic effects, an additional safety characteristic of our hybrid vectors. Expression of Rep, a likely immunogenic protein, could potentially elicit a cytotoxic immune response against cells transduced *in vivo* by a Rep-expressing vector. The drug-controlled expression system is expected to reduce the immunogenicity of Rep to a minimum, although it introduces an additional immunogenic

factor, the constitutively expressed Tet repressor protein. The immunogenic potential of the Tet repressor is a controversial issue, although it is conceivable that in cells or tissues in which episomal Ad vectors persist for long time (liver, for example) this might eventually turn out to be a problem. Anti-Rep and anti-Tet immune responses therefore need to be addressed in specific animal models for each vector delivery route.

Adenovirus-based integrating vectors could find practical application in both *ex vivo* and *in vivo* gene transfer protocols. We demonstrated that the large capacity of the Ad vector backbone allows the incorporation of large genes and eventually a complex regulatory systems into the vectors, a current limitation of retroviral vector technology. A high proportion of site-specific integration and a general preference for nontranscribed regions would reduce both the risk of insertional oncogenesis and the problem of position-dependent variability or silencing of transgene expression (195).

In my hands it was not possible to obtain any clone from keratinocyte primary cells. In all the experiments I made transducing keratinocytes both with the small integrating cassette (GFP-ΔNGFR) and with the large integrating virus (hCol7 + GFP) it was impossible to expand clones derived from the transduction of keratinocyte stem cells. This could be due to different events:

- Ad 5 serotype is not able to transduce the more immature keratinocytes.
- Rep78 is more toxic for these kind of cells.
- The population of more immature keratinocytes could be so small that we weren't able to clone enough cells to isolate any epidermal stem cell.
- Repopulating keratinocytes could silenciate the integrated cassete.

As discussed in my thesis the Ad 5 serotype need on the cell surface the presence of two receptor to transduce cells: CAR and the α_v integrin. It is so possible that the epidermal stem cell population is lacking on one or both receptors. Transduction experiments with other serotypes could be an alternative and the solution to this problem.

Rep 78 is a well known toxic protein, and maybe in the epidermal stem cell contest is too much toxic, giving the death of all the repopulating keratinocyte population. At the moment this problem can't be by-passed, Rep is needed to obtain integration.

Different limiting dilution experiments were done to clone a repopulating stem cell stable transduced with our integrating cassette. From different transduced populations of keratinocytes, thousand of cells were cloned, but no one of this single cells arised a repopulating clone. This could be due to the impossibility to clone a so low abbundant population and a more extensive effort is needed.

Repopulating cells are very active cells and methylation or other chromatin modification during differentiation or duplication could give raise to integrated cassette silencing. In this case maybe we were able to integrate our cassettes into the genome of a repopulating epidermal stem cell, but we neglected that clone who wasn't able to express the integrating cassette.

Optimisation of vector integration.

Previous reports demonstrated that the AAV-2 p5 promoter region contained a multifunctional element that was involved in *rep* gene expression, Rep-dependent replication, and site-specific integration (64, 27, 26). The aim of last part of my study was to isolate a minimal region of p5 able to integrate and investigate if the integration process is dependent on replication in the presence of Rep78 protein. In particular the main aim was to clarify the role of Rep mediated replication in AAV integration and if the presence of a p5 region flanking ITR in its wt position can improve the site specific integration frequency.

The minimal p5 element demonstrated functional *in vivo* replication assays was composed of a 55-bp region that included the TATA box, the Rep-binding site, the *trs*-1, and a

potential hairpin structure surrounding the *trs*. The Rep-binding site, the *trs*-1, and the hairpin structure were absolutely required for replication assays, whereas the TATA box was seen to be dispensable for *in vitro* replication (180).

A critical step for the characterization of the minimal p5 element consisted in the identification of the Rep nicking sites within the p5 region. Indeed, a previous study by Wang et al. (67) had indicated the presence of a cryptic *trs* at the transcription initiation site, without indicating the strand that was cleaved. The subsequent finding by Wu et al. (50) of no detectable nicking near the p5 Rep-binding site further put in question the presence of this *trs*. Using nicking assays, François et al. (180) confirmed the presence of a major *trs* at the transcription initiation site and localized it on the lower AAV's DNA strand between nucleotides 287 and 288. In addition, they showed that at least four other minor *trs* sites could be detected within the p5 region. Most of these nicking sites were not required for p5 replication and the minimal element characterized in François study (p5D10) contained only two *trs* sites, *trs*-1 and *trs*-12. The requirement for the former *trs* was demonstrated by the direct mutation of this site (p5m*trs*). The role of the second *trs* (*trs*-12) is presently unknown and difficult to evaluate since it localized within the Rep-binding site. Cleavage at this site could be explained by a nicking reaction occurring in *trans* by Rep protein bound on a DNA substrate, nicking a second DNA template. In both the viral ITR and the chromosome 19 AAVS1 region, the Rep proteins have been shown to cleave the DNA between two thymidine residues, resulting in the covalent attachment of Rep to the nicking site through a phosphotyrosyl linkage (7, 43, 46). It is interesting that none of the *trs* sites identified in the p5 resembled those found in the ITR or the AAVS1 region except for the presence of a thymidine residue to the nicking site. Also, great variability was observed in the spacer sequence separating the Rep-binding site from each *trs* within the p5, further distinguishing this substrate from the AAVS1 locus and the ITR. These observations, together with the experimental evidence demonstrating that most of these nicking sites, beside the *trs*-1, were not required for p5 replication, raise questions

about their biological relevance. Interestingly, an additional *trs* site was recently described within the ITR (181). In that study, nicking was observed only using a partially purified Rep preparation, further suggesting that a cellular factor was involved in this cleavage. Nevertheless, it remains possible that these cleavage sites, even if Rep dependent, represent artificial reaction products due to the conditions under which the nicking assay is performed. The sequence surrounding the major *trs*-1 was also important for replication of the p5 element. This domain can potentially form a hairpin structure that localizes the *trs*-1 on the extruded loop. Previous analyses on the viral ITR demonstrated that a potential stem-loop was present at the *trs* and that the extrusion of this structure was mediated by the ATPdependent helicase activity of Rep (51). A secondary structure was also recently described near the *trs* within the AAVS1 locus (52). It was demonstrated (180) that deletion of the nucleotides forming the stem of the hairpin impaired p5 replication. This result strongly supports the existence of secondary structure at the *trs*-1 and also suggests that cleavage at this site required the separation of the DNA strands through the helicase activity of Rep. Interestingly, in the case of the p5, the hairpin and the *trs*-1 localize within the YY1 recognition site, and binding of this factor to this site was previously shown to mediate TBP-independent initiation of transcription *in vitro* and DNA strand separation. It is tempting to speculate that formation of the hairpin structure at the p5 *trs*-1 is also favored by YY1 binding, further putting into question the relationships between replication and transcription initiation. Additional mutations affecting the YY1 binding site but not the *trs*-1 or the hairpin structure should help define the role of this cellular factor for Rep-dependent replication of the p5.

It was previously reported that TBP could bind to Rep78 *in vitro* and *in vivo* without, however, demonstrating any biological effect associated with this interaction (182). François results (180) indicated that the TATA box was absolutely required for *in vivo* replication of a minimal or a wild-type p5 element. In addition, they demonstrated that when the TATA box was present, TBP stimulated Rep binding at the Rep-binding site and

nicking at the *trs*-1. The biological relevance of these observations was further supported by enhancement of p5 replication observed in cells over-expressing TBP. On the basis of these findings and of previous observations concerning the Rep-ITR interactions, the following model can be proposed for the p5 element. *In vivo*, i.e., in live cells, in the absence of the TATA box, Rep proteins may not be able to bind the p5 Rep-binding site. If Rep binding occurs, it must not be very efficient and in any case, not sufficient to induce cleavage at the *trs*-1 since no replicative activity of the TATA-less p5 element was observed. In the presence of the TATA box, TBP increases the efficiency of Rep binding at the Rep-binding site, and also nicking at the *trs*-1, thus stimulating replication of the p5 element. Recent studies on the ITR have suggested that the interaction of Rep with the RBE induced a change in DNA conformation that resulted in the stimulation of the extrusion of the *trs* by Rep helicase activity (51). Similarly, in the case of the p5, an attractive hypothesis is that the interaction of Rep with TBP induces a conformational change that enhances Rep recognition of the Rep-binding site and favors the extrusion of the *trs*. Indeed, TBP is known to bend DNA once bound to the TATA box. This hypothesis is also supported by previous studies demonstrating that nicking at the AAVS1 *trs* by Rep was dependent upon topological constraints (183). Finally, an additional argument comes from the observation that high mobility group chromosomal protein 1 (HMG-1) increased Rep binding and nicking at the *trs* in the ITR. This protein, which influences DNA flexibility, also interacts directly with Rep (184). A similar effect on Rep activities was also demonstrated with some viral and cellular single-stranded DNA binding proteins (185). Several additional experiments should be performed to validate this hypothesis. Also, it is worth noting that the model presented does not take into account the complex interaction between TBP and the other factors that constitute the transcription initiation complex or the observation that Rep can form multimeric complexes upon binding its recognition site (181). It is interesting that the TATA box was completely dispensable for *in vitro* replication of the p5 element. This observation points out a different requirement

for cellular factors between *in vivo* and *in vitro* replication assays and further strengthens the hypothesis according to which the conformation of DNA is an essential parameter. Indeed, the template for *in vivo* replication is supercoiled plasmid DNA eventually wrapped by cellular histones, whereas *in vitro* replication is performed using naked linear double-stranded DNA molecules. The TBP was previously shown to interact with numerous cellular and viral proteins that are transcriptional regulators (186, 187). However, only a few reports describe an effect of TBP on the replication of viral origins. In particular, TBP was shown to inhibit the replication of viruses such as simian virus 40 and human papillomavirus by interacting with viral regulatory proteins or by preventing their binding to the origin of replication (14, 15). François results (180) demonstrated a positive effect of TBP on the replication of a viral element. Interestingly, it was previously reported that TBP could enhance eukaryotic DNA replication by binding to the replication origin in an *Saccharomyces cerevisiae* model (188).

In conclusion, these studies have contributed to the definition of a minimal replication-competent p5 region. It remained to be defined whether this minimal p5 element is also able to direct site-specific integration of plasmid DNA as previously demonstrated with a wild-type p5 region (26, 27) and to determine if p5 replication is required for this effect. Indeed, previous studies have shown that replication of the viral ITR was not required for site-specific integration. And more importantly, it remained to address the question of the role of this element in the context of the ITRs. It is possible, as previously suggested by Tullis et al. (65), that this element is required for optimal DNA replication.

We tried to answer to all the open questions starting to investigate the possible role of p5 element in an ITR contest. It remained to be defined if the minimal p5 element, alone, was able to direct a site-specific integration of plasmid DNA as previously demonstrated with a wt p5 region and if p5 replication is required for integration.

In our study using a different construct in respect to which François used and we confirmed the importance of TATA box in the p5 sequence. In our construct in fact it is

present the sequence containing the TATA box, but we abolished its function mutagenizing the TATA sequence to abolish the p5 promoter function.

The plasmid containing the p5ΔTATA sequence was able to integrate to a percentage similar to D10 plasmid, but in HIRT assay we showed that our construct was not replicated in presence of Rep protein.

Using the four constructs spanning different region of p5 region and using similar construct in except for the presence of TATA box region we obtained a series of interesting data.

First of all with a transfection approach we isolate a series of different clones. All the clones we then analysed showed the same percentage of integration, showing no difference in respect to the p5 region utilised.

We started our study modifying the 5' ITR putting in the wt position a p5ΔTATA element. From our data analysing 50 clones, 25 for the wt ITR and 25 for the mutated one we didn't see any dramatic effect on site-specific or overall integration. What we noticed was a very interesting and dramatic effect on vector copy number integrated in a site-specific way. In particular in the ITRp5ΔTATA contest we noticed a higher percentage of integration of multiple copies of the integrating cassette. The ITR wt was able to integrate only 1 or 2 copies of the cassette into the AAVS1 locus, while the ITRp5ΔTATA was seen to be able to integrate more than 2-3 copies into the AAVS1 locus.

What also we noticed was the ability of both the plasmids (the first one with the ITR wt and the second one with the ITRp5ΔTATA) to replicate the integrating cassette in presence of Rep. Whether the integration boost in presence of the p5 region was due to replication increase of the cassette, or the integration was independent from cassette replication, remains an open question.

Our replication assay using four different region spanning the p5 region and containing or not the TATA box have clarified this aspect.

In my hands from these four regions I obtained data very similar to François ones (180).

In particular I confirmed the importance of TATA box on the replication efficiency. Both D12 and p5ΔTATA were unable to replicate in presence of Rep, but able to integrate in these conditions. It is possible to conclude that replication of ITRp5ΔTATA we observed was due to the presence of ITR and the integration boost was not due to a more abundant replication of the integrating cassette.

Our data regarding the insertion of a p5 element following the ITR leave open a series of interesting approaches to improve the Rep mediated integration.

Expansion of vector tropism.

During our study we also asked to ourselves how to improve the transduction potential in human cell lines and also primary cells that are generally poorly transducible with Ad 5 serotype. We showed that HD-vectors containing B-group serotype 35 fiber knob domains (HD-Ad 5/35) efficiently transduced human leukemia cells and primary $CD34^+$ cells.

Another concern we wanted to face with was the relatively low transduction capacity of Ad 5 virus to transduce certain cell types, in particular the hematopoietic derived cell lines, primary cells and $CD34^+$ cells.

Currently existing adenovirus, rAAV, and onco-retrovirus vectors do not allow for efficient and stable transduction of human hematopoietic stem cells (HSCs). I used a capsid-modified adenovirus vector devoid of all viral genes for transient expression of GFP-DNGFr in hematopoietic derived stable cell lines and CD34. I wanted to test if using two different fiber knob domain in the same capsid type there were differences in transduction efficiency.

In the first step I decide to test the difference in transduction capacity of these two viruses. Without any doubt Ad 5/35 demonstrated to be able to transducer more efficiently hematopoietic derived cell lines and a lower MOI. But Ad 5/35 along the time

demonstrated a faster clearance from cells. Gene expression was lost faster than genes inserted with Ad 5. Our hypothesis was that maybe virus entrance was responsible for this phenomenon.

To evaluate our hypothesis that the primary attachment receptor largely determines the selection of intracellular trafficking routes by wild-type or capsid-modified Ads, we used Ad vectors with identical capsids except for the fiber knob domain, which is the capsid moiety responsible for high-affinity virus attachment to cell surface receptors. Anuj Gaggar et al. (163) demonstrate that the major difference in the trafficking of Ad 5 and Ad 5/35 was that Ad 5/35 virus particles were readily found in late endosomes/lysosomes for up to 4 hours after infection, whereas Ad 5 virus escaped rapidly to the cytosol and never co-localized with late endosomal/lysosomal markers. EM analyses showed that at 2 hours after virus infection, the majority (more than 80%) of Ad 5 virus particles could be found as free particles in the cytoplasm and in the perinuclear space and only 3% were found in the endosomes. However, at the same time point, more than 60% of Ad 5/35 virions were found within endosomes. This is in agreement with observations made for wild-type subgroup B and C viruses as well as with studies performed with chimeric Ad 5/7 vectors (162). Shayakhmetov et al. (152) argue that the ability of the fiber knob to interact with different attachment receptors accounts for the different trafficking pathways observed for Ad 5 and Ad 5/35 vectors independently of the length of the fiber shaft domain. CAR appears to be required only to hold the virus particle in a suitable position in order to allow α_v integrins to interact with the penton base. This interaction has been found to initiate the signaling allowing for virus internalization and endosome release. For the unknown Ad 35 receptor this signaling might be absent or different, resulting in a different trafficking route for the incoming virus. Notably, Ad 5/35 and Ad 5 vectors have identical capsids except for the fiber knob domain. This implies that both of these vectors have the same net charge of the capsid. This is important, considering that the net charge of the capsid may affect the pathway and efficiency of Ad internalization.

In my experiment I noticed that Ad 5/35 ensure a faster GFP expression in all cells we used but this not translate into a higher efficiency of gene transfer or level of transgene expression. My data indicate that this is at least in part due to a sort of genetic instability of viruses that passes from the endosomal/lysosomal cellular compartments. It seems that a earlier gene expression from that viruses do not correspond to a longer or constant gene expression. In general, molecules that enter cells via receptor-mediated endocytosis can follow one of two major routes: (i) the endocytic recycling pathway, in which membrane proteins and membrane-bound proteins are collected in a tubulovesicular compartment, termed the endocytic recycling compartment, prior to trafficking back to the cell surface; or (ii) the lysosomal pathway, in which a select set of membrane proteins, ligands that have dissociated from their receptors, and soluble materials occupy a compartment termed the sorting endosome, which later matures and acidifies to become a late endosome and finally a lysosome. It appears that trafficking of Ad 5/35 particles involves both pathways. Ad 5/35 particles achieve proximity to the nucleus by remaining inside late endosomes/lysosomes. It appears also that some of the Ad 5/35 particles enter the endocytic recycling pathway and are released from the cell. Finally, in comparison to the Ad 5-CAR interaction, the binding of Ad 5/35 particles to the receptor may lead to more destructive changes in structures that determine the infectivity of Ad particles. Other factors that may influence Ad 5/35 trafficking remain to be investigated, including whether fiber release occurs during internalization and which signaling pathways are activated. The development of Ad vectors that interact with receptors different from CAR requires a better understanding of events that follow the internalization of viral particles.

As I wrote before it could be of interest to test the capability of this new hybrid serotype to transduce the keratinocyte repopulating stem cell population. No stem cell keratinocyte marker is known, so is not possible to select this population as it is possible in a $CD34^+$ cell contest. The only proof of principle available in this case is transduce the total

keratinocyte population and see if it is possible to isolate a clone with the integrated cassette.

References

0. Hacein-Bey-Abina, S., Le Deist, F., Carlier, F., Bouneaud, C., Hue, C., De Villartay, J.P., Thrasher, A.J., Wulffraat, N., Sorensen, R., Dupuis-Girod, S. *et al.*, 2002. Sustained correction of X-linked severe combined immunodeficiency by ex vivo gene therapy. *N. Engl. J. Med.* **346**, pp. 1185–1193.

1. Schröder, A.R.W., Shinn, P., Chen, H., Berry, C., Ecker, J.R. and Bushman, F., 2002. HIV-1 integration in the human genome favors active genes and local hotspots. *Cell* **110**, pp. 521–529.

2. Wu, X., Li, Y., Crise, B. and Burgess, S.M., 2003. Transcription start regions in the human genome are favored targets for MLV integration. *Science* **300**, pp. 1749–1751.

3. Hacein-Bey-Abina, S., Von Kalle, C., Schmidt, M., McCormack, M.P., Wulffraat, N., Leboulch, P., Lim, A., Osborne, C.S., Pawliuk, R., Morillon, E. *et al.*, 2003. *LMO2*-associated clonal T cell proliferation in two patients after gene therapy for SCID-X1. *Science* **302**, pp. 415–419.

4. Kotin, R.M., Siniscalco, M., Samulski, R.J., Zhu, X., Hunter, L., Laughlin, C.A., McLaughlin, S., Muzyczka, N., Rocchi, M. and Berns, K.I., 1990. Site-specific integration by adeno-associated virus. *Proc. Natl. Acad. Sci. USA* **87**, pp. 2211–2215.

5. Samulski, R.J., Zhu, X., Xiao, X., Brook, J.D., Housman, D.E., Epstein, N. and Hunter, L.A., 1991. Targeted integration of adeno-associated virus (AAV) into human chromosome 19. *EMBO J.* **10**, pp. 3941–3950

6. Im, D. and Muzyczka, N., 1989. Factors that bind to adeno-associated virus terminal repeats. *J. Virol.* **63**, pp. 3095–3104.

7. Im, D. and Muzyczka, N., 1990. The AAV origin binding protein Rep68 is an ATP-dependent site-specific endonuclease with DNA helicase activity. *Cell* **61**, pp. 447–457.

8. Owens, R.A., Weitzman, M.D., Kyöstiö, S.R.M. and Carter, B.J., 1993. Identification of a DNA-binding domain in the amino terminus of adeno-associated virus Rep proteins. *J. Virol.* **67**, pp. 997–1005.

9. Davis, M.D., Wu, J. and Owens, R.A., 2000. Mutational analysis of adeno-associated virus type 2 Rep68 protein endonuclease activity on partially single-stranded substrates. *J. Virol.* **74**, pp. 2936–2942.

10. Smith, R.H. and Kotin, R.M., 1998. The Rep52 gene product of adeno-associated virus is a DNA helicase with 3′-to-5′ polarity. *J. Virol.* **72**, pp. 4874–4881.

11. Wilmott R H, Amin R S, Perez C R, Wert S E, Keller G, Boivin G P, Hirsch R, De Innocencio J, Lu P, Reising S F, et al Safety of adenovirus-mediated transfer of the human cystic fibrosis transmembrane conductance regulator cDNA to the lungs of nonhuman primates.. Hum Gene Ther. 1996;**7**:301–310.

12. Mitani K, Graham F L, Caskey C T, Kochanek S. Rescue, propagation, and partial purification of a helper virus-dependent adenovirus vector. Proc Natl Acad Sci USA. 1995;**92**:3854–3858.

13. Schiedner G, Morral N, Parks R J, Wu Y, Koopmans S C, Langston C, Graham F L, Beaudet A L, Kochanek S. Genomic DNA transfer with a high-capacity adenovirus vector results in improved in vivo gene expression and decreased toxicity. Nat Gen. 1998;**18**:180–183.

14. Surosky R T, Urabe M, Godwin S G, McQuiston S A, Kurtzman G J, Ozawa K, Natsoulis G. Adeno-associated virus Rep proteins target DNA sequences to a unique locus in the human genome. J Virol. 1997;**71**:7951–7959.

15. Lamartina S, Roscilli G, Rinaudo D, Delmastro P, Toniatti C. Lipofection of Purified Adeno-Associated Virus Rep68 Protein: toward a Chromosome-Targeting Nonviral ParticleJ Virol. 1998;**72**:7653–7658.

16. Pieroni L, Fipaldini C, Monciotti A, Cimini D, Sgura A, Fattori E, Epifano O, Cortese R, Palombo F, La Monica N. Targeted integration of adeno-associated virus-derived plasmids in transfected human cells.Virology. 1998;**249**:249–259.

17. Flotte T R, Carter B J. Adeno-associated virus vectors for gene therapy. Gene Ther. 1995;**2**:357–362.

18. Shelling A N, Smith M. Targeted integration of transfected and infected adeno-associated virus vectors containing the neomycin resistance gene. Gene Ther. 1994;**1**:165–169.

19. Balagué C, Kalla M, Zhang W W. Adeno-associated virus Rep78 protein and terminal repeats enhance integration of DNA sequences into the cellular genome.J Virol. 1997;**71**:3299–3306.

20. Srivastava, A., E. W. Lusby, and K. I. Berns. 1983. Nucleotide sequence and organization of the adeno-associated virus 2 genome. J. Virol. 45:555-564.

21. Berns, K. I. 1996. Parvoviridae: the viruses and their replication, p. 1017-1041. In B. N. Fields (ed.), Fundamental virology, 3rd ed. Lippincott-Raven Publishers, Philadelphia Pa.

22. Linden, R. M., and K. I. Berns. 1997. Site-specific integration by adeno-associated virus: a basis for a potential gene therapy vector. Gene Ther. 4:4-5.

23. Hacein-Bey-Abina, S., C. von Kalle, M. Schmidt, F. Le Deist, N. Wulffraat, E. McIntyre, I. Radford, J. L. Villeval, C. C. Fraser, M. Cavazzana-Calvo, and A. Fischer. 2003. A serious adverse event after successful gene therapy for X-linked severe combined immunodeficiency. N. Engl. J. Med. 348:255-256.

24. Inoue, N., R. Dong, R. K. Hirata, and D. W. Russell. 2001. Introduction of single base substitutions at homologous chromosomal sequences by adeno-associated virus vectors. Mol. Ther. 3:526-530.

25. Nakai, H., E. Montini, S. Fuess, T. A. Storm, M. Grompe, and M. A. Kay. 2003. AAV serotype 2 vectors preferentially integrate into active genes in mice. Nat. Genet. 34:297-302.

26. Philpott, N. J., C. Giraud-Wali, C. Dupuis, J. Gomos, H. Hamilton, K. I. Berns, and E. Falck-Pedersen. 2002. Efficient integration of recombinant adeno-associated virus DNA vectors requires a p5-rep sequence in cis. J. Virol. **76:**5411-5421.

27. Philpott, N. J., J. Gomos, K. I. Berns, and E. Falck-Pedersen. 2002. A p5 integration efficiency element mediates Rep-dependent integration into AAVS1 at chromosome 19. Proc. Natl. Acad. Sci. USA 99:12381-12385.].

28. Tan, I., C. H. Ng, L. A Lim, and T. A Leung. 2001. Phosphorylation of a novel myosin binding subunit of protein phosphatase 1 reveals a conserved mechanism in the regulation of actin cytoskeleton. J. Biol. Chem. **276:**21209-21216.

29. Giraud, C., E. Winocour, and K. I. Berns. 1995. Recombinant junctions formed by site-specific integration of adeno-associated virus into an episome. J. Virol. 69:6917-6924.

30. Dutheil, N., F. Shi, T. Dupressoir, and R. M. Linden. 2000. Adeno-associated virus site-specifically integrates into a muscle-specific DNA region. Proc. Natl. Acad. Sci. USA 97:4862-4866.

31. Srivastava, A. 1987. Replication of the adeno-associated virus DNA termini in vitro. Intervirology 27:138-147.

32. Hölscher, C., Hörer, M., Kleinschmidt, J. A., Zentgraf, H., Bürkle, A. & Heilbronn, R. (1994). Cell lines inducibly expressing the adeno-associated virus (AAV) *rep* gene: requirements for productive replication of *rep*-negative AAV mutants. *J Virol* 68, 7169–7177.

33. Labow, M. A., Graf, L. H., Jr & Berns, K. I. (1987). Adeno-associated virus gene expression inhibits cellular transformation by heterologous genes. *Mol Cell Biol* 7, 1320–1325.[

34. Hermonat, P. L. (1991). Inhibition of H-ras expression by the adeno-associated virus Rep78 transformation suppressor gene product. *Cancer Res* 51, 3373–3377.

35. Hermonat, P. L. (1994). Down-regulation of the human c-*fos* and c-*myc* proto-oncogene promoters by adeno-associated virus Rep78. *Cancer Lett* 81, 129–136.

36. Oelze, I., Rittner, K. & Sczakiel, G. (1994). Adeno-associated virus type 2 *rep* gene-mediated inhibition of basal gene expression of human immunodeficiency virus type 1 involves its negative regulatory functions. *J Virol* **68**, 1229–1233.

37. Hermanns, J., Schulze, A., Jansen-Dürr, P., Kleinschmidt, J. A., Schmidt, R. & zur Hausen, H. (1997). Infection of primary cells by adeno-associated virus type 2 results in a modulation of cell cycle-regulating proteins. *J Virol* 71, 6020–6027.

38. Hong, G., P. Ward, and K. I. Berns. 1994. Intermediates of adeno-associated virus DNA replication in vitro. J. Virol. 68:2011-2015.

39. Ni, T.-H., W. F. McDonald, I. Zolothukin, T. Melendy, S. Waga, B. Stillman, and N. Muzyczka. 1998. Cellular proteins required for adeno-associated virus DNA replication in the absence of adenovirus coinfection. J. Virol. 72:2777-2787.

40. Beaton, A., P. Palumbo, and K. I. Berns. 1989. Expression from the adeno-associated virus p5 and p19 promoters is negatively regulated in *trans* by the *rep* protein. J. Virol. 63:4450-4454.

41. Schmidt M, Chiorini JA, Afione S, Kotin R. 2002. Adeno-associated virus type 2 Rep78 inhibition of PKA and PRKX: fine mapping and analysis of mechanism. J Virol. 76(3):1033-42.

42. Snyder, R. O., D. S. Im, T. Ni, X. Xiao, R. J. Samulski, and N. Muzyczka. 1993. Features of the adeno-associated virus origin involved in substrate recognition by the viral Rep protein. J. Virol. 67:6096-6104.

43. Snyder, R. O., R. J. Samulski, and N. Muzyczka. 1990. In vitro resolution of covalently joined AAV chromosome ends. Cell 60:105-113.

44. Dyall J. & Berns, K. I. (1998) Site-Specific Integration of Adeno-Associated Virus into an Episome with the Target Locus via a Deletion-Substitution Mechanism *J. Virol.* 72, 6195-6198.

45. Linden R. M., Ward, P., Giraud, C., Winocour, E. & Berns, K. I. Site-specific integration by adeno-associated virus. (1996) *Proc. Natl. Acad. Sci. USA* 93, 11288-11294.

46. Urcelay E., Ward, P., Wiener, S. M., Safer, B. & Kotin, R. M. Asymmetric replication in vitro from a human sequence element is dependent on adeno-associated virus Rep protein. (1995) *J. Virol.* 69, 2038-2046.

47. Carlson, C. A., D. S. Steinwaerder, H. Stecher, D. M. Shayakhmetov, and A. Lieber. 2002. Rearrangements in adenoviral genomes mediated by inverted repeats. Methods Enzymol. 346:277-292.

48. Burgess Hickman, A., D. R. Ronning, Z. N. Perez, R. M. Kotin, and F. Dyda. 2004. The nuclease domain of adeno-associated virus Rep coordinates replication initiation using two distinct DNA recognition interfaces. Mol. Cell 13:403-414.

49. Ryan, J. H., S. Zolotukhin, and N. Muzyczka. 1996. Sequence requirements for binding of Rep68 to the adeno-associated virus terminal repeats. J. Virol. 70:1542-1553.

50. Wu, J., M. D. Davis, and R. A. Owens. 1999. Factors affecting the terminal reslution site endonuclease, helicase, and ATPase activities of adeno-associated virus type 2 Rep proteins. J. Virol. 73:8235-8244.

51. Brister, J. R., and N. Muzyczka. 2000. Mechanism of Rep-mediated adeno-associated virus origin nicking. J. Virol. 74:7762-7771.

52. Jang, M. Y., O. H. Yarborough, G. B. Conyers, P. McPhie, and R. A. Owens. 2005. Stable secondary structure near the nicking site for adeno-associated virus type 2 Rep proteins on human chromosome 19. J. Virol. 79:3544-3556.

53. Kogure, K., Urabe, M., Mizukami, H., Kume, A., Sato, Y., Monahan, J. & Ozawa, K. (2001). Targeted integration of foreign DNA into a defined locus on chromosome 19 in K562 cells using AAV-derived components. *Int J Hematol* 73, 469–475.

54. Xiao, W., K. H. Warrington, Jr., P. Hearing, J. Hughes, and N. Muzyczka. 2002. Adenovirus-facilitated nuclear translocation of adeno-associated virus type 2. J. Virol. 76:11505-11517.

55. Smith, R. H., and R. M. Kotin. 2000. An adeno-associated virus (AAV) initiator protein, Rep78, catalyzes the cleavage and ligation of single-stranded AAV ori DNA. J. Virol. 74:3122-3129.

56. Giraud, C., E. Winocour, and K. I. Berns. 1994. Site-specific integration by adeno-associated virus is directed by a cellular DNA sequence. Proc. Natl. Acad. Sci. USA 91:10039-10043.

57. Recchia, A., Parks, R.J., Lamartina, S., Toniatti, C., Pieroni, L., Palombo, F., Ciliberto, G., Graham, F.L., Cortese, R., La Monica, N. *et al.*, 1999. Site-specific integration mediated by a hybrid adenovirus/adeno-associated virus vector. *Proc. Natl. Acad. Sci. USA* **96**, pp. 2615–2620.

58. Costantini, L.C., Jacoby, D.R., Wang, S., Fraefel, C., Breakefield, X.O. and Isacson, O., 1999. Gene transfer to the nigrostriatal system by hybrid herpes simplex virus/adeno-associated virus amplicon vectors. *Hum. Gene Ther.* **10**, pp. 2481–2494.

59. Palombo, F., Monciotti, A., Recchia, A., Cortese, R., Ciliberto, G. and La Monica, N., 1998. Site-specific integration in mammalian cells mediated by a new hybrid baculovirus-adeno-associated virus vector. *J. Virol.* **72**, pp. 5025–5034.

60. Smith, R.H., Spano, A.J. and Kotin, R.M., 1997. The Rep78 gene product of adeno-associated virus (AAV) self-associates to form a hexameric complex in the presence of AAV *ori* sequences. *J. Virol.* **71**, pp. 4461–4471.

61. Weger, S., Wistuba, A., Grimm, D. & Kleinschmidt, J. A. (1997). Control of adeno-associated virus type 2 cap gene expression: relative influence of helper virus, terminal repeats, and Rep proteins. *J Virol* 71, 8437–8447.

62. Chiorini, J. A., Zimmermann, B., Yang, L., Smith, R. H., Ahearn, A., Herberg, F. & Kotin, R. M. (1998). Inhibition of PrKX, a novel protein kinase, and the cyclic AMP-dependent protein kinase PKA by the regulatory proteins of adeno-associated virus type 2. *Mol Cell Biol* 18, 5921–5929.

63. Di Pasquale, G. & Stacey, S. N. (1998). Adeno-associated virus Rep78 protein interacts with protein kinase A and its homolog PRKX and inhibits CREB-dependent transcriptional activation. *J Virol* 72, 7916–7925.

64. Nony, P., J. Tessier, G. Chadeuf, P. Ward, A. Giraud, M. Dugast, R. M. Linden, P. Moullier, and A. Salvetti. 2001. Novel *cis*-acting replication element in the adeno-associated virus type 2 genome is involved in amplification of integrated *rep-cap* sequences. J. Virol. 75:9991-9994.

65. Tullis, G. E., and T. Shenk. 2000. Efficient replication of adeno-associated virus type 2 vectors: a *cis*-acting element outside of the terminal repeats and a minimal size. J. Virol. 74:11511-11521.

66. Chang, L.-S., Y. Shi, and T. Shenk. 1989. Adeno-associated virus p5 promoter contains an adenovirus E1A-inducible element and a binding site for the major late transcription factor. J. Virol. 63:3479-3488.

67. Wang, X.-S., and A. Srivastava. 1997. A novel terminal resolution-like site in the adeno-associated virus type 2 genome. J. Virol. 71:1140-1146.

68. Pereira, D. J., D. M. McCarty, and N. Muzyczka. 1997. The adeno-associated virus (AAV) Rep protein acts as both a repressor and an activator to regulate AAV transcription during a productive infection. J. Virol. 71:1079-1088.

69. Wonderling, R. S., and R. A. Owens. 1997. Binding sites for adeno-associated virus Rep proteins within the human genome. J. Virol. **71:**2528-2534.

70. Chiorini, J. A., L. Yang, B. Safer, and R. M. Kotin. 1995. Determination of adeno-associated virus Rep68 and Rep78 binding sites by random sequence oligonucleotide selection. J. Virol. **69:**7334-7338.

71. Cho S, Wensink P. DNA binding by the male and female doublesex proteins of Drosophila melanogaster. J Biol Chem. 1997;**272**:3185–3189.

72. Kim J, Takeda Y, Matthews B, Anderson W. Kinetic studies on Cro repressor-operator DNA interaction. J Mol Biol. 1987;**196**:149–158.

73. McLaughlin S K, Collis P, Hermonat P L, Muzyczka N. Adeno-associated virus general transduction vectors: analysis of proviral structures. J Virol. 1988;**62**:1963–1973.

74. Lamartina S, Sporeno E, Toniatti C. In vitro and in vivo analysis of the AAV integration site in human chromosome 19. J Gene Med. 1999;**1**:68.

75. Cotmore S F, Tattersall P. High-mobility group 1/2 proteins are essential for initiating rolling-circle-type DNA replication at a parvovirus hairpin origin. J Virol. 1998;**72**:8477–8484.

76. Dyall J, Szabo P, Berns K I. Adeno-associated virus (AAV) site-specific integration: formation of AAV-AAVS1 junctions in an in vitro system. Proc Natl Acad Sci USA. 1999;**96**:12849–12854.

77. Syu L, Fluck M. Site-specific in situ amplification of the integrated polyomavirus genome: a case for a context-specific over-replication model of gene amplification. J Mol Biol. 1997;**271**:76–99.

78. Muzyczka N. Use of adeno-associated virus as a general transduction vector for mammalian cells. Curr Top Microbiol Immunol. 1992;**158**:97–129.

79. Onate S A, Prendergast P, Wagner J P, Nissen M, Reeves R, Pettijohn D E, Edwards D P. The DNA-bending protein HMG-1 enhances progesterone receptor binding to its target DNA sequences. Mol Cell Biol. 1994;**14**:3376–3391.

80. Isaacs A. and Lindenmann,J. (1957) Virus interference. I. The interferon. *Proc. R. Soc. Lond. B Biol. Sci.*, **147**, 258–267.

81. Sen G.C. (2001) Viruses and interferons. *Annu. Rev. Microbiol.*, **55**, 255–281.

82. Aubertin A.M., Guir,J. and Kirn,A. (1970) The inhibition of vaccinia virus DNA synthesis in KB cells infected with frog virus 3. *J. Gen. Virol.*, **8**, 105–111.

83. Garry R.F. (1988) Poliovirus protease 2A is required for interference with vesicular stomatitis virus-specified protein synthesis. *Arch. Virol.*, **103**, 133–137.

84. Aldabe R., Feduchi,E., Novoa,I. and Carrasco,L. (1995) Efficient cleavage of p220 by poliovirus 2Apro expression in mammalian cells: effects on vaccinia virus. *Biochem. Biophys. Res. Commun.*, **215**, 928–936.

85. Xiang J., Wunschmann,S., Diekema,D.J., Klinzman,D., Patrick,K.D., George,S.L. and Stapleton,J.T. (2001) Effect of coinfection with GB virus C on survival among patients with HIV infection. *N. Engl. J. Med.*, **345**, 707–714.

86. Atchison R.W., Casto,B.C. and Hammon,W.M. (1965) Adeno-associated defective virus particles. *Science*, **149**, 754–755.

87. McPherson R.A., Rosenthal,L.J. and Rose,J.A. (1985) Human cytomegalovirus completely helps adeno-associated virus replication. *Virology*, **147**, 217–222.

88. Buller R.M., Janik,J.E., Sebring,E.D. and Rose,J.A. (1981) Herpes simplex virus types 1 and 2 completely help adenovirus-associated virus replication. *J. Virol.*, **40**, 241–247.

89. Georg-Fries B., Biederlack,S., Wolf,J. and zur Hausen,H. (1984) Analysis of proteins, helper dependence and seroepidemiology of a new human parvovirus. *Virology*, **134**, 64–71.

90. Parks W.P., Melnick,J.L., Rongey,R. and Mayor,H.D. (1967) Physical assay and growth cycle studies of a defective adeno-satellite virus. *J. Virol.*, **1**, 171–180.

91. Schlehofer J.R., Ehrbar,M. and zur Hausen,H. (1986) Vaccinia virus, herpes simplex virus and carcinogens induce DNA amplification in a human cell line and support replication of a helpervirus dependent parvovirus. *Virology*, **152**, 110–117.

92. Walz C., Deprez,A., Dupressoir,T., Durst,M., Rabreau,M. and Schlehofer,J.R. (1997) Interaction of human papillomavirus type 16 and adeno-associated virus type 2 co-infecting human cervical epithelium. *J. Gen. Virol.*, **78**, 1441–1452.

93. Casto B.C., Atchison,R.W. and Hammon,W.M. (1967) Studies on the relationship between adeno-associated virus type I (AAV-1) and adenoviruses. I. Replication of AAV-1 in certain cell cultures and its effect on helper adenovirus. *Virology*, **32**, 52–59.

94. Bantel-Schaal U. and zur Hausen,H. (1988) Adeno-associated viruses inhibit SV40 DNA amplification and replication of herpes simplex virus in SV40-transformed hamster cells. *Virology*, **164**, 64–74.

95. Hermonat P.L. (1992) Inhibition of bovine papillomavirus plasmid DNA replication by adeno-associated virus. *Virology*, **189**, 329–333.

96. Hermonat P.L. (1994) Adeno-associated virus inhibits human papillomavirus type 16: a viral interaction implicated in cervical cancer. *Cancer Res.*, **54**, 2278–2281.

97. Antoni B.A., Rabson,A.B., Miller,I.L., Trempe,J.P., Chejanovsky,N. and Carter,B.J. (1991) Adeno-associated virus Rep protein inhibits human immunodeficiency virus type 1 production in human cells. *J. Virol.*, **65**, 396–404.

98. Schlehofer J.R. (1994) The tumor suppressive properties of adeno-associated viruses. *Mutat. Res.*, **305**, 303–313.

99. Suomalainen M., Nakano,M.Y., Boucke,K., Keller,S. and Greber,U.F. (2001) Adenovirus-activated PKA and p38/MAPK pathways boost microtubule-mediated nuclear targeting of virus. *EMBO J.*, **20**, 1310–1319.

100. Leza M.A. and Hearing,P. (1989) Independent cyclic AMP and E1A induction of adenovirus early region 4 expression. *J. Virol.*, **63**, 3057–3064.

101. Walsh D.A., Ashby,C.D., Gonzalez,C., Calkins,D., Fischer,E.H. and Kerbs,E.G. (1971) Purification and characterization of a protein inhibitor of adenosine 3′,5′-monophosphate-dependent protein kinases. *J. Biol. Chem.*, **246**, 1977–1987.

102. Steller H. Mechanisms and genes of cellular suicide. Science. 1995;**267**:1445–1449.

103. Vaux D L, Strasser A. The molecular biology of apoptosis. Proc Natl Acad Sci USA. 1996;**93**:2239–2244.

104. Earnshaw W C, Luis L M, Martins M, Kaufmann S H. Mammalian caspases: structure, activation, substrates, and functions during apoptosis. Annu Rev Biochem. 1999;**68**:383–424.

105. Yang Q, Chen F, Trempe J P. Characterization of cell lines that inducibly express the adeno-associated virus Rep proteins. J Virol. 1994;**68**:4847–4856.

106. Zhou C, Trempe J P. Induction of apoptosis by cadmium and the adeno-associated virus Rep proteins. Virology. 1999;**261**:280–287.

107. Louis N, Evelegh C, Graham F L. Cloning and sequencing of the cellular-viral junctions from the human adenovirus type 5 transformed 293 cell line. Virology. 1997;**233**:423–429.

108. Barry M, McFadden G. Apoptosis regulators from DNA viruses. Curr Opin Immunol. 1998;**10**:422–430.

109. Payette Y, Lachapelle M, Daniel C, Bernier J, Fournier M, Krzystyniak K. Decreased interleukin-2 receptor and cell cycle changes in murine lymphocytes exposed in vitro to low doses of cadmium chloride. Int J Immunopharmacol. 1995;**17**:235–246.

110. Bagchi D, Joshi S S, Bagchi M, Balmoori J, Benner E J, Kuszynski C A, Stohs S J. Cadmium- and chromium-induced oxidative stress, DNA damage, and apoptotic cell death in cultured human chronic myelogenous leukemic K562 cells, promyelocytic leukemic HL-60 cells, and normal human peripheral blood mononuclear cells. J Biochem Mol Toxicol. 2000;**14**:33–41.

111. Meerarani P, Ramadass P, Toborek M, Bauer H C, Bauer H, Hennig B. Zinc protects against apoptosis of endothelial cells induced by linoleic acid and tumor necrosis factor alpha. Am J Clin Nutr. 2000;**71**:81–87.

112. Caillet-Fauquet P, Perros M, Brandenburger A, Spegelaere P, Rommelaere J. Programmed killing of human cells by means of an inducible clone of parvoviral genes encoding non-structural proteins. EMBO J. 1990;**9**:2989–2995.

113. Op De Beeck A, Caillet-Fauquet P. The NS1 protein of the autonomous parvovirus minute virus of mice blocks cellular DNA replication: a consequence of lesions to the chromatin? J Virol. 1997;**71**:5323–5329.

114. Fisher K J, Kelley M W, Burda J F, Wilson J M. A novel adenovirus-adeno-associated virus hybrid vector that displays efficient rescue and delivery of the AAV genome. Hum Gene Ther. 1996;**7**:2079–2087.

115. Hitt M M, Addison C L, Graham F L. Human adenovirus vectors for gene transfer into mammalian cells. Adv Pharmacol. 1997;**40**:137–206.

116. Smith, A. E. (1995). Viral vectors in gene therapy. Annual Review of Microbiology 49: 807-838.

117. Verma, I. M. and Somia, N. (1997). Gene therapy - promises, problems and prospects. Nature 389: 239-242.

118. Graham, F. L., Smiley, J., Russell, W. L. and Nairn, R. (1997). Characterization of a human cell line transformation by DNA from adenovirus 5. General Virology 36: 59-72.

119. Engelhardt, J. F., Litsky, L., and Wilson, J. M. (1994). Prolonged gene expression in cotton rat lung with recombinant adenoviruses defective in E2a. Human Gene Therapy 5: 1217-1229.

120. Armentano, D., Zabner, J., Sacks, C., Sookdeo, C. C., Smith, M. P., St. George, J. A., Wadsworth, S. C., Smith, A. E. and Gregory, R. J. (1997). Effect of the E4 region on the presistence of transgene expression from adenovirus vectors. Journal of Virology 71: 2408-2416.

121. Chen, H., Mack, L. M., Kelly, R., Ontell, M., Kochanek, S. and Clemens, P. R. (1997). Persistence in muscle of an adenoviral vector that lacks all viral genes. Proceedings of the National Academy of Sciences of the U.S.A. 94: 1645-1650.

122. Worgall, S., Wolff, G., Falck-Pedersen, E. and Crystal R. G. (1997). Innate immune mechanisms dominate elimination of adenoviral vectors following in vivo administration. Human Gene Therapy 8: 37-44.

123. Yang, Y. and Wilson, J. M. (1995). Clearance of adenovirus-infected hepatocytes by MHC class I restricted CD4+ CTLs in vivo. Journal of Immmunology 155: 2564-2569.

124. Sparer, T. E., Wynn, S. G., Clark, D. J., Kaplan, J. M., Cardoza, L. M., Wadsworth, S. C., Smith, A. E. and Gooding, L. R. (1997). Generation of cytotoxic T

lymphocytes against immunorecessive epitopes after multiple immunizations with adenovirus vectors is dependent on haplotype. Journal of Virology 71: 2277-2284.

125. Kagami, H., Atkinson, J. C., Michalek, S. M., Handelman, B., Yu, S., Baum, B. J. and O'Connell, B. (1998). Repetitive adenovirus administration to the parotid gland: role of immunolgical barriers and induction of oral tolerance. Human Gene Therapy 9: 305-313.

126. Gahry-Sdard, H., Molinier-Frenkel, V., Le Boulaire, C., Saulnier, P., Opolon, P., Lengange, R., Gautier, E., Le Cesne, A., Zitvogel, L., Venet, A., Schatz, C., Courtney, M., Le Chevalier, T., Tursz, T., Guillet, J. and Farace, F. (1997). Phase I trial of recombinant adenovirus gene transfer in lung cancer. Journal of Clinical Investigation 100: 2218-2226.

127. Benihound K, Yeh P, Perricaudet M (1999) Adenovirus vector for gene delivery. *Curr Opin Biotech* **10:** 440-447.

128. Wang Y, Huang S (2000) Adenovirus technology for gene manipulation and functional studies. *Drug Disc Today* **5:** 10-16.

129. Chan L (1995) Use of somatic gene transfer to study lipoprotein metabolism in experimental animals *in vivo*. *Curr Opin Lipidol* **6:** 335-340.

130. Mountain A (2000) Gene therapy: the first decade. *Trends Biotechnol* **18:** 119-128.

131. Buttgereit P, Weineck S, Ropke G, Marten A, Brand K, Heinicke T, Caselmann WH, Huhn D, Schmidt-Wolf IG (2000) Efficient gene transfer into lymphoma cells using adenoviral vectors combined with lipofection. *Cancer Gene Ther* **7:** 1145-1155.

132. Zhang HG, Zhou T, Yang P, Edwards CK III, Curiel DT, Moutz DM (1998) Inhibition of TNF□ decreases inflammation and prolongs adenovirus gene expression in lung and liver. *Hum Gene Ther* **9:** 1875-1884.

133. Morral N, Parks R, Zhou H, Langston C, Schiedner G, Quinones J, Graham FL, Kochanek S, Beaudet AL (1998) High doses of a helper-dependent adenoviral vector yield supra-physiological levels of alpha1-antitripsin with negligible toxicity. *Hum Gene Ther* **9:** 2709-2716.

134. Toietta G, Pastore L, Cerullo V, Finegold M, Beaudet AL, Lee B (2002) Generation of helper-dependent adenoviral vectors by homologous recombination. *Mol Ther* **5:** 204-210.

135. Sakhuja K, Reddy PS, Ganesh S, Cantaniag F, Pattison S, Limbach P, Kayda DB, Kadan MJ, Kaleko M, Connelly S (2003) Optimization of the generation and propagation of gutless adenoviral vectors. *Hum Gene Ther* **14:** 243-254.

136. Ng P, Evelegh C, Cummings D, Graham FL (2002) Cre levels limit packaging signal excision efficiency in the Cre/loxP helper-dependent adenoviral vector system. *J Virol* **76:** 4181-4189.

137. Umana P, Gerdes CA, Stone D, Davis JR, Ward D, Castro MG, Lowenstein PR (2001) Efficient FLPe recombinase enables scalable production of helper-dependent adenoviral vectors with negligible helper-virus contamination. *Nat Biotechnol* **19:** 582-585

138. Bramson JL, Grinshtein N, Meulenbroek RA, Lunde J, Kottachchi D, Lorimer IA, Jasmin BJ, Parks RJ (2004) Helper-dependent adenoviral vectors containing modified fiber for improved transduction of developing and mature muscle cells. *Hum Gene Ther* **15:** 179-188.

139. Zou L, Zhou H, Postore L, Yang K (2000) Prolonged transgene expression mediated by a helper-dependent adenoviral vector in the central nervous system. *Mol Ther* **2:** 105-113.

140. Horwitz, M. The Adenoviridae and their replication. In: Fields B N, Knipe D M. , editors; Fields B N, Knipe D M. , editors. Virology. Vol. 2. New York, N.Y: Raven Press; 1990. pp. 1679–1721.

141. Eiz B, Pring-□kerblom P. Molecular characterization of the type-specific γ-determinant located on the adenovirus fiber. J Virol. 1997;**71**:6576–6581.

142. Hierholzer J C. Further subgrouping of the human adenoviruses by differential hemagglutination. J Infect Dis. 1973;**128**:541–550.

143. Horwitz, M. Adenoviruses. In: Fields B N, Knipe D M. , editors; Fields B N, Knipe D M. , editors. Virology. Vol. 2. New York, N.Y: Raven Press; 1990. pp. 1723–1740.

144. Bailey A, Mautner V. Phylogenetic relationships among adenovirus serotypes. Virology. 1994;**205**:438–452.

145. Bergelson J M, Cunningham J A, Droguett G, Kurt-Jones E A, Krithivas A, Hong J S, Horwitz M A, Crowell R L, Finberg R W. Isolation of a common receptor for Coxsackie B viruses and adenoviruses 2 and 5. Science. 1997;**275**:1320–1323.

146. Fender P, Kidd A H, Brebant R, Öberg M, Drouet E, Chroboczek J. Antigenic sites on the receptor-binding domain of human adenovirus type 2 fiber. Virology. 1995;**214**:110–117.

147. Krasnykh V N, Mikheeva G V, Douglas J T, Curiel D T. Generation of recombinant adenovirus vectors with modified fibers for altering viral tropism. J Virol. 1996;**70**:6839–6846.

148. Roelvink P, Kovesdi I, Wickham T. Comparative analysis of adenovirus fiber-cell interaction: Ad2 and Ad9 utilize the same cellular fiber receptor but use different binding strategies for attachment. J Virol. 1996;**70**:7614–7621.

149. Xia D, Henry L J, Gerard R D, Deisenhofer J. Crystal structure of the receptor-binding domain of adenovirus type 5 fiber protein at 1.7 □ resolution. Structure. 1994;**2**:1259–1270.

150. Douglas J T, Rogers B E, Rosenfeld M E, Michael S I, Feng M, Curiel D T. Targeted gene delivery by tropism-modified adenoviral vectors. Nat Biotechnol. 1996;**14**:1574–1578.

151. Mathias P, Wickham T, Moore M, Nemerow G. Multiple adenovirus serotypes use av integrins for infection. J Virol. 1994;**68**:6811–6814.

152. Shayakhmetov DM, Papayannopoulou T, Stamatoyannopoulos G, Lieber A. Efficient gene transfer into human CD34(+) cells by a retargeted adenovirus vector. J Virol. 2000 Mar;74(6):2567-83.

153. Stevenson S C, Rollence M, Marshall-Neff J, McClelland A. Selective targeting of human cells by a chimeric adenovirus vector containing a modified fiber protein. J Virol. 1997;**71**:4782–4790.

154. Wickham T J, Segal D M, Roelvink P W, Carrion M E, Lizonova G M, Kovesdi I. Targeted adenovirus gene transfer to endothelial and smooth muscle cells by using bispecific antibodies. J Virol. 1996;**70**:6831–6838.

155. Zabner J, Puga A, Freimuth P, Welsh M J. Lack of high affinity fiber receptor activity explains the resistance of ciliated airway epithelia to adenovirus infection. J Clin Investig. 1997;**100**:1144–1149.

156. Chillon M, Bosch A, Zabner J, Law L, Armentano D, Welsh M, Davidson B L. Group D adenoviruses infect primary central nervous system cells more efficiently than those from group C. J Virol. 1999;**73**:2537–2540.

157. Byk T, Haddada H, Vainchenker W, Louache F. Lipofectamine and related cationic lipids strongly improve adenoviral infection efficiency of primitive human hematopoietic cells. Hum Gene Ther. 1998;**9**:2493–2502.

158. Krasnykh V, Dmitriev I, Mikheeva G, Miller C R, Belousova N, Curiel D T. Characterization of an adenovirus vector containing a heterologous peptide epitope in the HI loop of the fiber knob. J Virol. 1998;**72**:1844–1852.

159. Crompton J, Toogood C I, Wallis N, Hay R T. Expression of a foreign epitope on the surface of the adenovirus hexon. J Gen Virol. 1994;**75**:133–139

160. Wickham T J, Carrion M E, Kovesdi I. Targeting of adenovirus penton base to new receptors through replacement of its RGD motif with other receptor-specific peptide motifs. Gene Ther. 1995;**2**:750–756.

161. Horwitz, M S. Adenoviruses. In: Fields B N, Knipe D M, Howley P M. , editors; Fields B N, Knipe D M, Howley P M. , editors. Virology. Vol. 2. Philadelphia, Pa: Lippincott-Raven Publishers Inc.; 1996. pp. 2149–2171.

162. Gall J, Kass-Eisler A, Leinwand L, Falck-Pedersen E. Adenovirus type 5 and 7 capsid chimera: fiber replacement alters receptor tropism without affecting primary immune neutralizing epitopes. J Virol. 1996;**70**:2116–2123.

163. Anuj Gaggar, Dmitry M Shayakhmetov & André Lieber. 2003. CD46 is a cellular receptor for group B adenoviruses. Nat. Med. 11(9):1408-12.

164. Burgeson, R. E. (1993) *J. Invest. Dermatol.* **101,** 252–255

165. Shimizu, H., Ishiko, A., Masunaga, T., Kurihara, Y., Sato, M., Bruckner-Tuderman, L., and Nishikawa, T. (1997) *Lab. Invest.* **76,** 753–763

166. Rousselle, P., Keene, D. R., Ruggiero, F., Champliaud, M.-F., van der Rest, M.,and Burgeson, R. E. (1997) *J. Cell Biol.* **138,** 719–728

167. Bruckner-Tuderman, L. (1996) *Biochem. Cell Biol.* **74,** 729–736

168. Bruckner-Tuderman, L., Ru¨ egger, S., Odermatt, B., Mitsuhashi, Y., andSchnyder, U. W. (1988) *Dermatologica (Basel)* **176,** 57–64

169. McGrath, J. A., Ishida-Yamamoto, A., O'Grady, A., Leigh, I. M., and Eady,R. A. J. (1993) *J. Invest. Dermatol.* **100,** 366–372

170. Hilal, H., Rochat, A., Duquesnoy, P., Blanchet-Bardon, C., Wechsler, J.,Martin, N., Christiano, A., and Uitto, J. (1993) *Nat. Genet.* **5,** 287–293

171. Hovnanian, A., Hilal, H., Blanchet-Bardon, C., Prost, Y., Christiano, A. M.,Uitto, J., and Goossens, M. (1994) *Am. J. Hum. Genet.* **55,** 289–296

172. Christiano, A. M., and Uitto, J. (1996) *Exp. Dermatol.* **5,** 1–11

173. Christiano, A. M., Anhalt, G., Gibbons, S., Bauer, E. A., and Uitto, J. (1994)*Genomics* **21,** 160–168

174. Prockop, D. J., and Kivirikko, K. I. (1995) *Annu. Rev. Biochem.* **64,** 403–434

175. Olsen, B. R. (1995) *Curr. Opin. Cell Biol.* **7,** 720–727Burgeson RE. The collagens of skin Curr Probl Dermatol. 1987;17:61-75.

176. Bentz H, Morris NP, Murray LW, Sakai LY, Hollister DW, Burgeson RE. Isolation and partial characterization of a new human collagen with an extended triple-helical structural domain. Proc Natl Acad Sci U S A. 1983 Jun;80(11):3168-72.

177. Lunstrum GP, Kuo HJ, Rosenbaum LM, Keene DR, Glanville RW, Sakai LY, Burgeson RE. Anchoring fibrils contain the carboxyl-terminal globular domain of

type VII procollagen, but lack the amino-terminal globular domain. J Biol Chem. 1987 Oct 5;262(28):13706-12.

178. Hofmann H, Voss T, Kuhn K, Engel J. Localization of flexible sites in thread-like molecules from electron micrographs. Comparison of interstitial, basement membrane and intima collagens. J Mol Biol. 1984 Jan 25;172(3):325-43.

179. Recchia, A., et al. (1999). Site-specific integration mediated by a hybrid adenovirus/adeno-associated virus vector. Proc. Natl. Acad. Sci. USA 96: 2615 – 2620.

180. Francois A, Guilbaud M, Awedikian R, Chadeuf G, Moullier P, Salvetti A. The cellular TATA binding protein is required for rep-dependent replication of a minimal adeno-associated virus type 2 p5 element. J Virol. 2005 Sep;79(17):11082-94.

181. Li, Z. L., R. Brister, D.-S. Im, and N. Muzyczka. 2003. Characterization of the adenoassociated virus Rep protein complex formed on the viral origin of DNA replication. Virology 313:364-376.

182. Hermonat, P. L., A. D. Santin, R. B. Batchu, and D. Zhan. 1998. The adeno-associated virus Rep78 major regulatory protein binds the cellular TATA-binding protein in vitro and in vivo. Virology 245:120-127.

183. Lamartina, S., S. Ciliberto, and C. Toniatti. 2000. Selective cleavage of AAVS1 substrates by the adeno-associated virus type 2 Rep68 protein is dependent on topological and sequence constraints. J. Virol. 74:8831-8842.

184. Costello, E., P. Saudan, E. Winocour, L. Pizer, and P. Beard. 1997. High mobility group chromosomal protein 1 binds to the adeno-associated virus replication protein (Rep) and promotes Rep-mediated site-specific cleavage of DNA, ATPase activity and transcriptional repression. EMBO J. 16:5943-5954.

185. Stracker, T. H., G. D. Cassell, P. Ward, Y. M. Loo, B. van Breukelen, S. D. Carrington-Lawrence, R. K. Hamatake, P. C. van der Vliet, S. K. Weller, T. Melendy, and M. D. Weitzmann. 2004. The Rep protein of adeno-associated virus type 2 interacts with single-stranded DNA-binding proteins that enhance viral replication. J. Virol. 78:441-453.

186. Boyd, J. M., P. M. Loewenstein, Q.-Q. Tang, L. Yu, and M. Green. 2002. Adenovirus E1A N-terminal amino acid sequence requirements for repression of transcription in vitro and in vivo correlate with those required for E1A interference with TBP-TATA complex formation. J. Virol. 76:1461-1474.

187. Das, D., and W. M. Scovell. 2001. The binding interaction of HMG-1 with the TATA-binding protein/TATA complex. J. Biol. Chem. 276:32597-32605.

188. Stagljar, I., U. Hübscher, and A. Barberis. 1999. Activation of DNA replication in yeast by recruitment of the RNA polymerase II transrciption complex. Biol. Chem. 380:525-530.

189. Antoni, B. A., Rabson, A. B., Miller, I. L., Trempe, J. P., Chejanovsky, N., and Carter, B. J. (1991). Adeno-associated virus Rep protein inhibits human immunodeficiency virus type 1 production in human cells. J. Virol. 65: 396 – 404.

190. Freundlieb, S., Schirra-Muller, C., and Bujard, H. (1999). A tetracycline controlled activation/repression system with increased potential for gene transfer into mammalian cells. J. Gene Med. 1: 4 – 12.

191. Olivares EC, Hollis RP, Chalberg TW, Meuse L, Kay MA, Calos MP. Site-specific genomic integration produces therapeutic Factor IX levels in mice. Nat Biotechnol. 2002;20:1124-1128.

192. Chen L, Woo SL. Complete and persistent phenotypic correction of phenylketonuria in mice by site-specific genome integration of murine phenylalanine hydroxylase cDNA. Proc Natl Acad Sci U S A. 2005;102:15581-15586.

193. Bushman F, Lewinski M, Ciuffi A, et al. Genome-wide analysis of retroviral DNA integration. Nat Rev Microbiol. 2005;3:848-858.

194. Nakai H, Montini E, Fuess S, Storm TA, Grompe M, Kay MA. AAV serotype 2 vectors preferentially integrate into active genes in mice. Nat Genet. 2003;34:297-302.

195. Recchia A, Perani L, Sartori D, Olgiati C, Mavilio F. Site-specific integration of functional transgenes into the human genome by adeno/AAV hybrid vectors. Mol Ther. 2004;10:660-670.

196. Yant SR, Ehrhardt A, Mikkelsen JG, Meuse L, Pham T, Kay MA. Transposition from a gutless adeno-transposon vector stabilizes transgene expression in vivo. Nat Biotechnol. 2002;20:999-1005.

197. Cavazzana-Calvo M, Thrasher A, Mavilio F. The future of gene therapy. Nature. 2004;427:779-781.

198. Coffin JM, Huges SH, Varmus HE. Retroviruses. Cold Spring Harbor, NY: Cold Spring Harbor Laboratory Press; 1997.

199. McCormack MP, Rabbitts TH. Activation of the T-cell oncogene LMO2 after gene therapy for X-linked severe combined immunodeficiency. N Engl J Med. 2004;350:913-922.